January 2009

Discovery Of Inactive E* Conformations In Thrombin And Other Vitamin K- Dependent Clotting Proteases

Alaji Bah
Washington University in St. Louis

WASHINGTON UNIVSERSITY IN ST. LOUIS

DEPARTMENT OF BIOCHEMISTRY & MOLECULAR BIOPHYSICS

Dissertation Committee:

Enrico Di Cera (Supervisor)

Carl Frieden (Chair)

Tom Ellenberger

Roberto Galletto

F. Scott Mathews

Douglas Tollefsen

Discovery Of Inactive E* Conformations In Thrombin And Other Vitamin K- Dependent Clotting Proteases

by

Alaji Bah

A dissertation presented to the Graduate School of Arts and Sciences

of Washington University in partial fulfillment of the

requirements for the degree

of Doctor of Philosophy

December, 2009

Saint Louis, Missouri. USA

ABSTRACT OF THE DISSERTATION

Discovery Of Inactive E* Conformations In Thrombin And Other Vitamin K- Dependent Clotting Proteases

by

Alaji Bah

Doctor of Philosophy in Biology and Biomedical Sciences (Biochemistry)

Washington University in St. Louis, 2009

Professor Enrico Di Cera, Supervisor

Serine proteases of the chymotrypsin family play important roles in the regulation and function of numerous biological processes including digestion, blood coagulation, fibrinolysis, development, fertilization, apoptosis and immunity. For many of these proteases, activity unfolds when a zymogen is activated by limited proteolysis and the associated conformational changes result in the formation of a proper active site and oxyanion hole, both of which are required for efficient hydrolysis of peptide bonds. The transition from zymogen to active enzyme, ***E***, thus provides critical temporal and spatial regulatory mechanism of protease function.

Catalytic activity of serine proteases belonging to Vitamin K-dependent clotting factors is significantly affected by Na^+ through an allosteric mechanism. Over the past 30 years, structural and biochemical studies revealed that Na^+ enhances the enzymatic properties of these proteases from a low activity, ***E***, to a high activity (***E:***Na^+) conformation. However, investigation of the effects of Na^+ on these proteases has mainly focused on the thermodynamics of interaction and the resulting catalytic enhancement, with little emphasis on characterizing the kinetics of Na^+ binding. In deed, the kinetic mechanism of Na^+ binding to many Na^+-activated enzymes remain for the most part unexplored due to lack of convenient probes to monitor the interaction or the difficulty of resolving rate constants for reactions that likely occur on a very fast time scale. My thesis project aims to fill this gap in the investigation of Na^+-activated proteases by elucidating the kinetic mechanism of Na^+ binding to vitamin K-dependent clotting factors.

While studying the kinetics of Na^+ binding to human α-thrombin, we observed a biphasic mechanism of binding whose analysis led to the discovery that in the absence of Na^+, the enzyme exists in dynamic equilibrium between two conformations, ***E**** and ***E***. Structural and kinetic studies indicate that ***E*** is the active form of the enzyme responsible for its catalytic properties while ***E**** is an inactive conformation that features a collapsed active site cleft, a disrupted oxyanion hole and an abrogated Na^+ binding site. ***E**** is not unique to α-thrombin, however, as we have observed a similar ***E**** to ***E*** transition in meizo-thrombin-des F1, factor IXa, factor Xa and activated protein C.

Discovery of ***E**** to ***E*** transition embedded in these trypsin-like enzymes is novel, and the observation of E*-like features in structures of other serine proteases reveal a level of unprecedented conformational plasticity present in the chymotrypsin fold. The inter-conversion between ***E**** and ***E*** has mechanistic significance on how these proteases function *in vivo*. Based on the physiological role of each protease, catalytic activity can be regulated by properly setting the E*–E equilibrium, favoring E* or E depending on whether that protease requires low or high catalytic activity for its *in vivo* function. More importantly, stabilization of E* through mutagenesis can provide a low activity enzyme incapable of interacting with substrate or binding inhibitor until an appropriate cofactor binds and unleashes its full catalytic activity.

Using α-thrombin, a key enzyme of blood coagulation as a model system, we demonstrated how each conformation could be stabilized through rational protein engineering using site-directed mutagenesis. Stabilization of its ***E**** form will turn α-thrombin into an effective anticoagulant agent that can be utilized for *in vivo* therapeutic purposes. In fact, α-thrombin mutants, E217K and W215A/E217A that show anticoagulant and antithrombotic effects in non-human primates both exhibit some structural features of ***E**** like partial collapse of the 215-217 β-strand and disruption of the oxyanion hole. Thus stabilization of ***E**** through mutagenesis or binding of a small molecule can provide an elegant regulatory control that can fine tune specificity along a particular pathway. In addition, discovery of ***E**** in Na^+-activated clotting proteases expands our understanding of allostery in monomeric enzymes in general and in

particular explains why the activity of some thrombin mutants is orders of magnitude lower than the activity of the wild-type in the absence of Na^+.

Findings from this thesis project reveal a fundamental property of structure-function regulation in the vitamin K dependent clotting enzymes and thus set the stage for further investigation of inactive conformations in other serine proteases of the chymotrypsin family. Whether the presence of ***E**** is a universal property of all serine proteases will await future studies.

DEDICATION

To my entire FAMILY

ACKNOWLEDGEMENTS

First, I would like to acknowledge and thank my family and friends for their friendship and patience as well as for their emotional and financial support throughout my academic career.

Next, I want to thank my dissertation committee (Carl Frieden, Tom Ellenberger, Roberto Galletto, F. Scott Mathews and Douglas Tollefsen) for their valuable time, helpful discussions and guidance.

To each and every current and past member of the Di Cera lab whom I interacted during my thesis research, I want to acknowledge their friendship and assistance. In particular, I will thank and acknowledge our laboratory manager, Leslie Bush-Pelc for her training, assistance, collaboration and technical knowledge. In fact, some of the mutants used in this dissertation were kindly provided by her. Raymond Chen and Austin Vogt are acknowledged for their immense scientific contribution in the work presented in chapters 4 and 5 respectively. Zhiwei Chen is thanked and acknowledged for all the crystallographic work presented in this dissertation. In addition, his training and guidance especially at APS is highly appreciated. Dr. Michael Page, Dr. Matthew Papaconstantinou and Prafull Gandhi are thanked for their help, advice and critical insights in every aspect of my research.

I also want to thank the following faculty members for giving me the opportunity to rotate in their laboratories; Prof. Peter Burgers, Jacques Baenziger and J. Mark Petrash. I

will also like to express my gratitude to our former Biochemistry Program Director, Prof. Kathleen Hall for her assistance and advice.

Finally, I am FOREVER indebted and grateful to Enrico for mentoring me during my graduate school career. He has always encouraged me to work hard and allowed me the freedom to engage in many different projects. Grazie infinite! Grazie molte! Ti ringrazio moltissimo!

CURRICULUM VITAE

Alaji Bah

Place of Birth — Banjul, The Gambia

2004-Present Doctoral Research Fellow
Department of Biochemistry & Molecular Biophysics.
Washington University School of Medicine
St. Louis, MO

2001-2004 BSc in Chemistry and BA in Mathematics: Department of Arts & Sciences

Associates in Liberal Studies: Whitney Young College of Leadership Studies

Kentucky State University
Frankfort, KY

Professional Experience

2005 –Present Doctoral Thesis — Supervisor: Prof Enrico Di Cera

2003 Summer Internship	Biomedical Research Apprentice Program Washington University in St. Louis St. Louis, MO
2002-2003	Undergraduate Research Experience The Land Grant Program Kentucky State University Frankfort, KY
2002	Summer Research Internship Supervisor: Dr. Ryan Vallance Universtiy of Kentucky Lexington, KY
1998-2000	Laboratory Technician Medical Research Council Laboratories Supervisor: Dr. Lorenz von Seidlein

Publications

1. Niu W, Chen Z, Bush-Pelc LA, **Bah A**, Gandhi PS, Di Cera E. The mutant N143P reveals how Na+ activates thrombin. J Biol Chem. (2009). [Epub ahead of print]

2. **Bah A**, Carrell CJ, Chen Z, Gandhi PS, Di Cera E. Stabilization of the E* form turns thrombin into an anticoagulant J Biol Chem. (2009) **284**: 20034-40.

3. Papaconstantinou ME, Gandhi PS, Chen Z, **Bah A**, Di Cera E. Na^+ binding to meizothrombin desF1. Cell Mol Life Sci. (2008) **65**:3688-97.

4. Papaconstantinou ME, **Bah A**, Di Cera E. Role of the A chain in thrombin function. Cell Mol Life Sci. (2008) **65** :1943-7.

5. Gianni S, Ivarsson Y, **Bah A**, Bush-Pelc LA, Di Cera E. Mechanism of Na^+ binding to thrombin resolved by ultra-rapid kinetics. Biophysical Chemistry (2007) **131**: 111-4

6. **Bah A**, Chen Z, Bush-Pelc LA, Mathews FS, Di Cera E. Crystal structures of murine thrombin in complex with the extracellular fragments of murine protease-activated receptors PAR3 and PAR4. Proc Natl Acad Sci U S A. (2007)**104**:11603-8.

7. **Bah A**, Garvey LC, Ge J, Di Cera E. Rapid kinetics of Na^+ binding to thrombin. J Biol Chem. (2006) **281**:40049-56.

8. Pineda AO, Chen ZW, **Bah A**, Garvey LC, Mathews FS, Di Cera E. Crystal structure of thrombin in a self-inhibited conformation. J Biol Chem. (2006) 281:32922-8.

INVITED REVIEWS

1. Di Cera E, Page MJ, **Bah A**, Bush-Pelc LA, Garvey LC. Thrombin allostery. Phys Chem Chem Phys. (2007) 9:1291-306.

ABSTRACTS

1. **Bah A**, Carrell CJ, Chen Z, Gandhi PS, Di Cera E. Stabilization of the E* form turns thrombin into an anticoagulant. (2009) Meeting of the American Crystallographic Association. Toronto, Canada.

2. **Bah A**, Carrell CJ, Chen Z, Gandhi PS, Di Cera E. Stabilization of the E* form turns thrombin into an anticoagulant. (2009) FASEB SUMMER RESEARCH CONFERENCES (Proteases in Hemostasis & Vascular Biology) Carefree, AZ.

3. **Bah A**, Chen Z, Bush-Pelc LA, Mathews FS, Di Cera E. Crystal structures of murine thrombin in complex with the extracellular fragments of murine protease-activated receptors PAR3 and PAR4. (2007). Meeting of the American Crystallographic Association. Salt Lake City, UT.

4. **Bah A**, Yin Z, Antonius G, Javed K, Wang C. *Calcium, Magnesium and Zinc Content in Green Peppers Grown on Soil Amendmended with Biosolids or Yard Waste Compost*. (2003) Association of 1890 Research Directors Biennial Research Symposium. Atlanta, Georgia.

5. **Bah A**, Gokel G.W, Rerndini R, Payeska Y, Payeski R, Hall M. *Synthesis of Ceramides Analogues.* (2003) SACNAS National Conference. Albuquerque, New Mexico.

6. **Bah A**, Vallance R, Javed KR, Trinkle CR. *Electrochemical Preparation of Tungsten Tip for Scanning Tunneling Microscope Probes*. 2002 Annual Biomedical Research Conference for Minority Students. New Orleans, Louisiana.

ACADEMIC HONORS

1. Biomarcromoles SIG Etter Student Lecturer award (2009) American Crystallography Association

2. Gerty T. Cori Predoctoral Fellowship (2008-9) Sigma-Aldrich

3. Linus Pauling Poster Award (2007) American Crystallography Association

4. Presidential Scholarship (2001-4) Kentucky State University

5. Certificate of Excellence (2004) Whitney College of Leadership Studies

6. Environmental Stewardship Poster Award (2003) Association of 1890 Research Directors Biennial Research Symposium

7. Certificate of Merit (1997) West African Examinations Council

TEACHING EXPERIENCE

1. Teaching assistant: Undergraduate biochemistry course at Washington University in St. Louis (Fall 2005).

2. Mathematics and Chemistry tutor: The Peers Empowering Peers Program (PEP) at Kentucky State University (Fall 2001-Spring 2004)

3. Teaching assistant: Calculus courses at Kentucky State University (Fall 2004).

4. Group leader: NSF sponsored Teams Enhancing Access to Minorities in the Sciences (TEAMS) Project at Kentucky State University (2003-2004)

TABLE OF CONTENTS

LIST OF FIGURES

Chapter I

Chapter IV

Chapter V

LIST OF TABLES

Chapter IV

Chapter V

ABBREVIATIONS

Å	Angstrom unit (1 Å = 0.1nm)
aPC	Activated protein C
ChCl	Choline Chloride
FPR	D-phenylalanine-proline-arginine-p-nitroanaline (similar for other substrates)
FVIIa	Activated coagulation factor VII (similar for other coagulation proteases)
k_{cat}	Catalytic constant
K_m	Michaelis constant
PEG	Poly(ethylene glycol)
s	k_{cat}/K_m
TM	Thrombomodulin
Tris-HCl	Tris(hydroxymethyl)aminomethane hydrochloride

CHAPTER I

Introduction

SERINE PROTEASES

Serine proteases, which derive their name from the nucleophilic serine residue in the enzyme active site, make up the largest group of proteolytic enzymes, forming more than a third of all known proteases (*1-3*). Serine proteases are present in every kingdom of cellular life, and are grouped into clans and families based on their catalytic mechanism and common ancestry respectively (*4*). They play critical roles in the function and regulation of many biological processes including digestion, coagulation, fibrinolysis, and complement activation as well as cell proliferation, activation and differentiation (*3*). Several excellent reviews are available in the literature that describes in depth the diversity, structure and functions of serine proteases (*1, 2, 5-8*). In what follows, I will give a brief overview of that aspect of serine proteases that is relevant to this thesis project.

The largest group of serine proteases belongs to the Clan PA, family S1 peptidases which are further divided into S1A and S1B subfamilies. S1A proteases are extracellular and are mostly found in eukaryotic organisms while S1B proteases participate in protein turnover in all organisms (*1, 5*). Although they are phylogenitically distinct, S1A and S1B proteases contain the same chymotrypsin fold and utilize the canonical catalytic triad of Ser^{195}, His^{57} and Asp^{102} (chymotrypsin numbering used throughout) in hydrolyzing a peptide bond (Figure 1.1) (*9*). The occurrence of this triad in identical spatial configuration in trypsins, subtilisin, prolyl oligopeptidase and ClpP peptidases is an indication of its success as efficient catalytic machinery *(1)*.

Peptidase activity occurs via two tetrahedral intermediates and is divided into three main stages: (i) formation of an enzyme-substrate Michaelis-Menten complex (ii) acylation and(iii) de-acylation steps (Figure 1.2). Even though the majority of serine proteases are endopeptidases that hydrolyze peptide bonds within polypeptide chains, there are some exopeptidases that cleave residues from either the N- or C-terminal of substrates. Many S1 peptidases usually require proteolytic activation from a zymogen precursor. Cleaving between residues 15 and 16 results in the formation of ion pair between the nascent N-terminus and Asp^{194}, which induces a conformational change that stabilizes an accessible active site architecture and proper formation of an oxyanion hole (*10-12*) (Figure 1.1).

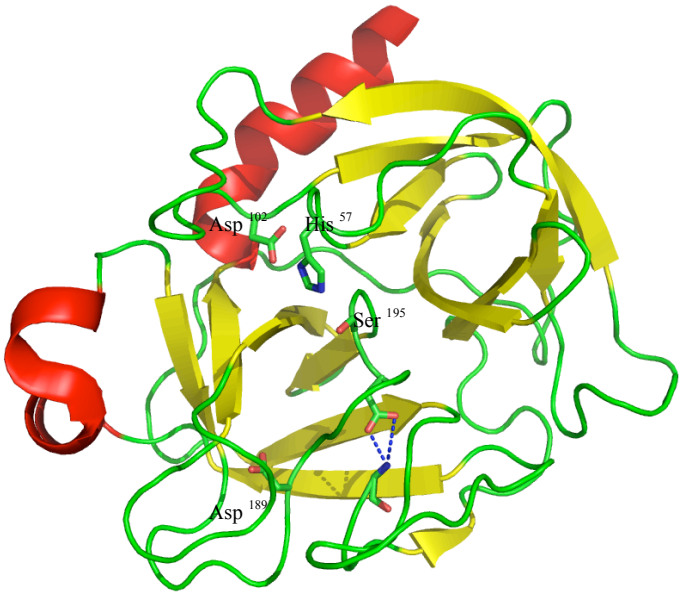

Figure 1.1 Cartoon representation of the 3-D structure of a typical serine protease of the S1 family of proteases. Residues of the catalytic triad located between the two β-barrel (yellow), ion-pair (blue dashes) between residues 16 and 194 & Asp189 at the bottom of primary specificity pocket are all shown in stick model. PDB Code (2PTN).

I

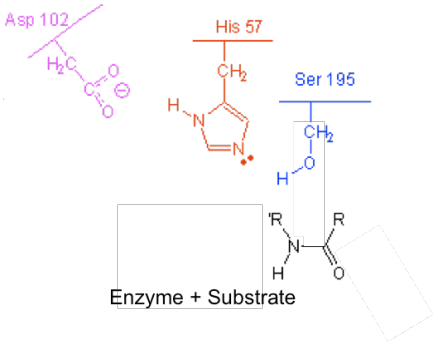

Enzyme + Substrate

II

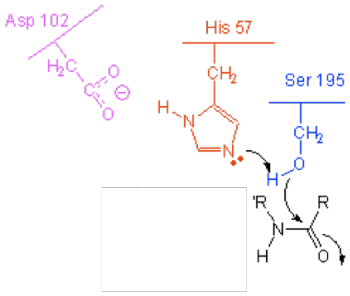

Formation of Michaelis-Menten Complex

III

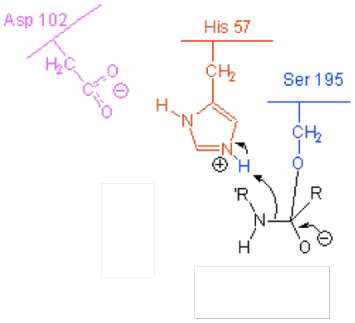

Tetrahedral Intermediate

IV

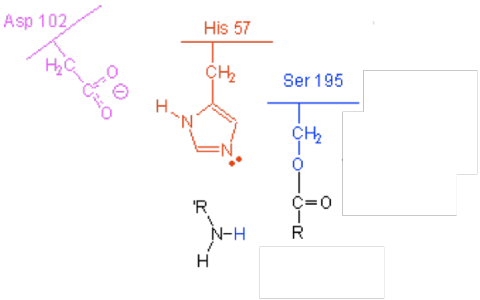

Acyl-enzyme Intermediate & Release of N-terminus

V

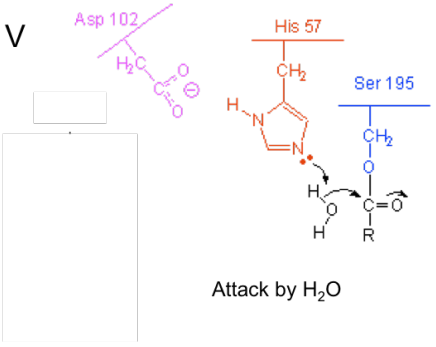

Attack by H_2O

VI

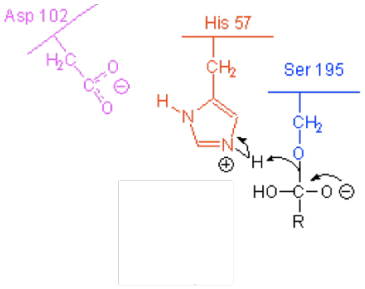

Tetrahedral Intermediate

VII

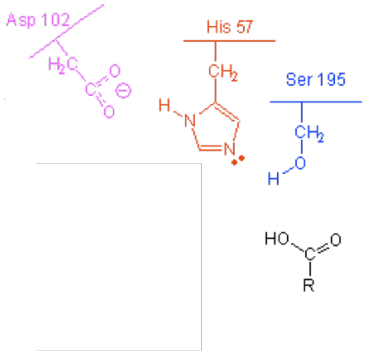

Free C-terminus generation

Figure 1.2 Catalytic mechanism of serine protease peptide bond hydrolysis.

With the aid of His^{57} acting as a general base, the hydroxyl group of the catalytic ser^{195} attacks the carbonyl group of the amide substrate. This leads to the formation of a tetrahedral anion intermediate, which is stabilized by the oxyanion hole, a net positively charge pocket formed by the N atoms of Ser^{195} and Gly^{193}. Collapse of the tetrahedral intermediate results in the formation of an acyl-enzyme complex and stabilization of the new N-terminus by His^{57}. Finally, a water molecule displaces the free N-terminus product and then attacks the acyl-enzyme intermediate to form another tetrahedral intermediate. The collapse of this intermediate releases the new C-terminus of the product (*2*).

In the chymotrypsin fold, residues responsible for catalysis and regulation are distributed across the entire protein. The catalytic triad is strategically located at the interface of two six-stranded β-barrels with His^{57} and Asp^{102} residing at the N-terminal β-barrel while Ser^{195} and the oxyanion hole are located in the C-terminal β-barrel (*13*) (Figure 1.1). The active site face is defined by surface exposed loops that mediate substrate specificity and allostery through interaction with substrates, cations or macromolecular cofactors (*1*). As a result, within the same fold for instance, trypsin is optimized to cleave after Arg/Lys residues while chymotrypsin prefer aromatic side chains.

The molecular origin of the difference in substrate specificity within S1 proteases is not fully understood (*3*). The architecture of the primary specificity pocket partly determines their corresponding specificity since its engineering is necessary but not sufficient for converting one protease into another. However, extensive additional mutations at loops not directly in contact with substrate are also required to generate substrate specificity conversion (*14*). Nonetheless, the resulting catalytic activity of these engineered mutants are poor relative to the wild type enzyme. For example, the swapping of chymotrypsin

into trypsin or trypsin into elastase is never fully realized (*15, 16*). These results demonstrate our current lack of understanding of the determinants of substrate specificity in S1 serine proteases. The linkage between structure and function underlying the mechanism of protease specificity is missing a key element. The considerable conformational plasticity and the allosteric pathways embedded in the chymotrypsin fold may be the missing link (*3*).

THE BLOOD COAGULATION CASCADE

Serine proteases of the chymotrypsin family play important roles in the blood coagulation cascade. Blood coagulation, a key component of homeostasis, evolved as a specialization of the complement system and immune response (*17*). The coagulation cascade involves several proteins that act together following vascular injury to generate a clot that prevents a severe loss of body fluids and/or pathogenic invasion (*18*). The initiation and termination of the clotting process is timely and localized, otherwise uncontrolled clot formation will result in the occlusion of blood vessels and thrombosis, which can lead to cardiovascular diseases such as strokes and heart attacks. Thus, a tightly-regulated coagulation cascade is essential for survival to prevent excessive bleeding or widespread clot deposits (*18*).

The blood coagulation cascade can be initiated through two pathways known as the intrinsic (contact) and extrinsic (tissue factor) pathways (Figure 1.3) (*18*). Each pathway consists of a series of zymogen activation steps where a newly activated enzyme

catalyzes the activation of the next zymogen in the series until prothrombin is converted to thrombin. Thrombin then cleaves fibrinogen to form an insoluble clot that anchors the activated platelets to the site of lesion to initiate the process of wound repair. In addition, thrombin stabilizes the clot by generating the transglutaminase, FXIIIa, that crosslinks the nascent clot, and down regulates the fibrinolytic system by activating Thrombin-activatable fibrinolysis inhibitor (TAFI). TAFIa removes C-terminal lysines and arginine residues from fibrin, hence reducing the ability of fibrin to initiate the fibrinolyic response(*17*).

Laboratory and clinical data have shown that the primary route of initiating the coagulation cascade after vascular injury is the extrinsic pathway (*18*). This pathway is composed of three procoagulant vitamin K-dependent enzyme complexes and one anticoagulant enzyme complex (Figure 1.3). Each haemostatic complex consists of a vitamin K dependent clotting enzyme and a macromolecular cofactor, assembled in a Ca^{2+} dependent manner on a phospholipids membrane of activated or damaged cells. The central event of the coagulation cascade is the formation of thrombin, and can be divided into three distinct phases (initiation, propagation and termination).

Thrombin generation begins by exposure of tissue factor that forms a complex with factor VIIa and results in the generation of small quantities of factors IXa and Xa (*19, 20*). This small concentration of Xa produces minute amounts of thrombin (initial phase) that can activate factor XI and cofactors VIII and V. During the propagation phase, the procoagulant complexes are assembled, and they enhance the generation of FXa and

thrombin in the tenase (IXa, VIIIa, Ca^{2+}, phospholipids, X) and prothrombinase (Xa, Va, Ca^{2+}, phospholipids, prothrombin) complexes by ~5 orders of magnitude relative to their free enzymes.

The termination phases involves the coordination of stoichiometric and dynamic inhibitors that down regulate the explosive generation of thrombin to halt the progression of the coagulation cascade. Although antithrombin III (AT-III) and the tissue factor pathway inhibitor (TFPI) are the principal stoichiometric inhibitors, heparin cofactor II, α_2-macroglobulin, α_1-antitrypsin, activated protein C inhibitor are essential inhibitors that contribute in regulating the coagulation cascade as well (*21, 22*). AT-III is a potent neutralizer of all the procoagulant enzymes while TFPI shuts down the generation of Factors IXa and Xa by effectively inhibiting the tissue factor-VIIa-Xa complex (Figure 1.3).

The dynamic inhibitory system is composed of the thrombin-thrombomodulin-protein C system (*23*). Binding of thrombin onto thrombomodulin, a receptor constitutively expressed on the surface of the endothelium, prevents the cleavage of fibrinogen and the activation of PARs, but enhances the activation of protein C over a 1000-fold. Activated protein C binds and cleaves cofactors VIIIa and Va thereby inactivating the tenase and prothrombinase complexes respectively. As a result, the exponential amplification of α-thrombin generation is down regulated.

In addition to its roles in the coagulation cascade, other important effects are triggered by thrombin upon cleavage of protease-activated receptors (PARs), which are members of the G-protein-coupled receptor super family. Four PARs have been cloned and they all share similar mechanism of activation (*24*). Thrombin and other proteases, derived from the circulatory and inflammatory cells, cleave at a specific site within the extracellular N-terminus to expose a new N-terminal tethered ligand domain, which binds to and activates the cleaved receptors (*25*). Thrombin activates PAR1 (*26*), PAR3 (*27, 28*) and PAR4 (*29-31*) through this mechanism and elicit several cellular responses. Consequently, thrombin is a potent mitogen that affects the physiology of many cell types including smooth muscles, macrophages and endothelial cells. In addition, thrombin is by far the most potent platelet activator. PAR1 is responsible for platelet activation in humans at low thrombin concentrations and its action is reinforced by PAR4 at higher concentrations of the enzyme (*25*). Activation of PAR1 and PAR4 triggers platelet activation and aggregation and unfolds the **prothombotic** role of thrombin in the blood.

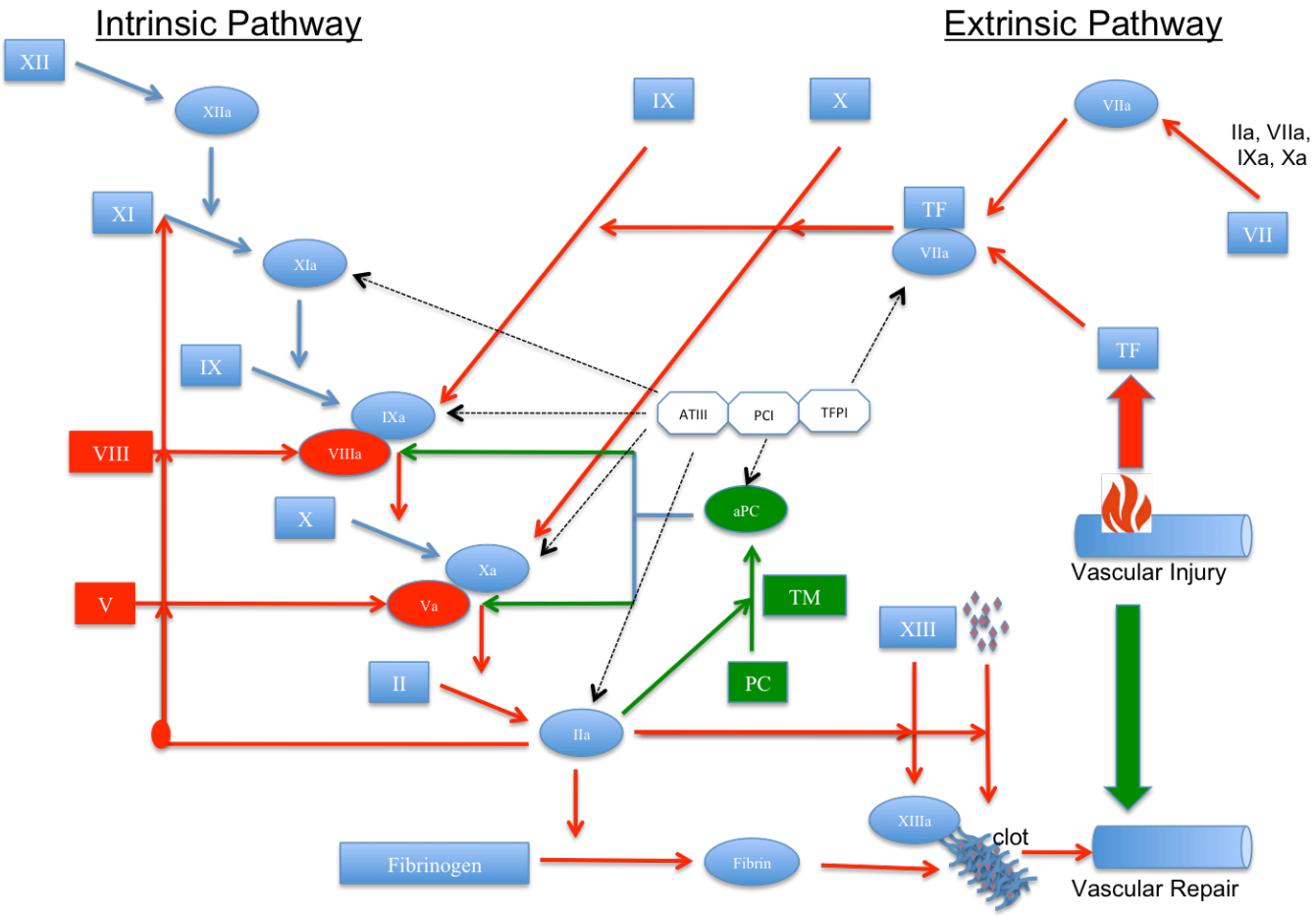

Figure 1.3 The Blood Coagulation Cascade. Shown are the intrinsic (contact) and extrinsic (tissue factor) pathways of initiation thrombin generation. Zymogens (squares), procoagulant enzymes (blue ovals), cofactors (red ovals), anticoagulant enzymes (green ovals), platelets (red diamonds) and inhibitors (white pentagons) (*17, 18, 24*).

Na^+ ACTIVATION & VITAMIN K-DEPENDENT CLOTTING FACTORS

Metal ions play a key role in serine proteases of the vitamin K dependence clotting factors as well as in many other enzyme-catalyzed biological processes (*32-34*). The first observation of monovalent cation (M^+) activation of enzymes was made by Boyer *et. al.* (*35*) when they discovered that K^+ was absolutely required by pyruvate kinase for catalytic activity (*36*). Later, Monod demonstrated Na^+-dependent catalytic rate enhancement in β-galactosidase (*37*) and thereafter, the activities of many enzymes were observed to be modulated by M^+ (*38*). Due to the tight control of the $[M^+]$ *in vivo*, M^+ are not regulators of enzyme activity. They function by lowering the energy barriers in the ground or transition states, hence affecting substrate binding or catalysis (*39*).

A recent classification of M^+-activated enzymes groups them according to the selectivity of the effect and the mechanism of activation, as established from kinetic and structural analysis respectively (*40*). The mechanism of activation can be can be either cofactor-like or allosteric. In the former case known as type I, M^+ is absolutely required for catalysis because it anchors the substrate to the enzyme's active site. However, in the later case called Type II, M^+ enhances enzyme activity through conformational changes induced upon binding to a distant site where M^+ makes no direct interaction with the substrate. In this case, that is most relevant to the vitamin K- dependent family of clotting enzymes (*1, 41*), the M^+ acts as an allosteric effector and is not absolutely required for catalysis since the enzyme is still active in the absence of M^+.

Na^+ influences the activity of all vitamin K -dependent clotting enzymes. Orthner and Kosow were the first to show that factor Xa (*42*) and thrombin (*43*) are optimally active in the presence of Na^+ while Steiner and Castellino made a similar observation in activated protein C (*44-47*). Since then, it has been demonstrated that Na^+ had a significant influence on the activity of factor VIIa (*48, 49*), factor IXa (*50*) and meizothrombin-desF1 (*51, 52*).

Wells and Di Cera first established that the Na^+ activation of human thrombin is specific and allosteric, and involves the transition of the enzyme between two active forms (*53*) leading to an increase in k_{cat} and a decrease in K_m. These forms are E with low activity and E: Na^+ with high activity, originally defined as the slow and fast forms respectively (*53*). Because the K_d for Na^+ binding to thrombin is 110 mM at 37^{o}C, the physiological concentration of NaCl of 140 mM is not enough to saturate thrombin. As a result, both the E and E: Na^+ forms of thrombin are significantly populated (2:3 ratio) *in vivo* (*53-56*). Na^+ is required for the optimal cleavage of fibrinogen, PAR1, PAR3 and PAR4 as well as activation of factors V, VIII and XI. More importantly, however, Na^+ binding is dispensable for activation of the anticoagulant protein C with or without thrombomodulin (Figure 1.4). Therefore, Na^+ binding is the major driving force behind the procoagulant, prothrombotic and signaling functions of the blood (*57*). This explains why several naturally occurring mutations of the prothrombin gene that affect residues linked to Na^+ are associated with bleeding and why all anticoagulants thrombins engineered to date are defective for Na^+ binding (*58*).

Further insights into how Na^+ regulates the function of human thrombin came from the work of Bush *et. al.* who observed that murine thrombin lacks Na^+ activation, yet it retains high catalytic activity towards all its physiological substrates (*59*). Structural and kinetic analysis later revealed that the murine enzyme is adopts an E:Na^+ conformation both in the presence (personal communication) and absence of Na^+ binding (*60*). The lack of Na^+ activation allows the murine enzyme to be more resistant to mutations that destabilize the Na^+ binding environment or the transmission of that binding to function.

After being overlooked in previous crystal structures, the Na^+ binding site of thrombin was finally identified unequivocally using Rb^+ replacement in 1995 (*61*) and its definition facilitated the subsequent identification of the analogous Na^+ binding sites in Factor Xa (*62, 63*), Factor IXa (*50*) Factor VIIa (*64*), activated protein C (*65*) and the thrombin precursor meizothrombin-desF1 (*51*) (Figure 1.5). Structural analysis of E and E: Na^+ reveals that a network of water molecules transmits the effect of Na^+ from its binding site to the active site. However, spectroscopic and mutagenesis evidence indicate that Na^+ binding has long range allosteric effects that globally affect the enzyme (*56, 66*).

Because Na^+ has a significant influence on the activity of all the vitamin K - dependent clotting factors (*42-44, 48-50, 52, 53*) investigating the molecular determinants and mechanism of its binding is key to understand the function and regulation of this family of clotting enzymes. However, investigation of the effects of Na^+ on these proteases has mainly focused on thermodynamics of interaction and the resulting catalytic enhancement, with little emphasis on characterizing the kinetic mechanism of Na^+

binding. In general, the kinetics of M^+ binding to M^+-activated enzymes remain for the most part unexplored due to lack of convenient probes to monitor the interaction or the difficulty of resolving rate constants for reactions that likely occur on a very fast time scale.

My thesis project aims to fill this gap in the investigation of Type II Na^+-activated proteases by elucidating the kinetic mechanism of Na^+ binding to vitamin K-dependent clotting factors. Stopped flow and ultra-rapid continuous flow fluorescence techniques were utilized to investigate the mechanism of Na^+ binding by monitoring the associated conformational changes in the μs and ms timescales. These studies, along with structural analysis reveal the presence of inactive E* conformation that interconvert with the active E form. To further understand the molecular determinants of E* and gain insight into its role in substrate specificity, investigation of its properties were performed using a combination of site-directed mutagenesis, enzyme catalysis, calorimetry and X-ray crystallographic studies.

Several important questions are addressed in this thesis. What is the kinetic mechanism of Na^+ binding in all vitamin K-dependent clotting factors? What are the structural and kinetic features of E* and what is the physiological role of the E* to E equilibrium? Finally, can we alter substrate specificity by stabilizing E*? Due to the diversity of its substrate and cofactor interactions, as well as its wealth of kinetic and structural data, thrombin offers a unique opportunity to explore these questions.

Chapter 2 gives a detailed description of the kinetics and thermodynamic properties of the E* to E transition in human α-thrombin using stopped-flow measurements of intrinsic fluorescence. The stopped-flow data presented in chapter 2 is complemented with the ultra-rapid kinetic investigation from our collaborators in Stefano Gianni's group to establish the complete analysis of Na^+ binding of thrombin.

Having established the presence of E* inactive conformation in wild type α-thrombin, Chapter 3 explores the potential of stabilizing E* to abrogate catalytic function until a suitable cofactor restores activity by triggering the E* to E transition. In α-thrombin, this strategy can be utilized to turn off the procoagulant and prothrombotic functions of the enzyme that do not require a cofactor, while maintaining the protein C anticoagulant pathway in the presence of the cofactor TM. Stabilization of E* through mutation of the autolysis loop provides a molecular mechanism to turn thrombin into an anticoagulant with potential therapeutics for *in vivo* application.

Chapter 4 builds upon the results from the previous chapters and extend the mutagenesis studies on the autolysis loop to explore the effects of its length and amino acid composition in the E* to E transition and Na^+ dependent allostery. Murine thrombin, which is stabilized in an E: Na^+ -like conformation, was utilized as a model to dissect the role of the autolysis loop in the stabilization of E and E: Na^+ conformations of human thrombin.

Chapter 5 describes the investigation of the kinetic mechanism of Na^+ binding in clotting factors VIIa, IXa, Xa and activated protein C. A binding mechanism similar to human α-thrombin was observed in activated protein C, Factors IXa and Xa, indicating the presence of E* is not unique to thrombin.

Finally, in chapter 6, we discuss how the knowledge gained from this thesis work can be applied in future to enhance our understanding of protease function and to generate more proficient enzymes for biological or industrial use.

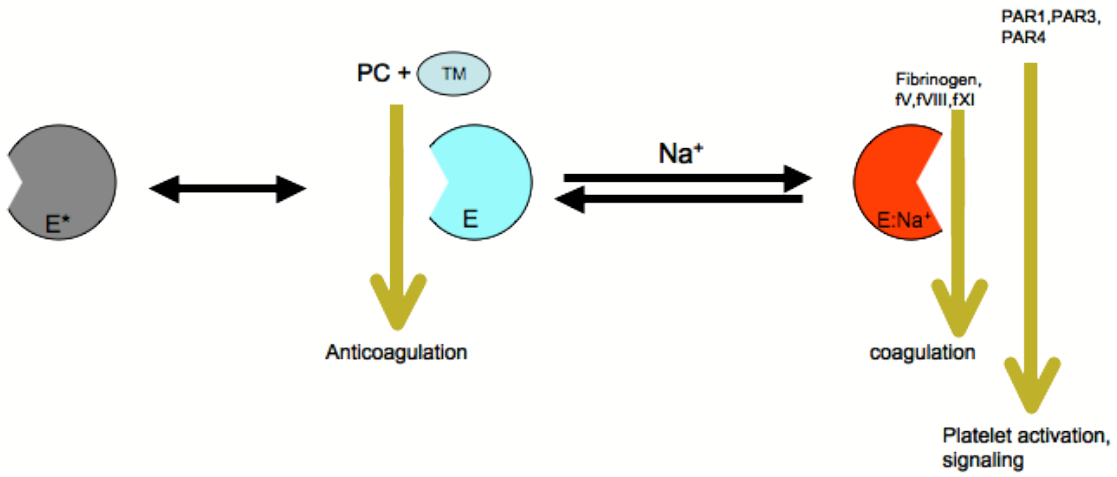

Figure 1.4 Role of Na^+ in the multiple roles of thrombin function. Na^+ is the major driving force for the procoagulant and prothrombotic functions of human thrombin. However, it is dispensable for the activation of protein C. The E* is an inactive conformation incapable of interacting with Na^+, substrates or inhibitors.

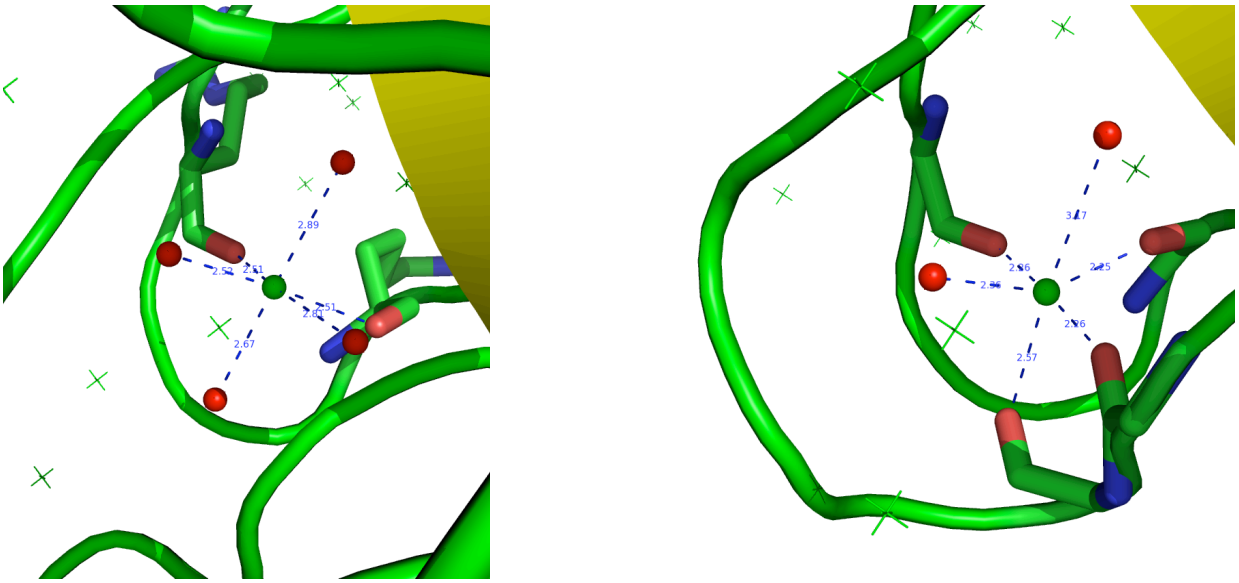

Figure 1.5 The Na^+ binding site of Vitamin K-dependent clotting factors. (A) In thrombin Na^+ is coordinated by four water molecules and two backbone carbonyl oxygens (221a, 224) while (B), the reverse is true for FXa, two water molecules and four carbonyl oxygens (185a, 186, 222, 224). Note how only a single loop is involved in thrombin but both 186- and 220-loops are coordinating the Na^+ in FXa. The Na^+ sites in the other vitamin K-dependent clotting factors are similar to that of FXa. PDB codes (1SG8, thrombin & 2BOK, FXa)

References:

1. Page, M. J., and Di Cera, E. (2008) Serine peptidases: classification, structure and function, *Cell Mol Life Sci 65*, 1220-1236.
2. Hedstrom, L. (2002) Serine protease mechanism and specificity, *Chem Rev 102*, 4501-4524.
3. Di Cera, E. (2009) Serine proteases, *IUBMB life 61*, 510-515.
4. Rawlings, N. D., Morton, F. R., Kok, C. Y., Kong, J., and Barrett, A. J. (2007) MEROPS: the peptidase database, *Nucleic Acids Res*.
5. Page, M. J., and Di Cera, E. (2007) Serine Proteases, in *Encyclopedia of Life Sciences*, John Wiley & Sons, Ltd., Chichester.
6. Page, M. J., and Di Cera, E. (2008) Serine Protease and Serine Protease Inhibitors, in *Encyclopedia of Chemical Biology*, John Wiley & Sons, Ltd., Chichester.
7. Perona, J. J., and Craik, C. S. (1995) Structural basis of substrate specificity in the serine proteases, *Protein Sci 4*, 337-360.
8. Hedstrom, L. (1996) Trypsin: a case study in the structural determinants of enzyme specificity, *Biological chemistry 377*, 465-470.
9. Polgar, L. (2005) The catalytic triad of serine peptidases, *Cell Mol Life Sci 62*, 2161-2172.
10. Neurath, H., and Dixon, G. H. (1957) Structure and activation of trypsinogen and chymotrypsinogen, *Fed Proc 16*, 791-801.
11. Fehlhammer, H., Bode, W., and Huber, R. (1977) Crystal structure of bovine trypsinogen at 1-8 A resolution. II. Crystallographic refinement, refined crystal structure and comparison with bovine trypsin, *Journal of molecular biology 111*, 415-438.
12. Bode, W., Fehlhammer, H., and Huber, R. (1976) Crystal structure of bovine trypsinogen at 1-8 A resolution. I. Data collection, application of patterson search techniques and preliminary structural interpretation, *Journal of molecular biology 106*, 325-335.
13. Page, M. J., Macgillivray, R. T., and Di Cera, E. (2005) Determinants of specificity in coagulation proteases, *J Thromb Haemost 3*, 2401-2408.
14. Hedstrom, L., Szilagyi, L., and Rutter, W. J. (1992) Converting trypsin to chymotrypsin: the role of surface loops, *Science (New York, N.Y 255*, 1249-1253.
15. Venekei, I., Szilagyi, L., Graf, L., and Rutter, W. J. (1996) Attempts to convert chymotrypsin to trypsin, *FEBS Lett 383*, 143-147.
16. Hung, S. H., and Hedstrom, L. (1998) Converting trypsin to elastase: substitution of the S1 site and adjacent loops reconstitutes esterase specificity but not amidase activity, *Protein Eng 11*, 669-673.
17. Di Cera, E. (2003) Thrombin interactions, *Chest 124*, 11S-17S.
18. Mann, K. G. (2003) Thrombin formation, *Chest 124*, 4S-10S.
19. Gailani, D., and Broze, G. J., Jr. (1991) Factor XI activation in a revised model of blood coagulation, *Science (New York, N.Y 253*, 909-912.
20. Girard, T. J., MacPhail, L. A., Likert, K. M., Novotny, W. F., Miletich, J. P., and Broze, G. J., Jr. (1990) Inhibition of factor VIIa-tissue factor coagulation activity by a hybrid protein, *Science (New York, N.Y 248*, 1421-1424.

21. Tollefsen, D. M. (2007) Heparin Cofactor II Modulates the Response to Vascular Injury, *Arterioscler Thromb Vasc Biol 27*, 454-460.
22. Gettins, P. G. (2002) Serpin structure, mechanism, and function, *Chem Rev 102*, 4751-4804.
23. Esmon, C. T. (2003) The protein C pathway, *Chest 124*, 26S-32S.
24. Brass, L. F. (2003) Thrombin and platelet activation, *Chest 124*, 18S-25S.
25. Coughlin, S. R. (2000) Thrombin signalling and protease-activated receptors, *Nature 407*, 258-264.
26. Vu, T. K., Wheaton, V. I., Hung, D. T., Charo, I., and Coughlin, S. R. (1991) Domains specifying thrombin-receptor interaction, *Nature 353*, 674-677.
27. Ishihara, H., Connolly, A. J., Zeng, D., Kahn, M. L., Zheng, Y. W., Timmons, C., Tram, T., and Coughlin, S. R. (1997) Protease-activated receptor 3 is a second thrombin receptor in humans, *Nature 386*, 502-506.
28. Sambrano, G. R., Weiss, E. J., Zheng, Y. W., Huang, W., and Coughlin, S. R. (2001) Role of thrombin signalling in platelets in haemostasis and thrombosis, *Nature 413*, 74-78.
29. Kahn, M. L., Zheng, Y. W., Huang, W., Bigornia, V., Zeng, D., Moff, S., Farese, R. V., Jr., Tam, C., and Coughlin, S. R. (1998) A dual thrombin receptor system for platelet activation, *Nature 394*, 690-694.
30. Nakanishi-Matsui, M., Zheng, Y. W., Sulciner, D. J., Weiss, E. J., Ludeman, M. J., and Coughlin, S. R. (2000) PAR3 is a cofactor for PAR4 activation by thrombin, *Nature 404*, 609-613.
31. Xu, W. F., Andersen, H., Whitmore, T. E., Presnell, S. R., Yee, D. P., Ching, A., Gilbert, T., Davie, E. W., and Foster, D. C. (1998) Cloning and characterization of human protease-activated receptor 4, *Proceedings of the National Academy of Sciences of the United States of America 95*, 6642-6646.
32. Ibers, J. A., and Holm, R. H. (1980) Modeling coordination sites in metallobiomolecules, *Science (New York, N.Y 209*, 223-235.
33. Castagnetto, J. M., Hennessy, S. W., Roberts, V. A., Getzoff, E. D., Tainer, J. A., and Pique, M. E. (2002) MDB: The Metalloprotein Database and Browser at The Scripps Research Institute, *Nucleic Acids Research 30*, 379-382.
34. Tainer, J. A., Roberts, V. A., and Getzoff, E. D. (1992) Protein metal-binding sites, *Current Opinion in Biotechnology 3*, 378-387.
35. Boyer, P. D., Lardy, H. A., and Phillips, P. H. (1942) The role of potassium in muscle phosphorylations, *J Biol Chem 146*, 673-681.
36. Kachmar, J. F., and Boyer, P. D. (1953) Kinetic analysis of enzyme reactions. II. The potassium activation and calcium inhibition of pyruvic phosphoferase, *J Biol Chem 200*, 669-682.
37. Cohn, M., and Monod, J. (1951) [Purification and properties of the beta-galactosidase (lactase) of Escherichia coli.], *Biochim Biophys Acta 7*, 153-174.
38. Suelter, C. H. (1970) Enzymes activated by monovalent cations, *Science (New York, N.Y 168*, 789-795.
39. Page, M. J., and Di Cera, E. (2006) Role of Na+ and K+ in enzyme function, *Physiological reviews 86*, 1049-1092.
40. Di Cera, E. (2006) A structural perspective on enzymes activated by monovalent cations, *J Biol Chem 281*, 1305-1308.

41. Di Cera, E. (2008) Thrombin, *Mol Aspects Med 29*, 203-254.
42. Orthner, C. L., and Kosow, D. P. (1978) The effect of metal ions on the amidolytic acitivity of human factor Xa (activated Stuart-Prower factor), *Arch Biochem Biophys 185*, 400-406.
43. Orthner, C. L., and Kosow, D. P. (1980) Evidence that human alpha-thrombin is a monovalent cation-activated enzyme, *Arch Biochem Biophys 202*, 63-75.
44. Steiner, S. A., Amphlett, G. W., and Castellino, F. J. (1980) Stimulation of the amidase and esterase activity of activated bovine plasma protein C by monovalent cations, *Biochem Biophys Res Commun 94*, 340-347.
45. Steiner, S. A., and Castellino, F. J. (1982) Kinetic studies of the role of monovalent cations in the amidolytic activity of activated bovine plasma protein C, *Biochemistry 21*, 4609-4614.
46. Steiner, S. A., and Castellino, F. J. (1985) Effect of monovalent cations on the pre-steady-state kinetic parameters of the plasma protease bovine activated protein C, *Biochemistry 24*, 1136-1141.
47. Steiner, S. A., and Castellino, F. J. (1985) Kinetic mechanism for stimulation by monovalent cations of the amidase activity of the plasma protease bovine activated protein C, *Biochemistry 24*, 609-617.
48. Dang, Q. D., and Di Cera, E. (1996) Residue 225 determines the Na(+)-induced allosteric regulation of catalytic activity in serine proteases, *Proceedings of the National Academy of Sciences of the United States of America 93*, 10653-10656.
49. Petrovan, R. J., and Ruf, W. (2000) Role of residue Phe225 in the cofactor-mediated, allosteric regulation of the serine protease coagulation factor VIIa, *Biochemistry 39*, 14457-14463.
50. Schmidt, A. E., Stewart, J. E., Mathur, A., Krishnaswamy, S., and Bajaj, S. P. (2005) Na+ site in blood coagulation factor IXa: effect on catalysis and factor VIIIa binding, *Journal of molecular biology 350*, 78-91.
51. Papaconstantinou, M. E., Gandhi, P. S., Chen, Z., Bah, A., and Di Cera, E. (2008) Na(+) binding to meizothrombin desF1, *Cell Mol Life Sci 65*, 3688-3697.
52. Kroh, H. K., Tans, G., Nicolaes, G. A. F., Rosing, J., and Bock, P. E. (2007) Expression of allosteric linkage between the sodium ion binding site and exosite I of thrombin during prothrombin activation, *J Biol Chem 282*, 16095-16104.
53. Wells, C. M., and Di Cera, E. (1992) Thrombin is a Na(+)-activated enzyme, *Biochemistry 31*, 11721-11730.
54. Griffon, N., and Di Stasio, E. (2001) Thermodynamics of Na+ binding to coagulation serine proteases, *Biophys Chem 90*, 89-96.
55. Guinto, E. R., and Di Cera, E. (1996) Large heat capacity change in a protein-monovalent cation interaction, *Biochemistry 35*, 8800-8804.
56. Bah, A., Garvey, L. C., Ge, J., and Di Cera, E. (2006) Rapid kinetics of Na+ binding to thrombin, *J Biol Chem 281*, 40049-40056.
57. Di Cera, E., Page, M. J., Bah, A., Bush-Pelc, L. A., and Garvey, L. C. (2007) Thrombin allostery, *Phys Chem Chem Phys 9*, 1292-1306.
58. Di Cera, E. (2007) Thrombin as procoagulant and anticoagulant, *J Thromb Haemost 5*, 196-202.
59. Bush, L. A., Nelson, R. W., and Di Cera, E. (2006) Murine thrombin lacks Na+ activation but retains high catalytic activity, *J Biol Chem 281*, 7183-7188.

60. Marino, F., Chen, Z. W., Ergenekan, C., Bush-Pelc, L. A., Mathews, F. S., and Di Cera, E. (2007) Structural basis of Na+ activation mimicry in murine thrombin, *J Biol Chem 282*, 16355-16361.
61. Di Cera, E., Guinto, E. R., Vindigni, A., Dang, Q. D., Ayala, Y. M., Wuyi, M., and Tulinsky, A. (1995) The Na+ binding site of thrombin, *J Biol Chem 270*, 22089-22092.
62. Zhang, E., and Tulinsky, A. (1997) The molecular environment of the Na+ binding site of thrombin, *Biophys Chem 63*, 185-200.
63. Scharer, K., Morgenthaler, M., Paulini, R., Obst-Sander, U., Banner, D. W., Schlatter, D., Benz, J., Stihle, M., and Diederich, F. (2005) Quantification of cation-pi interactions in protein-ligand complexes: crystal-structure analysis of Factor Xa bound to a quaternary ammonium ion ligand, *Angew Chem Int Ed Engl 44*, 4400-4404.
64. Bajaj, S. P., Schmidt, A. E., Agah, S., Bajaj, M. S., and Padmanabhan, K. (2006) High Resolution Structures of p-Aminobenzamidine- and Benzamidine-VIIa/Soluble Tissue Factor: UNPREDICTED CONFORMATION OF THE 192-193 PEPTIDE BOND AND MAPPING OF Ca2+, Mg2+, Na+, AND Zn2+ SITES IN FACTOR VIIa., *J. Biol. Chem. 281*, 24873-24888.
65. Schmidt, A. E., Padmanabhan, K., Underwood, M. C., Bode, W., Mather, T., and Bajaj, S. P. (2002) Thermodynamic linkage between the S1 site, the Na+ site, and the Ca2+ site in the protease domain of human activated protein C (APC). Sodium ion in the APC crystal structure is coordinated to four carbonyl groups from two separate loops, *J Biol Chem 277*, 28987-28995.
66. Pineda, A. O., Carrell, C. J., Bush, L. A., Prasad, S., Caccia, S., Chen, Z. W., Mathews, F. S., and Di Cera, E. (2004) Molecular dissection of Na+ binding to thrombin., *J Biol Chem 279*, 31842-31853.

CHAPTER II

Rapid Kinetics of Na^+ Binding to Thrombin

THE JOURNAL OF BIOLOGICAL CHEMISTRY VOL. 281, NO. 52, pp. 40049–40056, December 29, 2006

Rapid Kinetics of Na^+ Binding to Thrombin*[S]

Received for publication, September 6, 2006, and in revised form, October 30, 2006 Published, JBC Papers in Press, October 30, 2006, DOI 10.1074/jbc.M608600200

Alaji Bah, Laura C. Garvey, Jingping Ge, and Enrico Di Cera[1]

From the Department of Biochemistry and Molecular Biophysics, Washington University School of Medicine, St. Louis, Missouri 63110

The kinetic mechanism of Na^+ binding to thrombin was resolved by stopped-flow measurements of intrinsic fluorescence. Na^+ binds to thrombin in a two-step mechanism with a rapid phase occurring within the dead time of the spectrometer (<0.5 ms) followed by a single-exponential slow phase whose k_{obs} decreases hyperbolically with increasing [Na^+]. The rapid phase is due to Na^+ binding to the enzyme *E* to generate the *E*:Na^+ form. The slow phase is due to the interconversion between *E and *E*, where *E** is a form that cannot bind Na^+. Temperature studies in the range from 5 to 35 °C show significant enthalpy, entropy, and heat capacity changes associated with both Na^+ binding and the *E* to *E** transition. As a result, under conditions of physiologic temperature and salt concentrations, the *E** form is negligibly populated (<1%) and thrombin is almost equally partitioned between the *E* (40%) and *E*:Na^+ (60%) forms. Single-site Phe mutations of all nine Trp residues of thrombin enabled assignment of the fluorescence changes induced by Na^+ binding mainly to Trp-141 and Trp-215, and to a lesser extent to Trp-148, Trp-207, and Trp-237. However, the fast phase of fluorescence increase is influenced to different extents by all Trp residues. The distribution of these residues over the entire thrombin surface demonstrates that Na^+ binding induces long-range effects on the structure of the enzyme as a whole, contrary to the conclusions drawn from recent structural studies. These findings elucidate the mechanism of Na^+ binding to thrombin and are relevant to other clotting factors and enzymes allosterically activated by monovalent cations.**

Numerous enzymes with widely different functions, structures, and mechanisms require a monovalent cation (M^+) for optimal catalytic activity (1–3). In practically all cases reported to date, M^+ activation is mediated by Na^+ or K^+ with high selectivity (3, 4). Remarkable progress has been made during the past decade in the structural characterization of such enzymes. Structural studies have uncovered two basic mechanisms of activation, one in which M^+ functions as a cofactor by bridging atoms of the protein and substrate in the active site and another in which M^+ binds away from substrate and influences recognition and catalysis through an allosteric mechanism. A simple classification of M^+-activated enzymes has been proposed recently by merging information from kinetic and structural studies (3). The classification groups enzymes based on their M^+ specificity (Na^+ or K^+) and the mechanism of activation, cofactor-like (Type I) or allosteric (Type II).

Among Na^+-activated Type II enzymes, thrombin has been studied in considerable detail both functionally and structurally (5–7). Na^+ binds near the primary specificity pocket, nestled between the 186 and 220 loops (8, 9), and is required for efficient cleavage of the procoagulant factors fibrinogen (10), factors V (11), VIII (12), XI (13), and the prothrombotic factor PAR1 (14), but not for activation of the anticoagulant protein C (10, 15). Hence, Na^+ binding to thrombin controls key reactions responsible for the initiation, amplification, and feedback inhibition of the coagulation cascade (16) as well as platelet aggregation (7). Indeed, several naturally occurring mutations of the prothrombin gene, like prothrombin Frankfurt (17), Salakta (18), Greenville (19), Scranton (20), Copenhagen (21), and Saint Denis (22), affect residues responsible for Na^+ binding (9) and are often associated with bleeding. Furthermore, thrombin can be engineered for optimal anticoagulant activity *in vitro* and *in vivo* by mutating residues linked to Na^+ binding (15, 23–26).

Thrombin and a few other M^+-activated enzymes like Trp synthase (27, 28), pyruvate kinase (29, 30), Hsc70 (31), β-galactosidase (32, 33), and inosine monophosphate dehydrogenase (34) have been the subject of detailed treatments of the kinetics of M^+ activation. At steady state, Na^+ promotes diffusion into the active site and acylation of substrate by thrombin (35–37). The binding affinity is relatively weak, with a K_d in the millimolar range (35) as found for many other M^+-activated enzymes (1–4), and changes significantly with temperature (38–40). However, the kinetics of M^+ binding to M^+-activated enzymes in general remain for the most part unexplored due to the difficulty of resolving rate constants for reactions that likely occur on a very fast time scale (4). In the case of thrombin, earlier studies have suggested that Na^+ binds in a two-step mechanism with a fast phase occurring within the dead time of the spectrometer (2 ms), followed by a slow phase in the 30-ms time scale at 5 °C (41). In the present study, we revisit these earlier observations and address the kinetic mechanism of Na^+ binding to thrombin in more detail. We identify the Trp residues responsible for the spectral changes and the precise mechanism that gives rise to the two-step components of Na^+ binding.

MATERIALS AND METHODS

Site-directed mutagenesis of human thrombin was carried out in a HPC4-modified pNUT expression vector (15, 42), using the QuikChange site-directed mutagenesis kit from Stratagene

* This work was supported in part by National Institutes of Health Grants HL49413, HL58141, and HL73813. The costs of publication of this article were defrayed in part by the payment of page charges. This article must therefore be hereby marked "*advertisement*" in accordance with 18 U.S.C. Section 1734 solely to indicate this fact.

[S] The on-line version of this article (available at http://www.jbc.org) contains supplemental Figs. S1 and S2.

[1] To whom correspondence should be addressed. Tel.: 314-362-4185; Fax: 314-747-5354; E-mail: enrico@wustl.edu.

(La Jolla, CA) as described (9, 39). Expression of thrombin mutants was carried out in baby hamster kidney cells. Mutants were activated with the prothrombinase complex between 40 and 60 min at 37 °C. Enzymes used in the activation were from Enzyme Research (South Bend, IN). Mutants were purified to homogeneity by fast protein liquid chromatography using Resource Q and S columns with a linear gradient from 0.05 to 0.5 M choline chloride (ChCl), 5 mM MES, pH 6, at room temperature. Active site concentrations were determined by titration with hirudin (43). All nine Trp residues of thrombin were mutated to Phe by single-site substitutions. The conservative replacement did not change the kinetic properties of the constructs, which retained activity toward substrates and Na^+ activation comparable with wild-type (data not shown). Murine thrombin was prepared as reported elsewhere (44).

Stopped-flow fluorescence measurements of Na^+ binding to thrombin were carried out with an Applied Photophysics SX20 spectrometer, using an excitation of 280 nm and a cutoff filter at 305 nm. Samples of thrombin at a final concentration of 50 nM were mixed 1:1 with 60-μl solutions of the same buffer (5 mM Tris, 0.1% polyethylene glycol (PEG),[2] pH 8.0, at 15 °C) containing variable amounts of NaCl (up to 400 mM) kept at constant ionic strength of 400 mM with ChCl. The baseline was measured with 400 mM ChCl in the mixing syringe. Each trace was determined in quadruplicate. Na^+ binding studies were carried out for wild-type thrombin in the temperature range 5–35 °C. The pH was precisely adjusted at room temperature to obtain the value of 8.0 at the desired temperature. Tris buffer has a pK_a of 8.06 at 25 °C and a temperature coefficient of $\Delta pK_a/\Delta T$ of −0.027 (45). These properties ensured buffering over the entire temperature range examined.

The fluorescence increase observed upon Na^+ binding has an initial rapid phase that cannot be resolved within the dead time (<0.5 ms) of the spectrometer, followed by a single exponential slow phase with a k_{obs} that decreases as $[Na^+]$ increases (see "Results"). The total change in fluorescence calculated from the sum of the amplitudes of the fast and slow phases coincides with the value of F determined by equilibrium measurements of intrinsic fluorescence. The value of F as a function of $[Na^+]$ was fit according to Equation 1 (39)

$$F = \frac{F_0 + F_1 K_{app}[Na^+]}{1 + K_{app}[Na^+]} \quad \text{(Eq. 1)}$$

where F_0 and F_1 are the values of F in the absence and under saturating $[Na^+]$ and K_{app} is the apparent equilibrium association constant for Na^+ binding (see below). The value of F_0 corresponds to the base-line reading.

The simplest kinetic scheme accounting for the two-step mechanism of Na^+ binding detected by stopped-flow measurements is given by Scheme 1.

$$E^* \underset{k_1}{\overset{k_{-1}}{\rightleftharpoons}} E \overset{K_A}{\Leftrightarrow} E{:}Na^+$$

SCHEME 1

The free enzyme exists in equilibrium between two forms, E^* and E, that interconvert with kinetic rate constants k_1 and k_{-1}. Of these forms, only E can interact with Na^+ with an equilibrium association constant K_A to generate the E:Na^+ form. The fast phase detected by rapid kinetics is due to the binding of Na^+ to E to generate E:Na^+. Analysis of the fast phase was carried out according to Equation 2, which is analogous to Equation 1,

$$F = \frac{F_0 + F_i K_A[Na^+]}{1 + K_A[Na^+]} \quad \text{(Eq. 2)}$$

where F_i is the value of F under saturating $[Na^+]$ ($F_i < F_1$) and K_A is the intrinsic equilibrium association constant for Na^+ binding. The slow phase is due to the interconversion between E^* and E with an observed rate constant as shown in Equation 3.

$$k_{obs} = k_1 + k_{-1}\frac{1}{1 + K_A[Na^+]} \quad \text{(Eq. 3)}$$

The value of k_{obs} is expected to decrease with increasing $[Na^+]$ from $k_1 + k_{-1}$ ($[Na^+] = 0$) to k_1 ($[Na^+] = \infty$). Analysis of k_{obs} yields k_1, k_{-1}, and a value of K_A that is independent from that derived from analysis of the amplitude of the fast phase according to Equation 2. In the event of a mutation that abrogates the fast phase, the effect of Na^+ binding can still be detected from measurements of k_{obs} (see "Results"). The alternative two-step mechanism as shown in Scheme 2

$$E \overset{K_A}{\Leftrightarrow} E{:}Na^+ \underset{k_1}{\overset{k_{-1}}{\rightleftharpoons}} E^*{:}Na^+$$

SCHEME 2

where a slow isomerization follows the rapid binding of Na^+ leads to an observed rate constant as shown in Equation 4.

$$k_{obs} = k_{-1} + k_1\frac{K_A[Na^+]}{1 + K_A[Na^+]} \quad \text{(Eq. 4)}$$

In this case, the value of k_{obs} is expected to increase with increasing $[Na^+]$ from k_{-1} ($[Na^+] = 0$) to $k_1 + k_{-1}$ ($[Na^+] = \infty$). Hence, the dependence of k_{obs} on $[Na^+]$ is of diagnostic value and rules out Scheme 2 in favor of Scheme 1 (see "Results").

There is a relationship between the *apparent* equilibrium association constant K_{app} derived from Equation 1 and the *intrinsic* equilibrium association constant K_A derived from Equation 2 or 3. The value of K_{app} can also be derived from equilibrium titrations of intrinsic fluorescence (35, 39–41, 46, 47) or linkage studies (38, 46, 48). The value of K_A, on the other hand, can only be derived from rapid kinetic studies. Because of the presence of E, E^*, and E:Na^+ in Scheme 1, at equilibrium one has (49) Equation 5.

$$K_{app} = \frac{K_A}{1 + \frac{k_{-1}}{k_1}} = \frac{K_A}{1 + r} \quad \text{(Eq. 5)}$$

The parameter $r = [E^*]/[E]$ measures the population of E^* relative to E. Under conditions where $r \ll 1$ and the free form is

[2] The abbreviations used are: PEG, polyethylene glycol; MES, 4-morpholineethanesulfonic acid.

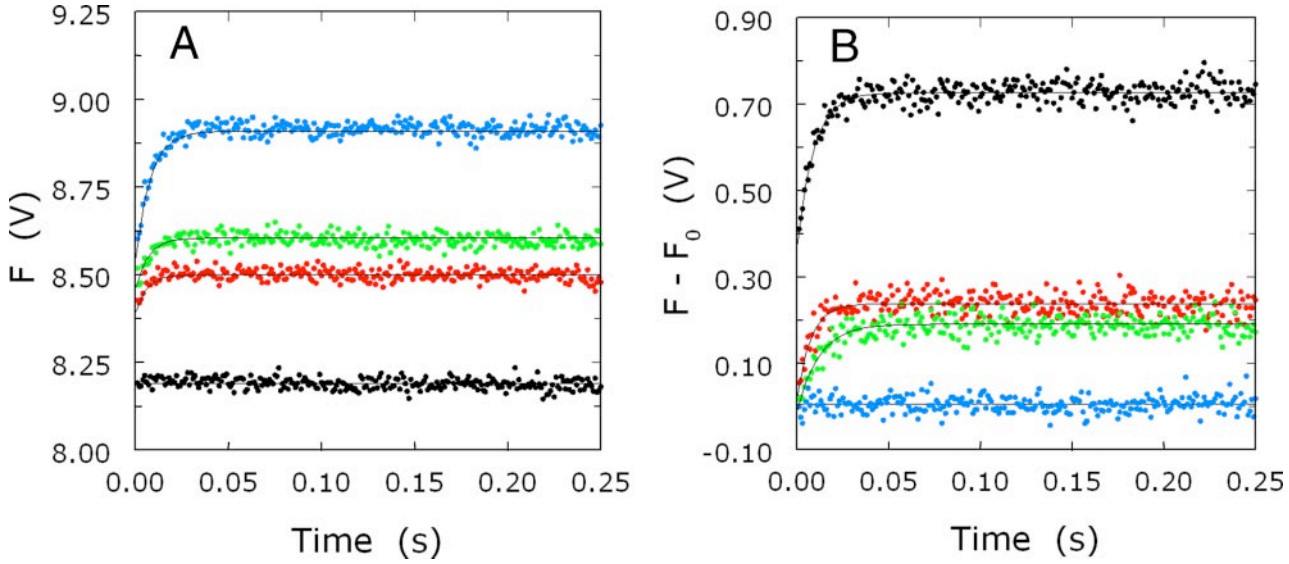

FIGURE 1. *A*, kinetic traces of Na^+ binding to human thrombin in the 0–250-ms time scale. Shown are the traces obtained at 0 (*black circles*), 5 (*red circles*), 10 (*green circles*), and 50 (*blue circles*) mM Na^+. Notice how the binding of Na^+ obeys a two-step mechanism, with a fast phase completed within the dead time (<0.5 ms) of the spectrometer, followed by a single-exponential slow phase. The k_{obs} for the slow phase decreases with increasing [Na^+] (see also Fig. 2), as is evident from the plot. Experimental conditions were 50 nM thrombin, 5 mM Tris, 0.1% PEG, pH 8.0, at 15 °C. The [Na^+] was changed by keeping the ionic strength constant at 400 mM with ChCl. Continuous lines were drawn using the expression $a\{1 - \exp(-k_{obs}t)\} + b$ with best-fit parameter values: *black circles*, $a = 0 \pm 0$ V, $k_{obs} = 0 \pm 0\ s^{-1}$, $b = 8.19 \pm 0.01$ V; *red circles*, $a = 0.11 \pm 0.02$ V, $k_{obs} = 170 \pm 10\ s^{-1}$, $b = 8.39 \pm 0.02$ V; *green circles*, $a = 0.15 \pm 0.02$ V, $k_{obs} = 150 \pm 10\ s^{-1}$, $b = 8.46 \pm 0.02$ V; *blue circles*, $a = 0.37 \pm 0.01$ V, $k_{obs} = 130 \pm 10\ s^{-1}$, $b = 8.54 \pm 0.01$ V. *B*, kinetic traces of Na^+ binding to thrombin wild type and mutants in the 0–250-ms time scale expressed relative to the base-line value F_0 to enable comparison. Shown are the traces obtained at 200 mM Na^+ for human thrombin (*black circles*), mutants W141F (*red circles*), and W215F (*green circles*). Also shown, as a control, is the trace obtained at 200 mM Na^+ for murine thrombin (*blue circles*), which is devoid of Na^+ activation. Notice how mutation of Trp-141 and Trp-215 essentially abolishes the fast phase seen in the wild type (see *panel A*) and reduces significantly the total fluorescence change associated with Na^+ binding (see also Fig. 3 and Table 2). Experimental conditions were 50 nM thrombin, 5 mM Tris, 0.1% PEG, pH 8.0, at 15 °C. Continuous lines were drawn using the expression $a\{1 - \exp(-k_{obs}t)\}$ with best-fit parameter values: *black circles*, $a = 0.36 \pm 0.02$ V, $k_{obs} = 111 \pm 7\ s^{-1}$, $b = 0.37 \pm 0.02$ V; *red circles*, $a = 0.21 \pm 0.02$ V, $k_{obs} = 84 \pm 8\ s^{-1}$, $b = 0.02 \pm 0.02$ V; *green circles*, $a = 0.20 \pm 0.01$ V, $k_{obs} = 130 \pm 10\ s^{-1}$, $b = -0.01 \pm 0.01$ V; *blue circles*, $a = 0 \pm 0$ V, $k_{obs} = 0 \pm 0\ s^{-1}$, $b = 0.00 \pm 0.01$ V.

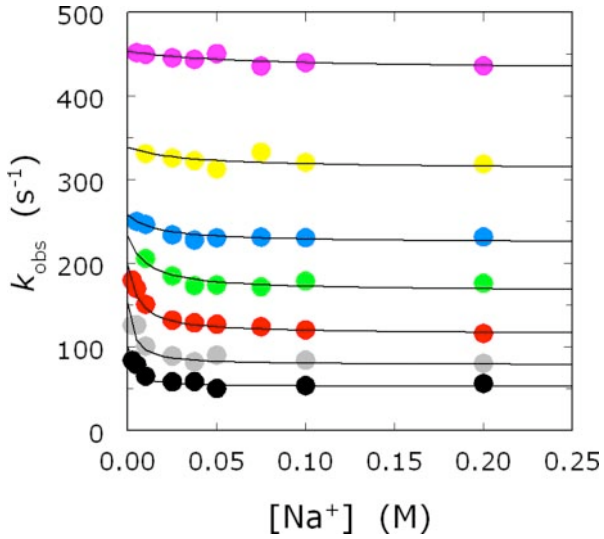

FIGURE 2. **Values of k_{obs} for the slow phase of fluorescence increase due to Na^+ binding to thrombin (see Fig. 1) as a function of [Na^+] in the temperature range 5–35 °C.** Shown are the results pertaining to 5 (*black circles*), 10 (*gray circles*), 15 (*red circles*), 20 (*green circles*), 25 (*blue circles*), 30 (*yellow circles*), and 35 (*magenta circles*) °C. Experimental conditions were 50 nM thrombin, 5 mM Tris, 0.1% PEG, pH 8.0. The [Na^+] was changed by keeping the ionic strength constant at 400 mM with ChCl. Continuous lines were drawn according to Equation 3 under "Materials and Methods" with best-fit parameter values listed in Table 1.

essentially all *E*, the value of K_{app} coincides with K_A. However, under conditions where *r* is significant, a sizable fraction of free thrombin exists in the *E** form and the value of K_{app} underestimates the true Na^+ binding affinity K_A. Hence, it is very important to know how *r* changes under conditions of interest to correctly interpret Na^+ binding in terms of the process that converts *E* to *E*:Na^+.

The temperature dependence of K_{app}, K_A, and *r* yields the thermodynamic parameters associated with the underlying processes according to Equation 6 (39)

$$-\ln K = \frac{\Delta H_0}{R}\frac{1}{T} - \frac{\Delta S_0}{R} + \frac{\Delta C_P}{R}\left(1 - \frac{T_0}{T} - \ln\frac{T}{T_0}\right) \qquad \text{(Eq. 6)}$$

where *K* is K_{app}, K_A, or *r*, ΔH_0 and ΔS_0 are the enthalpy and entropy changes at the reference temperature $T_0 = 298.15$ K, ΔC_P is the heat capacity change, *R* the gas constant, *T* the absolute temperature. The van't Hoff plot of $-\ln K$ *versus* $1/T$ is linear when $\Delta C_P = 0$ and curves upward when $\Delta C_P < 0$.

RESULTS

Na^+ binding to human thrombin gives rise to a significant increase in intrinsic fluorescence (35, 39–41, 46, 47). The change occurs in two steps, clearly revealed by stopped-flow measurements (Fig. 1*A*). A fast phase, whose amplitude increases with [Na^+], occurs within the dead time of the spectrometer (<0.5 ms) and is followed by a single-exponential slow phase whose k_{obs} decreases with increasing [Na^+]. Control experiments run with murine thrombin, an enzyme devoid of Na^+ activation (44), show no change in fluorescence even at 200 mM Na^+ (Fig. 1*B*). The dependence of k_{obs} on [Na^+] is hyperbolic (Fig. 2) and is consistent with the mechanism

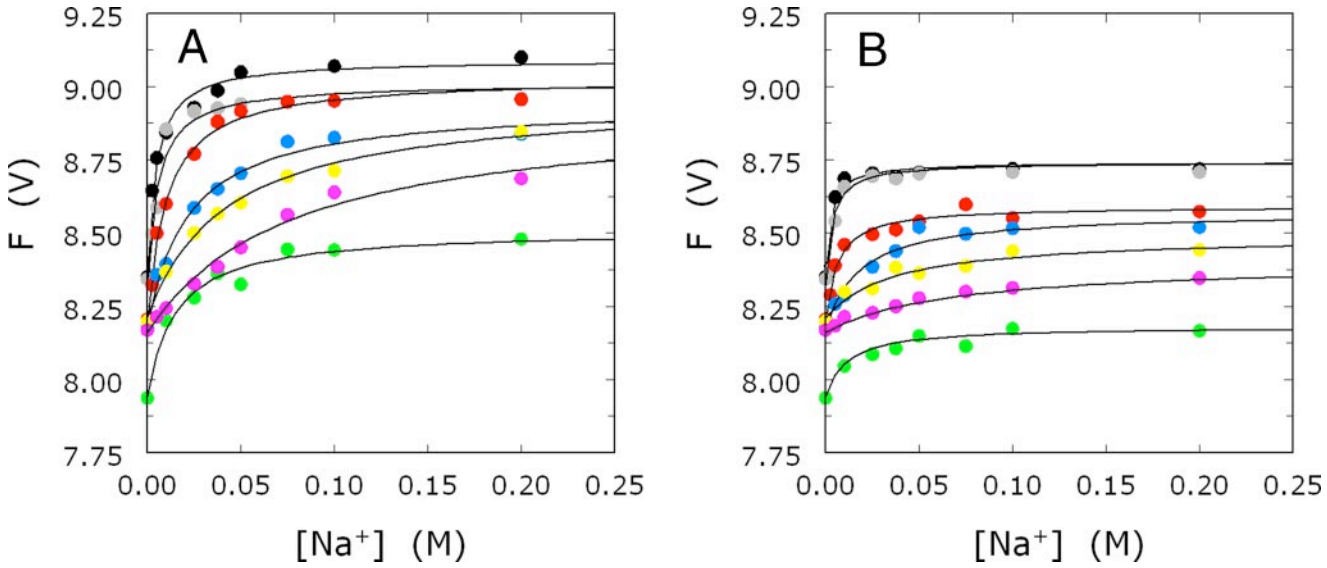

FIGURE 3. *A*, Na^+ binding curves of thrombin obtained from the total change in intrinsic fluorescence measured as the sum of the amplitudes of the fast and slow phases determined by stopped-flow kinetics (see Fig. 1). Shown are the results pertaining to 5 (*black circles*), 10 (*gray circles*), 15 (*red circles*), 20 (*green circles*), 25 (*blue circles*), 30 (*yellow circles*), and 35 (*magenta circles*) °C. Experimental conditions were 50 nM thrombin, 5 mM Tris, 0.1% PEG, pH 8.0. The [Na^+] was changed by keeping the ionic strength constant at 400 mM with ChCl. Continuous lines were drawn according to Equation 1 under "Materials and Methods", with best-fit parameter values listed in Table 1. *B*, Na^+ binding curves of thrombin obtained from the amplitude of the fast phase of fluorescence increase determined by stopped-flow kinetics (see Fig. 1). Shown are the results pertaining to 5 (*black circles*), 10 (*gray circles*), 15 (*red circles*), 20 (*green circles*), 25 (*blue circles*), 30 (*yellow circles*), and 35 (*magenta circles*) °C. Experimental conditions were 50 nM thrombin, 5 mM Tris, 0.1% PEG, pH 8.0. The [Na^+] was changed by keeping the ionic strength constant at 400 mM with ChCl. Continuous lines were drawn according to Equation 2 under "Materials and Methods" with best-fit parameter values listed in Table 1.

TABLE 1

Fluorescence and Na^+ binding parameters for wild-type thrombin as a function of temperature

The parameters F_0, F_i, and F_1 defining $\Delta F_i = F_i - F_0$ and $\Delta F_t = F_1 - F_0$ were derived from analysis of the data in Fig. 3, *A* and *B*, using Equations 1 and 2 under "Materials and Methods." The values of K_{app} were derived from analysis of the data in Fig. 3*A* according to Equation 1. The values of K_A were derived from analysis of the data in Fig. 3*B* according to Equation 2, and Fig. 2 according to Equation 3, together with the values of k_1 and k_{-1}. *r* is the ratio k_{-1}/k_1. Note how the values of K_{app} and K_A obtained independently obey Equation 5 under "Materials and Methods."

T	F_0	F_i	F_1	$\Delta F_i/F_0$	$\Delta F_t/F_0$	K_{app}	K_A	k_1	k_{-1}	*r*
°C	*V*	*V*	*V*	%	%	M^{-1}	M^{-1}	s^{-1}	s^{-1}	
5	8.36 ± 0.02	8.74 ± 0.02	9.09 ± 0.02	4.5	8.7	220 ± 20	370 ± 40	52 ± 2	48 ± 2	0.92
10	8.32 ± 0.03	8.74 ± 0.03	9.01 ± 0.03	5.0	8.3	180 ± 20	300 ± 40	78 ± 4	75 ± 4	0.96
15	8.19 ± 0.01	8.59 ± 0.02	9.03 ± 0.01	4.9	10.3	100 ± 10	160 ± 20	115 ± 3	83 ± 6	0.72
20	7.94 ± 0.03	8.18 ± 0.03	8.51 ± 0.03	3.0	7.1	68 ± 7	90 ± 9	166 ± 4	65 ± 8	0.39
25	8.18 ± 0.03	8.57 ± 0.03	8.94 ± 0.03	4.8	9.3	46 ± 5	57 ± 4	224 ± 4	34 ± 4	0.15
30	8.21 ± 0.02	8.49 ± 0.02	8.96 ± 0.02	3.4	9.1	24 ± 2	28 ± 2	312 ± 4	27 ± 8	0.086
35	8.16 ± 0.02	8.40 ± 0.02	8.93 ± 0.02	2.9	9.4	13 ± 1	15 ± 1	431 ± 10	23 ± 4	0.053

depicted in Scheme 1 and Equation 3. That supports the conclusion that, in the absence of Na^+, thrombin exists in equilibrium between two conformations, *E** and *E*, and that only *E* can be converted to the *E*:Na^+ form. The binding of Na^+ to *E* gives rise to the fast phase. The slow phase detected by stopped-flow measurements is the result of the interconversion between *E** and *E* that takes place on a time scale of milliseconds.

The sum of the amplitudes of the slow and fast phases changes hyperbolically with [Na^+] (Fig. 3*A*) and recapitulates the behavior observed by intrinsic fluorescence measurements at equilibrium (35, 39–41, 46, 47). Analysis of such curves in the temperature range 5–35 °C enables determination of K_{app} from Equation 1 (Table 1). A van't Hoff plot of the K_{app} values is shown in Fig. 4 and reveals a curvature conducive to the presence of a heat capacity change of −500 cal/mol/K, consistent with previous results (38–40). Analysis of the amplitude of the fast phase as a function of [Na^+] (Fig. 3*B*) according to Equation 2 enables the determination of K_A (Table 1). These values of K_A are practically identical to those derived independently from analysis of k_{obs} as a function of [Na^+] according to Equation 3 (Fig. 2), which also enables resolution of k_1 and k_{-1} (Table 1). The van't Hoff plot of the K_A values is curved, as for K_{app}, due to a heat capacity change of −500 cal/mol/K (Fig. 4). This proves that the heat capacity change reported previously for the values of K_{app} (38–40) reflects an intrinsic property of Na^+ binding to thrombin and is not the result of the pre-existing equilibrium between *E* and *E**. In fact, from the definition of K_{app} in Equation 5, it can be seen that the *E*-*E** equilibrium gives rise to an apparent heat capacity change when the value of *r* changes with temperature, even if no heat capacity change is associated with K_A and/or *r*. The direct determination of K_A from rapid kinetic data resolves the transition from *E* to *E*:Na^+ in Scheme 1 and decouples this process from the linked equilibrium between *E* and *E**. The temperature dependence of K_A then offers direct validation of the heat capacity change associated with Na^+ binding as a basic thermodynamic property of thrombin (38–40).

Binding of Na^+ is characterized by a large enthalpy change of

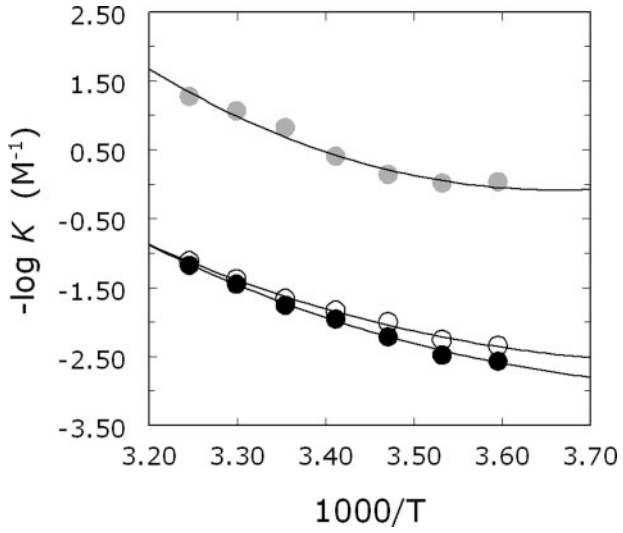

FIGURE 4. **van't Hoff plots of Na^+ binding to thrombin.** Shown are the values of K_{app} (*open circles*) and K_A (*black circles*) obtained from stopped-flow kinetics in the temperature range 5–35 °C (see Table 1). The plot is curved in both cases, signaling the presence of a heat capacity change. Also shown is the temperature dependence of $-\log r$ (*gray circles*, dimensionless units), measuring the equilibrium between *E* and *E** in Scheme 1 (see Table 1). This parameter too is associated with significant curvature in the plot, signaling a large heat capacity change. Experimental conditions were 5 mM Tris, 0.1% PEG, pH 8.0. Continuous lines were drawn according to Equation 6 under "Materials and Methods" with best-fit parameter values: *open circles*, $\Delta H_0 = -18.9 \pm 0.9$ kcal/mol, $\Delta S_0 = -56 \pm 3$ cal/mol/K, $\Delta C_P = -500 \pm 100$ cal/mol/K; *black circles*, $\Delta H_0 = -21.5 \pm 0.9$ kcal/mol, $\Delta S_0 = -64 \pm 3$ cal/mol/K, $\Delta C_P = -500 \pm 100$ cal/mol/K; *gray circles*, $\Delta H_0 = -23 \pm 2$ kcal/mol, $\Delta S_0 = -81 \pm 8$ cal/mol/K, $\Delta C_P = -900 \pm 300$ cal/mol/K.

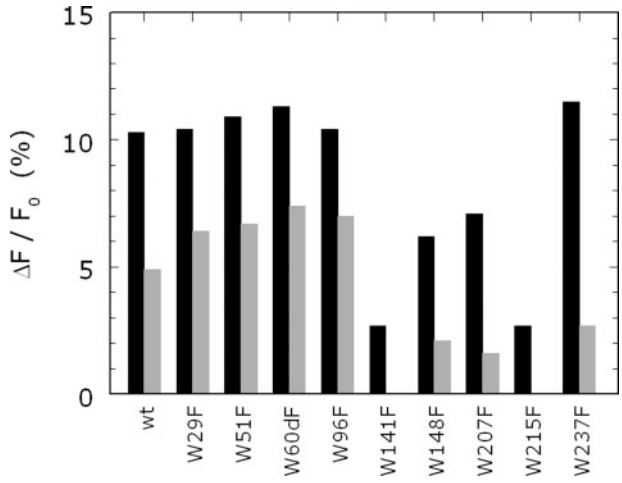

FIGURE 5. **Fluorescence change induced by Na^+ binding to wild type and the Phe mutants of all nine Trp residues of human thrombin.** Shown are the values listed in Table 2 for the total change in intrinsic fluorescence measured as $F_1 - F_0$ (*black bars*) or the amplitude of the fast phase measured as $F_i - F_0$ (*gray bars*). All values are expressed as % change relative to F_0. Experimental conditions were 50 nM thrombin, 5 mM Tris, 0.1% PEG, pH 8.0, at 15 °C. The [Na^+] was changed by keeping the ionic strength constant at 400 mM with ChCl.

−22 kcal/mol that is compensated by a large entropy loss of −64 cal/mol/K (Fig. 4). The enthalpy change is due to formation of the six ligating interactions in the coordination shell that also involve four buried water molecules (3, 4, 9). The entropy change reflects the uptake and ordering of water molecules within the channel embedding the primary specificity pocket and the active site linked to the occupancy of the Na^+ site (9). As a result of the enthalpy-entropy energetic compensation, the binding affinity of Na^+ is relatively weak (K_d in the mM range), as seen for many other M^+-activated enzymes (3, 4). An important consequence of the large enthalpy change is that the value of K_A becomes only about 10 M^{-1} at 37 °C, which implies that under physiologic conditions of temperature and [NaCl] = 140 mM thrombin is only 60% bound to Na^+, as first documented in 1992 (35). This makes thrombin optimally poised for allosteric regulation *in vivo*, where the Na^+-bound and Na^+-free forms are targeted toward procoagulant and anticoagulant roles, respectively (7, 10).

It is of particular importance to structurally assign the spectral changes linked to Na^+ binding to thrombin. Trp-215 in the aryl binding site has been identified as a major fluorophore responsible for the spectral change (48), but a rigorous test of the contribution of all nine Trp residues of thrombin has not been carried out. Previous studies investigated the role of Trp-60d, Trp-96, Trp-148, Trp-207, and Trp-215 with Phe substitutions, but the analysis involved the activity toward thrombin substrates and not Na^+ binding (50). Fig. 5 shows the fluorescence enhancement due to Na^+ binding for the Phe mutants of all nine Trp residues of thrombin. The Phe mutations of the nine Trp residues of thrombin cause few, if any, changes in the kinetic and equilibrium properties of the enzyme toward Na^+ (Table 2). The Trp → Phe substitution therefore provides an optimal adiabatic perturbation of the indole moiety and probes selectively the changes monitored by fluorescence spectroscopy. The data in Fig. 5 refer to the total fluorescence change, $F_1 - F_0$ in Equation 1 (*black bars*) or the amplitude of the fast phase, $F_i - F_0$ in Equation 2 (*gray bars*), both relative to the base-line value F_0. The 10% total increase in fluorescence observed for wild type is retained by five Trp mutants, namely, W29F, W51F, W60dF, W96F, and W237F. Two mutants, W148F and W207F, experience >30% loss in total fluorescence change. On the other hand, W141F and W215F lose >70% of the total fluorescence change. Inspection of the fast component of the fluorescence change is even more informative. This phase monitors directly Na^+ binding to *E* to generate the *E*:Na^+ form. In the wild type, the amplitude of the fast phase, $F_i - F_0$ (see Table 1 and Figs. 1*B* and 3*B*), is about half the amplitude of the total fluorescence change, $F_1 - F_0$ (see Table 1 and Figs. 1*A* and 3*A*). The amplitude of the fast phase is perturbed in all Trp mutants, even when the total fluorescence change is the same as for wild type (Figs. 1 and 5). Because Trp residues are distributed over the entire structure of thrombin, and their distance from the bound Na^+ ranges from 13 (Trp-215) to 35 (Trp-51) Å, binding of Na^+ to *E* likely elicits effects well beyond the immediate environment of the Na^+ site and perturbs the structure of thrombin as a whole. This is in agreement with recent functional mapping of the Na^+-induced allosteric transition of thrombin (51). The amplitude of the fast phase increases significantly relative to wild type for the W29F, W51F, W60dF, and W96F mutants. On the other hand, the amplitude decreases significantly for W148F, W207F, and W237F and completely disappears for W141F and W215F. Hence, Trp-215 but also Trp-141 are major reporters of the process of Na^+ binding to thrombin. Trp-148, Trp-207, and Trp-237 also contribute to

TABLE 2
Fluorescence and Na^+ binding parameters for wild-type thrombin and mutants

	F_o	F_i	F_1	$\Delta F_i/F_o$	$\Delta F_1/F_o$	K_{app}	K_A	k_1	k_{-1}	r	D^a
	V	*V*	*V*	%	%	M^{-1}	M^{-1}	s^{-1}	s^{-1}		Å
wt	8.19 ± 0.01	8.59 ± 0.02	9.03 ± 0.01	4.9	10.3	100 ± 10	160 ± 20	115 ± 3	83 ± 6	0.72	
W29F	8.17 ± 0.02	8.69 ± 0.02	9.02 ± 0.02	6.4	10.4	58 ± 6	85 ± 7	126 ± 4	74 ± 4	0.59	24
W51F	8.15 ± 0.01	8.70 ± 0.02	9.04 ± 0.01	6.7	10.9	100 ± 10	170 ± 30	114 ± 3	87 ± 6	0.76	35
W60dF	8.13 ± 0.01	8.73 ± 0.03	9.05 ± 0.01	7.4	11.3	89 ± 6	140 ± 10	132 ± 2	77 ± 9	0.58	21
W96F	8.13 ± 0.03	8.70 ± 0.03	8.98 ± 0.03	7.0	10.4	70 ± 10	110 ± 10	133 ± 2	69 ± 2	0.52	27
W141F	8.02 ± 0.01	8.02 ± 0.01	8.24 ± 0.01	0.0	2.7	110 ± 10	170 ± 10	79 ± 1	40 ± 9	0.51	23
W148F	8.18 ± 0.02	8.35 ± 0.02	8.69 ± 0.02	2.1	6.2	81 ± 8	130 ± 10	95 ± 2	72 ± 4	0.76	21
W207F	8.15 ± 0.01	8.28 ± 0.02	8.73 ± 0.01	1.6	7.1	120 ± 10	190 ± 10	89 ± 2	78 ± 2	0.88	23
W215F	8.12 ± 0.01	8.12 ± 0.01	8.34 ± 0.01	0.0	2.7	59 ± 8	110 ± 10	118 ± 3	81 ± 7	0.69	13
W237F	8.14 ± 0.02	8.36 ± 0.01	9.08 ± 0.01	2.7	11.5	110 ± 10	170 ± 10	101 ± 2	68 ± 3	0.67	30

[a] Distance from the Cε2 atom of the Trp residue to the bound Na^+ in the crystal structure of the Na^+-bound form 1SG8 (9). All parameters were derived as shown in Table I. Note how the values of K_{app} and K_A obtained independently obey Equation 5 under "Materials and Methods."

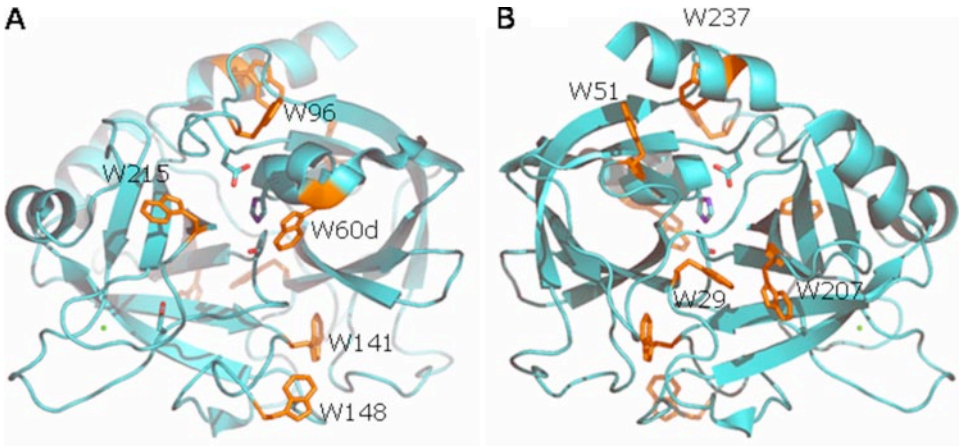

FIGURE 6. ***Ribbon plot* of thrombin in the Na^+-bound form, portraying the structure 1SG8 (9) with the active site in the front (*A*) or rotated 180° along the *y*-axis (*B*).** Shown are the side chains of the catalytic residues His-57, Asp-102, and Ser-195 and the side chain of Asp-189. Na^+ is rendered as a *green ball*. The nine Trp residues of the enzyme are shown with their side chains in *orange*. The contribution of these residues to the fluorescence change induced by Na^+ binding is shown in Fig. 5 and Table 2. The A chain was removed for clarity.

the spectral change, whereas Trp-29, Trp-51, Trp60d, and Trp-96 produce changes that oppose those of the other fluorophores because their replacement to Phe actually enhances the fluorescence change due to Na^+ binding.

DISCUSSION

The results presented here expand and clarify the scenario offered by the only previous investigation of Na^+ binding to thrombin using rapid kinetics (41). The earlier study was carried out at 5 °C and ionic strength values of 0.3 and 2.0 M, using 500 nM thrombin. Two phases were identified, as shown in Fig. 1*A*, but no dependence of k_{obs} on [Na^+] could be detected below 500 mM [Na^+]. This made interpretation of the results particularly cumbersome and did not support the use of simple mechanisms like Scheme 1 or Scheme 2. The study, however, uncovered the pre-existing equilibrium between *E* and *E** as depicted in Scheme 1. There are several reasons why our results, and especially the dependence of k_{obs} on [Na^+], differ in part from those reported previously. The SX20 spectrometer is a much improved version of the SX17 model used previously (41) and features a shorter dead time and higher signal resolution and stability. The thrombin concentration used in our measurements (50 nM) did not result in any photobleaching, thereby eliminating the need to correct for the effect when fitting experimental data. When using 500 nM thrombin, as in the previous study (41), we did observe significant photobleaching that affected base-line stability, reproducibility, and extent of fluorescence change (see supplemental data). When we further reduced the thrombin concentration down to 5 nM, the results lacked the optimal reproducibility observed at 50 nM. Significant photobleaching was acknowledged in the previous study (41), but not resolved. The previous study was carried out at 5 °C, where condensation in the cell is very significant and must be eliminated with constant N_2 flushing. We found that the temperature range of 15–25 °C is optimal to resolve the range of k_{obs} linked to Na^+ binding. Last, but not least, the pK_a of Tris buffer at 5 °C is 8.60 (45), which makes it problematic to buffer a solution at pH 7.4 as used in the previous study (41).

Our results add mechanistic significance to previous studies of Na^+ binding because of the use of Phe mutations of all nine Trp residues of thrombin. The fast phase of fluorescence increase directly linked to the transition from *E* to *E*:Na^+ in Scheme 1 is affected in all Phe mutants, vouching for a global effect of Na^+ binding on thrombin structure. The contributions of single Trp residues are not additive, lending support to the hypothesis that some of the environments in which they reside may be coupled allosterically. The coupling may ensure propagation of long-range effects originating at the Na^+ site via a limited number of structural conduits. Trp-141 and Trp-215 make a large contribution to the fluorescence change induced by Na^+ binding, and their mutation to Phe abrogates the fast phase completely. This implies that the environments of Trp-141 and Trp-215 change in the *E** to *E* conversion, and more drastically in the conversion of *E* to *E*:Na^+. The important role of Trp-215 has been reported before (48). This is the closest Trp residue to the bound Na^+ (13 Å) and defines most of the aryl binding site involved in substrate recognition (5, 9, 52). The importance of Trp-141 is unanticipated. However, recent structures of thrombin document a flip in the indole ring of Trp-141 in the absence of Na^+ similar to that observed for

Trp-215 (49). Trp-141 is buried in a strategic location between the autolysis loop and exosite I, and its linkage with the bound Na^+, situated 23 Å away, vouches for a pivotal role in communicating changes from the Na^+ site to exosite I (Fig. 6). Among the other residues that contribute to the fluorescence change and the fast phase, Trp-148 is located in the middle of the highly flexible autolysis loop, 21 Å away from the bound Na^+, and is 62% exposed to solvent (52), whereas Trp-207 is completely buried in the back of the catalytic chain, 23 Å away from the bound Na^+, and in hydrophobic contact with Trp-29 and residues of the A chain (Fig. 6). Because of their proximity, Trp-207 and Trp-29 may function as a single fluorophore and/or quench each other. It is interesting that the Phe mutation of Trp-29 enhances the amplitude of the fast phase, as though changes affecting Trp-207 are better reported in the absence of Trp-29. A similar scenario can be envisioned for Trp-51 and Trp-237 (Fig. 6), whose hydrophobic coupling may result in overlapping spectral effects with Trp-51 actually hindering the full response of Trp-237 to Na^+ binding. Finally, the effects seen with the highly solvent-exposed Trp-60d and Trp-96 (Fig. 6) suggest that these residues may be quite flexible and capable of probing different environments that reduce the fluorescence response to Na^+ binding.

It is of interest to correlate the new information arising from stopped-flow measurements of the mechanism of Na^+ binding to thrombin with existing structural data. The three species in Scheme 1 portray thrombin in the Na^+-free (*E* and *E**) and Na^+-bound (*E*:Na^+) forms, and the data presented here demonstrate that Na^+ binds to thrombin in a two-step mechanism consistent with Scheme 1. The activation effect of Na^+ on thrombin has very clear kinetic signatures and specifically involves an increase in k_{cat} and a decrease in K_m (35–37, 49, 53, 54). Such a "modifier" effect on k_{cat} has long been known to be of diagnostic value (55) and unequivocally proves the existence of two active forms in equilibrium, one Na^+ free with low k_{cat} and one Na^+ bound with high k_{cat} (4, 49). *E* and *E*:Na^+ in Scheme 1 are the two active forms of thrombin that account for the dependence of k_{cat} on [Na^+] and correspond to the slow (*E*) and fast (*E*:Na^+) forms originally defined by Wells and Di Cera (35). The structures of these two forms have been solved recently (9). Basic differences between them involve the orientation of Asp-189 in the primary specificity pocket, Ser-195 in the active site, and the reorganization of a water network that connects the Na^+ site to the active site Ser-195 located 16 Å away. The orientation of Asp-189 in the fast form optimizes docking of the guanidinium group of Arg at the P1 position of substrate. The Oγ atom of Ser-195 in the fast form is within H-bonding distance of the catalytic His-57. The H-bond is required for efficient catalysis (56) and is broken in the slow form. The network of water molecules ensures the long-range communication between the bound Na^+ and the active site that is at the basis of thrombin allostery. The increase in the number and ordering of water molecules linked to Na^+ binding also explains the large entropy loss and negative heat capacity change associated with this process. Unfortunately, the differences between the slow and fast forms reported recently (9) do not involve Trp residues that contribute to the spectral changes linked to Na^+ binding. Either such changes are too subtle to be unraveled under the constrained environment of a crystal lattice or available structures of the slow and/or fast forms are not representative of the full landscape of conformational transitions induced by Na^+ binding. Indeed, functional mapping of the slow → fast transition suggests a more global involvement of thrombin residues (51).

Structural assignments for the *E** form are equally problematic. In a previous study on the kinetics of Na^+ binding to thrombin, *E** was interpreted as an "inactive" slow form unable to bind Na^+ and substrate or inhibitors at the active site (41). The conclusion was drawn from data showing that the binding of inhibitors to thrombin was also linked to increases in intrinsic fluorescence and obeyed a mechanism similar to that of Na^+ binding (41). The hypothesis of *E** being an inactive conformation of the slow form, as originally suggested by Lai *et al.* (41), has gained prominence recently in the context of several structures of inactive forms of thrombin in the Na^+-free form that have appeared in the literature. These structures differ drastically from the active slow form *E* (9, 57) and share disorder or collapse of the Na^+ site and steric blockage of the active site (49, 58–61). We have recently shown (62) that these inactive structures are likely the result of mutations introduced in the enzyme (58, 59) and/or artifacts of crystal packing (49, 60, 61). A recent structure of thrombin obtained in the absence of inhibitors and salts appears to be a genuine inactive slow form, devoid of artifactual effects due to mutations in the Na^+ site or crystal packing (62). The structure has the Na^+ site obliterated by the side chain of Arg-187 and the active site occluded by the repositioning of the side chains of Trp-215 and Arg-221a. The drastic movement of Trp-215 would do justice to the dominant role played by this residue in the fluorescence changes reported in our study. However, even this structure lacks significant changes around all other Trp residues. Hence, evidence that thrombin can assume an inactive slow form under crystallographic conditions is strong (62), but the connection with the functional properties of the enzyme in solution remains weak. The kinetic signatures of Na^+ activation do not require inactive conformations of thrombin and indeed refute (4, 49) simplistic "alternative" models based on the equilibrium of active and inactive forms (61).

The data presented in this study vouch for *E** being a form of thrombin unable to bind Na^+ and not necessarily inactive toward substrates or inhibitors. In fact, a conformation of thrombin with the pore of entry to the Na^+ binding site (4, 39) occluded would fit the description of *E** and would still retain activity toward substrates and inhibitors. Whether inactive conformations of thrombin in the slow form exist in solution remains to be demonstrated by future studies of rapid kinetics involving the library of Trp mutants presented here in order to structurally assign the observed spectral changes and confirm that they have the same origin as those linked to Na^+ binding. However, even if future studies in solution prove that *E** is indeed an inactive slow form, then its possible physiologic role should be clarified. Based on the data in Fig. 5, *E** represents <1% of the population of thrombin molecules at 37 °C, which raises questions about its possible functional role *in vivo*. This conundrum does not apply to the active slow form, which contributes 40% of the thrombin molecules *in vivo* and whose anti-

coagulant role is well established (7, 10, 15). Nonetheless, *E** carries considerable mechanistic significance for Na^+ binding to thrombin and may become populated under the effect of mutations or conditions that involve allosteric effectors to be identified. In addition, *E** is an intriguing new variable to be taken into consideration when studying Na^+ binding to other clotting factors and M^+-activated enzymes.

REFERENCES

1. Suelter, C. H. (1970) *Science* **168,** 789–795
2. Evans, H. J., and Sorger, G. J. (1966) *Annu. Rev. Plant. Physiol.* **17,** 47–76
3. Di Cera, E. (2006) *J. Biol. Chem.* **281,** 1305–1308
4. Page, M. J., and Di Cera, E. (2006) *Physiol. Rev.* **86,** 1049–1092
5. Bode, W. (2006) *Blood Cells Mol. Dis.* **36,** 122–130
6. Davie, E. W., and Kulman, J. D. (2006) *Semin. Thromb. Hemostasis* **32,** Suppl. 1, 3–15
7. Di Cera, E. (2003) *Chest* **124,** 11S–17S
8. Di Cera, E., Guinto, E. R., Vindigni, A., Dang, Q. D., Ayala, Y. M., Wuyi, M., and Tulinsky, A. (1995) *J. Biol. Chem.* **270,** 22089–22092
9. Pineda, A. O., Carrell, C. J., Bush, L. A., Prasad, S., Caccia, S., Chen, Z. W., Mathews, F. S., and Di Cera, E. (2004) *J. Biol. Chem.* **279,** 31842–31853
10. Dang, O. D., Vindigni, A., and Di Cera, E. (1995) *Proc. Natl. Acad. Sci. U. S. A.* **92,** 5977–5981
11. Myles, T., Yun, T. H., Hall, S. W., and Leung, L. L. (2001) *J. Biol. Chem.* **276,** 25143–25149
12. Nogami, K., Zhou, Q., Myles, T., Leung, L. L., Wakabayashi, H., and Fay, P. J. (2005) *J. Biol. Chem.* **280,** 18476–18487
13. Yun, T. H., Baglia, F. A., Myles, T., Navaneetham, D., Lopez, J. A., Walsh, P. N., and Leung, L. L. (2003) *J. Biol. Chem.* **278,** 48112–48119
14. Ayala, Y. M., Cantwell, A. M., Rose, T., Bush, L. A., Arosio, D., and Di Cera, E. (2001) *Proteins* **45,** 107–116
15. Dang, Q. D., Guinto, E. R., and Di Cera, E. (1997) *Nat. Biotechnol.* **15,** 146–149
16. Page, M. J., and Di Cera, E. (2006) *Thromb. Haemostasis* **95,** 920–921
17. Degen, S. J., McDowell, S. A., Sparks, L. M., and Scharrer, I. (1995) *Thromb. Haemostasis* **73,** 203–209
18. Miyata, T., Aruga, R., Umeyama, H., Bezeaud, A., Guillin, M. C., and Iwanaga, S. (1992) *Biochemistry* **31,** 7457–7462
19. Henriksen, R. A., Dunham, C. K., Miller, L. D., Casey, J. T., Menke, J. B., Knupp, C. L., and Usala, S. J. (1998) *Blood* **91,** 2026–2031
20. Sun, W. Y., Smirnow, D., Jenkins, M. L., and Degen, S. J. (2001) *Thromb. Haemostasis* **85,** 651–654
21. Stanchev, h., Philips, M., Villoutreix, B. O., Aksglaede, L., Lethagen, S., and Thorsen, S. (2006) *Thromb. Haemostasis* **95,** 195–198
22. Rouy, S., Vidaud, D., Alessandri, J. L., Dautzenberg, M. D., Venisse, L., Guillin, M. C., and Bezeaud, A. (2006) *Br. J. Haematol.* **132,** 770–773
23. Gibbs, C. S., Coutre, S. E., Tsiang, M., Li, W. X., Jain, A. K., Dunn, K. E., Law, V. S., Mao, C. T., Matsumura, S. Y., Mejza, S. J., Paborsky, L. R., and Leung, L. L. K. (1995) *Nature* **378,** 413–416
24. Cantwell, A. M., and Di Cera, E. (2000) *J. Biol. Chem.* **275,** 39827–39830
25. Tsiang, M., Paborsky, L. R., Li, W. X., Jain, A. K., Mao, C. T., Dunn, K. E., Lee, D. W., Matsumura, S. Y., Matteucci, M. D., Coutre, S. E., Leung, L. L., and Gibbs, C. S. (1996) *Biochemistry* **35,** 16449–16457
26. Gruber, A., Cantwell, A. M., Di Cera, E., and Hanson, S. R. (2002) *J. Biol. Chem.* **277,** 27581–27584
27. Woehl, E., and Dunn, M. F. (1999) *Biochemistry* **38,** 7118–7130
28. Woehl, E., and Dunn, M. F. (1999) *Biochemistry* **38,** 7131–7141
29. Mesecar, A. D., and Nowak, T. (1997) *Biochemistry* **36,** 6803–6813
30. Mesecar, A. D., and Nowak, T. (1997) *Biochemistry* **36,** 6792–6802
31. O'Brien, M. C., and McKay, D. B. (1995) *J. Biol. Chem.* **270,** 2247–2250
32. Xu, J., McRae, M. A., Harron, S., Rob, B., and Huber, R. E. (2004) *Biochem. Cell Biol.* **82,** 275–284
33. Neville, M. C., and Ling, G. N. (1967) *Arch. Biochem. Biophys.* **118,** 596–610
34. Digits, J. A., and Hedstrom, L. (1999) *Biochemistry* **38,** 2295–2306
35. Wells, C. M., and Di Cera, E. (1992) *Biochemistry* **31,** 11721–11730
36. Ayala, Y. M., and Di Cera, E. (2000) *Protein Sci.* **9,** 1589–1593
37. Krem, M. M., Prasad, S., and Di Cera, E. (2002) *J. Biol. Chem.* **277,** 40260–40264
38. Guinto, E. R., and Di Cera, E. (1996) *Biochemistry* **35,** 8800–8804
39. Prasad, S., Wright, K. J., Roy, D. B., Bush, L. A., Cantwell, A. M., and Di Cera, E. (2003) *Proc. Natl. Acad. Sci. U. S. A.* **100,** 13785–13790
40. Griffon, N., and Di Stasio, E. (2001) *Biophys. Chem.* **90,** 89–96
41. Lai, M. T., Di Cera, E., and Shafer, J. A. (1997) *J. Biol. Chem.* **272,** 30275–30282
42. Guinto, E. R., Vindigni, A., Ayala, Y. M., Dang, Q. D., and Di Cera, E. (1995) *Proc. Natl. Acad. Sci. U. S. A.* **92,** 11185–11189
43. Dang, Q. D., and Di Cera, E. (1994) *J. Protein Chem.* **13,** 367–373
44. Bush, L. A., Nelson, R. W., and Di Cera, E. (2006) *J. Biol. Chem.* **281,** 7183–7188
45. Stoll, V. S., and Blanchard, J. S. (1990) *Methods Enzymol.* **182,** 24–38
46. Ayala, Y., and Di Cera, E. (1994) *J. Mol. Biol.* **235,** 733–746
47. De Filippis, V., De Dea, E., Lucatello, F., and Frasson, R. (2005) *Biochem. J.* **390,** 485–492
48. Arosio, D., Ayala, Y. M., and Di Cera, E. (2000) *Biochemistry* **39,** 8095–8101
49. Carrell, C. J., Bush, L. A., Mathews, F. S., and Di Cera, E. (2006) *Biophys. Chem.* **121,** 177–184
50. Bell, R., Stevens, W. K., Jia, Z., Samis, J., Cote, H. C. F., MacGillivray, R. T. A., and Nesheim, M. E. (2000) *J. Biol. Chem.* **275,** 29513–29520
51. Mengwasser, K. E., Bush, L. A., Shih, P., Cantwell, A. M., and Di Cera, E. (2005) *J. Biol. Chem.* **280,** 23997–27003
52. Bode, W., Turk, D., and Karshikov, A. (1992) *Protein Sci.* **1,** 426–471
53. Vindigni, A., and Di Cera, E. (1996) *Biochemistry* **35,** 4417–4426
54. Orthner, C. L., and Kosow, D. P. (1980) *Arch. Biochem. Biophys.* **202,** 63–75
55. Botts, J., and Morales, M. (1953) *Trans Faraday Soc.* **49,** 696–707
56. Fuhrmann, C. N., Daugherty, M. D., and Agard, D. A. (2006) *J. Am. Chem. Soc.* **128,** 9086–9102
57. Pineda, A. O., Savvides, S. N., Waksman, G., and Di Cera, E. (2002) *J. Biol. Chem.* **277,** 40177–40180
58. Carter, W. J., Myles, T., Gibbs, C. S., Leung, L. L., and Huntington, J. A. (2004) *J. Biol. Chem.* **279,** 26387–26394
59. Pineda, A. O., Chen, Z. W., Caccia, S., Cantwell, A. M., Savvides, S. N., Waksman, G., Mathews, F. S., and Di Cera, E. (2004) *J. Biol. Chem.* **279,** 39824–39828
60. Papaconstantinou, M. E., Carrell, C. J., Pineda, A. O., Bobofchak, K. M., Mathews, F. S., Flordellis, C. S., Maragoudakis, M. E., Tsopanoglou, N. E., and Di Cera, E. (2005) *J. Biol. Chem.* **280,** 29393–29396
61. Johnson, D. J., Adams, T. E., Li, W., and Huntington, J. A. (2005) *Biochem. J.* **392,** 21–28
62. Pineda, A. O., Chen, Z. W., Bah, A., Garvey, L. C., Mathews, F. S., and Di Cera, E. (2006) *J. Biol. Chem.* **281,** 32922–32928

CHAPTER III

Stabilization of the E* form turns thrombin into an anticoagulant

THE JOURNAL OF BIOLOGICAL CHEMISTRY VOL. 284, NO. 30, pp. 20034–20040, July 24, 2009

Stabilization of the *E** Form Turns Thrombin into an Anticoagulant*

Received for publication, April 23, 2009, and in revised form, May 14, 2009 Published, JBC Papers in Press, May 27, 2009, DOI 10.1074/jbc.M109.012344

Alaji Bah, Christopher J. Carrell, Zhiwei Chen, Prafull S. Gandhi, and Enrico Di Cera[1]

From the Department of Biochemistry and Molecular Biophysics, Washington University School of Medicine, St. Louis, Missouri 63110

Previous studies have shown that deletion of nine residues in the autolysis loop of thrombin produces a mutant with an anticoagulant propensity of potential clinical relevance, but the molecular origin of the effect has remained unresolved. The x-ray crystal structure of this mutant solved in the free form at 1.55 Å resolution reveals an inactive conformation that is practically identical (root mean square deviation of 0.154 Å) to the recently identified *E form. The side chain of Trp^{215} collapses into the active site by shifting >10 Å from its position in the active *E* form, and the oxyanion hole is disrupted by a flip of the Glu^{192}–Gly^{193} peptide bond. This finding confirms the existence of the inactive form *E** in essentially the same incarnation as first identified in the structure of the thrombin mutant D102N. In addition, it demonstrates that the anticoagulant profile often caused by a mutation of the thrombin scaffold finds its likely molecular origin in the stabilization of the inactive *E** form that is selectively shifted to the active *E* form upon thrombomodulin and protein C binding.**

Serine proteases of the trypsin family are responsible for digestion, blood coagulation, fibrinolysis, development, fertilization, apoptosis, and immunity (1). Activation of the protease requires the transition from a zymogen form (2) and formation of an ion pair between the newly formed amino terminus of the catalytic chain and the side chain of the highly conserved residue Asp^{194} (chymotrypsinogen numbering) next to the catalytic Ser^{195}. This ensures substrate access to the active site and proper formation of the oxyanion hole contributed by the backbone N atoms of Ser^{195} and Gly^{193} (3). The zymogen → protease conversion is classically associated with the onset of catalytic activity (3, 4) and provides a useful paradigm for understanding key features of protease function and regulation.

Recent kinetic (5) and structural (6, 7) studies of thrombin, the key protease in the blood coagulation cascade (8), have drawn attention to a significant plasticity of the trypsin fold that impacts the function of the enzyme in a decisive manner. The active form of the protease, *E*, coexists with an inactive form, *E**, that is distinct from the zymogen conformation (9). The *E** form features a collapse of the 215–217 β-strand into the active site and a flip of the peptide bond between residues Glu^{192} and Gly^{193} that disrupts the oxyanion hole. Importantly, the ion pair between Ile^{16} and Asp^{194} remains intact, suggesting that *E** is not equivalent to the zymogen form of the protease and that the *E**-*E* equilibrium is established after the conversion from the zymogen form has taken place. Indeed, existing structures of the zymogen forms of trypsin (10), chymotrypsin (11), and chymase (12) feature a broken Ile^{16}–Asp^{194} ion pair but no collapse of the 215–217 β-strand. Stopped-flow experiments show that the *E**-*E* conversion takes place on a time scale of <10 ms (5), as opposed to the much longer (100–1000 ms) time scale required for the zymogen-protease conversion (13, 14).

The *E** form is not a peculiarity of thrombin. The collapse of the 215–217 β-strand into the active site is observed in the inactive form of αI-tryptase (15), the high temperature requirement-like protease (16), complement factor D (17), granzyme K (18), hepatocyte growth factor activator (19), prostate kallikrein (20), and prostasin (21). A disrupted oxyanion hole is observed in complement factor B (22) and the arterivirus protease Nsp4 (23). The most likely explanation for the widespread occurrence of inactive conformations of trypsin-like proteases is that the *E**-*E* equilibrium is a basic property of the trypsin fold that fine tunes activity and specificity once the zymogen → protease conversion has taken place (9).

The new paradigm established by the *E**-*E* equilibrium has obvious physiological relevance. In the case of complement factors, kallikreins, tryptase, and some coagulation factors must be kept to a minimum until binding of a trigger factor ensues. Stabilization of *E** may afford a resting state of the protease waiting for action, as seen for other systems (24–28). For example, factor B is mostly inactive until binding of complement factor C3 unleashes catalytic activity at the site where amplification of C3 activation is most needed prior to formation of the membrane attack complex (29). Indeed, the crystal structure of factor B reveals a conformation with the oxyanion hole disrupted by a flip of the 192–193 peptide bond (22), as observed in the *E** form of thrombin (6, 7).

The allosteric equilibrium as shown in Scheme 1,

$$E^* \underset{k_{-1}}{\overset{k_1}{\rightleftharpoons}} E$$

SCHEME 1

* This work was supported, in whole or in part, by National Institutes of Health Grants HL49413, HL58141, and HL73813 (to E. D. C.).

The atomic coordinates and structure factors (code 3gic) have been deposited in the Protein Data Bank, Research Collaboratory for Structural Bioinformatics, Rutgers University, New Brunswick, NJ (http://www.rcsb.org/).

[1] To whom correspondence should be addressed: Dept. of Biochemistry and Molecular Biophysics, Washington University School of Medicine, Box 8231, St. Louis, MO 63110. Tel.: 314-362-4185; Fax: 314-362-4311; E-mail: enrico@wustl.edu.

involves the rates for the $E^* \rightarrow E$ transition, k_1, and backward, k_{-1}, that define the equilibrium constant $r = k_{-1}/k_1 = [E^*]/[E]$ (5). The value of k_{cat}/K_m for an enzyme undergoing the E^*-E equilibrium is as shown in Equation 1 (30),

$$\frac{k_{cat}}{K_m} = s = \frac{s_E}{1 + r} \quad \text{(Eq. 1)}$$

where s_E is the value of s for the E form, and obviously $s_{E^*} = 0$. Likewise, the binding of an inhibitor to the enzyme undergoing the E^*-E equilibrium is shown in Equation 2,

$$K = \frac{K_E}{1 + r} \quad \text{(Eq. 2)}$$

where K_E is the value of the equilibrium association constant K for the E form, and $K_{E^*} = 0$. As the value of r increases upon stabilization of E^*, the values of s and K in Equations 1 and 2 decrease without limits. Hence, stabilization of E^* has the potential to completely abrogate substrate hydrolysis ($s \rightarrow 0$) or inhibitor binding ($K \rightarrow 0$). However, binding of a suitable cofactor could restore activity by triggering the $E^* \rightarrow E$ transition. This suggests a simple explanation for the anticoagulant profile observed in a number of thrombin mutants that have poor activity toward all physiological substrates but retain activity toward the anticoagulant protein C in the presence of the cofactor thrombomodulin (31–34). Here we report evidence that stabilization of E^* provides a molecular mechanism to turn thrombin into an anticoagulant.

MATERIALS AND METHODS

The human thrombin mutant Δ146–149e was constructed, expressed, and purified to homogeneity as reported elsewhere (32, 35, 36), using the QuikChange site-directed mutagenesis kit from Stratagene (La Jolla, CA) in an HPC4-modified pNUT expression vector containing the human prethrombin-1 gene. Values of $s = k_{cat}/K_m$ for the hydrolysis of the chromogenic substrates H-D-Phe-Gly-Arg-*p*-nitroanilide, H-D-Phe-Pro-Phe-*p*-nitroanilide, H-D-Phe-Pro-Lys-*p*-nitroanilide, and H-D-Phe-Pro-Arg-*p*-nitroanilide (FPR),[2] the release of fibrinopeptide A from fibrinogen, cleavage of the protease-activated receptors PAR1, PAR3, and PAR4, and activation of protein C in the absence or presence of 100 nM thrombomodulin and 5 mM $CaCl_2$ were determined as reported elsewhere (32, 37, 38) under physiological experimental conditions of 5 mM Tris, 0.1% PEG8000, 145 mM NaCl, pH 7.4, at 37 °C.

Binding of the active site inhibitor argatroban (39) was studied directly by isothermal titration calorimetry under experimental conditions of 5 mM Tris, 0.1% PEG8000, 145 mM NaCl, pH 7.4, at 37 °C, using an iTC200 calorimeter (MicroCal Inc. Northampton, MA) with the sample cell containing thrombin and the syringe injecting argatroban. The sample volume for iTC200 is 204.6 μl and the total volume of injected ligand is 39.7 μl. The thermal equilibration step at 37 °C, was followed by an initial 60-s delay step and subsequently an initial 0.2-μl injection. Typically, 19 serial injections of 2 μl and 1 last injection of 1.5 μl of ligand were performed at an interval of 180 s. The stirring speed was maintained at 1000 rpm, and the reference power was kept constant at 5 μcal/s. The heat associated with each injection of ligand was integrated and plotted against the molar ratio of ligand to macromolecule. Thermodynamic parameters were extracted from a curve fit to the data using the software (Origin 7.0) provided by MicroCal according to a one-site binding model. Experiments were performed in triplicate with excellent reproducibility (<10% variation in thermodynamic parameters).

Crystals of human thrombin Δ146–149e were obtained using the hanging drop vapor-diffusion method. A solution of Δ146–149e (8 mg/ml in 1 μl) in 50 mM NaCl, 20 mM Tris, pH 7.5, was mixed with an equal volume reservoir solution containing 20% PEG20000 and 100 mM Tris, pH 8.5, at 25 °C. Crystals were tetragonal, space group $P4_3$, with unit cell parameters $a = b = 58.2$ Å, $c = 119.6$ Å, and contained one molecule in the asymmetric unit. Crystals were flash-frozen in liquid nitrogen after soaking in artificial mother liquor containing 15% (v/v) glycerol. X-ray diffraction data were recorded on an ADSC Quantum 315 CCD at beamline 14-BM-C at BIOCARS (Argonne, IL). One pass of 150° with steps of 0.5° was collected and processed to 1.55 Å resolution. Integration and scaling of diffraction data were carried out with the HKL-2000 package (40). The structure was solved by molecular replacement using the CCP4 suite (41) and Protein Data Bank accession code 2GP9 (7) as a search model. Rounds of positional and isotropic temperature factor refinement in REFMAC (42) were alternated with model building in COOT (43). After most of the model was found, TLS tensors modeling rigid-body anisotropic temperature factors were calculated and applied to the model using REFMAC. This was alternated with more model building in COOT until the final model was produced. Ramachandran plots were calculated using PROCHECK (44). Statistics for data collection and refinement are summarized in Table 1. Coordinates of the structure of the human thrombin mutant Δ146–149e have been deposited to the Protein Data Bank (accession code 3GIC).

RESULTS

Once generated in the blood from its inactive precursor prothrombin, thrombin acts as a procoagulant when it converts fibrinogen into an insoluble fibrin clot (45) and acts as a prothrombotic when it cleaves protease-activated receptors (PARs) (46, 47). However, upon interaction with the endothelial cell receptor thrombomodulin, thrombin loses both procoagulant and prothrombotic functions and increases its activity >1,000-fold toward the anticoagulant protein C (48). A thrombin mutant stabilized in the E^* form would have little or no activity toward physiological substrates. If this mutant could be converted to the E form upon binding of thrombomodulin, then a selective anticoagulant response would be elicited upon activation of protein C in the vascular endothelium where thrombomodulin is present.

The mutant Δ146–149e carries a deletion of the nine residues ^{146}ETWTANVGK^{149e} in the autolysis loop and was originally constructed to assess the role of this highly flexi-

[2] The abbreviations used are: FPR, H-D-Phe-Pro-Arg-*p*-nitroanilide; r.m.s.d., root mean square deviation; PC, protein C; TM, thrombomodulin; PAR, protease-activated receptor.

TABLE 1

Crystallographic data for the thrombin mutant Δ146–149e (Protein Data Bank code 3GIC)

Data collection	
Wavelength	0.9 Å
Space group	$P4_3$
Unit cell dimension	$a = b = 58.23$, $c = 119.56$ Å
Molecules/asymmetric unit	1
Resolution range	40.0–1.55 Å
Observations	220,618
Unique observations	54,240
Completeness	94.3% (76.1%)
R_{sym} (%)	3.7% (27.9%)
$I/\sigma(I)$	27.7 (2.3)
Refinement	
Resolution	40.0–1.55 Å
$\|F\|/\sigma(\|F\|)$	>0
R_{cryst}, R_{free}	0.188, 0.224
Reflections (working/test)	51,479/2747
Protein atoms	2295
Solvent molecules	257
r.m.s.d. bond lengths[a]	0.012 Å
r.m.s.d. angles[a]	1.4°
r.m.s.d. ΔB (Å^2) (mm/ms/ss)[b]	0.86/0.67/2.21
$\langle B \rangle$ protein	18.6 Å^2
$\langle B \rangle$ solvent	28.6 Å^2
Ramachandran plot	
Most favored	98.3%
Generously allowed	1.3%
Disallowed	0.4%

[a] Root mean square deviations from ideal bond lengths and angles and r.m.s.d. values in *B*-factors of bonded atoms are shown.

[b] mm indicates main chain-main chain; ms indicates main chain-side chain; and ss indicates side chain-side chain.

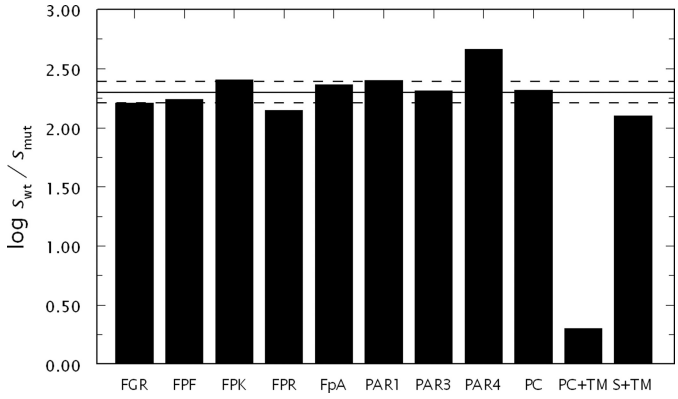

FIGURE 1. **Functional properties of the thrombin mutant Δ146–149e.** Shown are the values of $s = k_{cat}/K_m$ for the hydrolysis of chromogenic substrates H-D-Phe-Gly-Arg-*p*-nitroanilide (*FGR*), H-D-Phe-Pro-Phe-*p*-nitroanilide (*FPF*), H-D-Phe-Pro-Lys-*p*-nitroanilide (*FPK*), and FPR, fibrinogen (*FpA*), PAR1, PAR3, PAR4, protein C (*PC*), and protein C (*PC+TM*) or FPR (*S+TM*) in the presence of 100 nM thrombomodulin and 5 mM $CaCl_2$ for wild-type (s_{wt}) relative to the thrombin mutant Δ146–149e (s_{mut}). All substrates, except PAR4, experience a loss of activity that equals 2.30 log units (*solid line*) with a standard deviation of 0.09 log units (*broken lines*). This supports perturbation of the *E*-E* equilibrium in favor of the inactive form *E** (see Equations 1 and 3 in the text). The larger loss for PAR4 (>4 S.D. compared with the other substrates) is likely due to direct interaction of the substrate with residues of the autolysis loop (55) that are missing in the Δ146–149e mutant. In the presence of thrombomodulin, the mutant experiences only a 2-fold drop in activity toward protein C compared with wild type. However, thrombomodulin binding alone does not restore activity toward the chromogenic substrate FPR. Experimental conditions are as follows: 5 mM Tris, 0.1% PEG8000, 145 mM NaCl, pH 7.4, at 37 °C. The values of s_{wt} are as follows: 0.52 ± 0.05 μM^{-1} s^{-1} H-D-Phe-Gly-Arg-*p*-nitroanilide (*FGR*), 0.28 ± 0.03 μM^{-1} s^{-1} H-D-Phe-Pro-Gly-*p*-nitroanilide (*FGF*), 4.2 ± 0.2 $\mu M^{-1} s^{-1}$ H-D-Phe-Pro-Gly-*p*-nitroanilide (*FGK*), 37 ± 1 μM^{-1} s^{-1} H-D-Phe-Pro-Arg-*p*-nitroanilide (*FPR*), 17 ± 1 μM^{-1} s^{-1} fibrinogen (*FpA*), 39 ± 1 $\mu M^{-1} s^{-1}$ PAR1, 0.35 ± 0.02 μM^{-1} s^{-1} PAR3, 0.34 ± 0.01 μM^{-1} s^{-1} PAR4, 59 ± 3 M^{-1} s^{-1} PC, 0.22 ± 0.01 $\mu M^{-1} s^{-1}$ PC+TM, 64 ± 2 $\mu M^{-1} s^{-1}$ S+TM.

ble domain in thrombin function (49). The sequence ^{149a}ANVGK^{149e} is not present in trypsin and chymotrypsin and can be deleted without functional consequences (49). Also, swapping the entire ^{146}ETWTANVGK^{149e} sequence of thrombin with the ^{146}SSGT^{149} sequence of trypsin (50) or deleting the ^{146}ETW^{148} sequence (51) produces perturbations of function that are recapitulated by the single mutations E146A and R221aA (32, 35). Residue Glu^{146} makes an important ion pair interaction with Arg^{221a} in the adjacent 220-loop in the *E* form but not in the *E** form (6, 7, 35). The entire autolysis loop likely participates in the long range communication seen in the *E*-E* equilibrium (6) between the 220-loop, the active site, and exosite I where thrombomodulin binds (8). Deletion of the entire sequence ^{146}ETWTANVGK^{149e} in the Δ146–149e mutant causes a significant loss of activity toward chromogenic and physiological substrates, but binding of thrombomodulin almost completely restores activity toward the anticoagulant protein C (Fig. 1). Importantly, thrombomodulin has only a modest effect on the hydrolysis of a chromogenic substrate (Fig. 1), as already documented for other anticoagulant thrombin mutants (52) and wild type (53). These properties suggest that the Δ146–149e mutation shifts the *E*-E* equilibrium of thrombin in favor of *E**, and thrombomodulin in complex with protein C can switch the mutant back into the active conformation *E*.

Evidence that the thrombin mutant Δ146–149e is stabilized in the *E** form in solution comes from inspection of the values of k_{cat}/K_m for chromogenic and natural substrates. The data in Fig. 1 reveal a remarkable similarity in the loss of activity toward fibrinogen, PAR1, PAR3, and protein C for the Δ146–149e mutant compared with wild type. Likewise, a comparable loss of activity is observed toward several chromogenic substrates bearing replacements at the P1 or P2 positions (54). On the average, the loss is about 200-fold. For a mutation that selectively shifts the *E*-E* equilibrium in favor of *E**, without introducing additional effects on substrate or inhibitor recognition, the values of *s* and *K* in Equations 1–2 must decrease by the same amount. Specifically, the ratio shown in Equation 3 between the wild-type (WT) and mutant values of *s* and *K* must be the same for all substrates and inhibitors.

$$\frac{s_{WT}}{s_{mut}} = \frac{K_{WT}}{K_{mut}} = \frac{1 + r_{mut}}{1 + r_{WT}} \qquad \text{(Eq. 3)}$$

The data in Fig. 1 are consistent with the prediction from Equation 3. Perturbation of PAR4 recognition is significantly more pronounced compared with all other substrates, but this is consistent with the direct interactions that this substrate makes with residues of the autolysis loop (55). Further support for stabilization of *E** in the Δ146–149e mutant comes from calorimetric measurements of the binding of the inhibitor argatroban (39) to the active site. The value of *K* (see Equation 2) drops 135-fold in the mutant compared with wild type (Fig. 2), as expected from Equation 3.

Addition of thrombomodulin restores activity of the mutant toward protein C (Fig. 1), indicating that although the mutation stabilizes *E**, the active form *E* is still present in solution and can be populated for protein C activation in the presence of cofac-

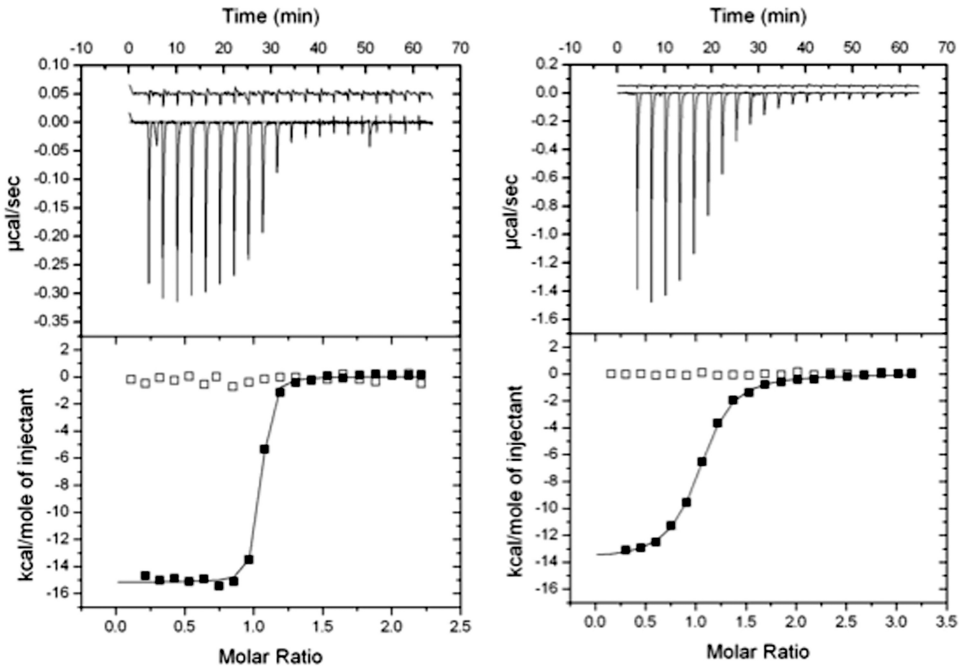

FIGURE 2. **Argatroban binding to thrombin wild type (*left*) and Δ146–149e (*right*) measured by isothermal titration calorimetry.** The *top panel* shows the heat exchanged in each individual titration for the thrombin sample (*bottom trace*) and the argatroban buffer control (*top trace*). The *bottom panel* is the integration of the data to yield the overall heat exchanged as a function of the ligand/protein molar ratio. Experimental conditions are 5 mM Tris, 0.1% polyethylene glycol, 145 mM NaCl, pH 7.4, 37 °C. The enzyme and argatroban concentrations are as follows: 13.44 and 140 μM (thrombin wild type); 52.5 and 777 μM (Δ146–149e). Titration curves were fit using the Origin software of the iTC200, with best fit parameter values as follows: thrombin wild type, $K = 1.0 \pm 0.1\ 10^8\ M^{-1}$, $\Delta G = -11.3 \pm 0.1$ kcal/mol, $\Delta H = -15.2 \pm 0.1$ kcal/mol, and $T\Delta S = -3.9 \pm 0.1$ kcal/mol; Δ146–149e, $K = 7.4 \pm 0.4\ 10^5\ M^{-1}$, $\Delta G = -8.3 \pm 0.1$ kcal/mol, $\Delta H = -13.8 \pm 0.1$ kcal/mol, and $T\Delta S = -5.5 \pm 0.1$ kcal/mol. The value of the stoichiometric constant *N* was 1.01 ± 0.01 for thrombin wild type and the Δ146–149e mutant.

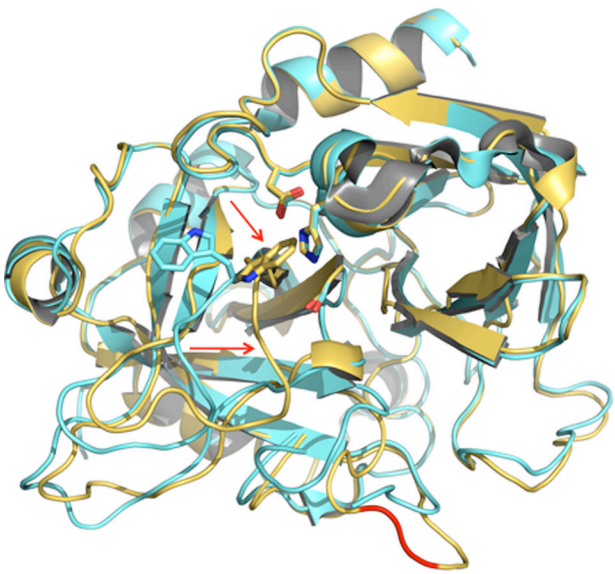

FIGURE 3. **Ribbon representation of the structure of the thrombin mutant Δ146–149e (*gold*) overlaid with the structure of thrombin in the *E* conformation (35) (*cyan*).** The newly formed peptide bond between Lys^{145} and Gly^{150} is indicated in *red* in the shortened autolysis loop of Δ146–149e (see also Fig. 4), and the loop in the *E* conformation is not visible between residues Trp^{148} and Lys^{149e}. The 215–217 β-strand in the mutant collapses into the primary specificity pocket (*red open arrowheads*), with the side chain of Trp^{215} (*stick model*) repositioned into the active site (residues of the catalytic triad His^{57}, Asp^{102}, and Ser^{195} shown as *stick models*) in hydrophobic interaction with Trp^{60d}, Tyr^{60a}, Leu^{99}, and His^{57}. This represents a drastic change (r.m.s.d. 0.384 Å) from the conformation of *E* where the side chain of Trp^{215} is positioned 10.5 Å away and leaves the active site accessible to substrate. The conformation of Δ146–149e is remarkably similar (r.m.s.d. 0.154 Å) to that of *E** determined recently (6, 7).

tor. Evidence that binding to exosite I, the major thrombin epitope for thrombomodulin recognition (56, 57), can convert *E** to *E* has been provided recently by the structure of the thrombin mutant D102N bound to a fragment of the platelet receptor PAR1 (6). Therefore, the thrombin mutant Δ146–149e likely functions as an allosteric switch stabilized into the inactive form *E** until the combined binding of thrombomodulin and protein C shifts *E** to *E* and restores activity.

To gain direct information on the conformational properties of the Δ146–149e mutant, its crystal structure was solved in the free form at 1.55 Å resolution. Consistent with the functional data, the mutant assumes a collapsed conformation that is practically identical (r.m.s.d. 0.154 Å) to the *E** form identified recently from the structure of the thrombin mutant D102N (6, 7). The Δ146–149e mutant folds in a self-inhibited conformation (Fig. 3) due to a collapse of the 215–217 β-strand into the active site that moves the indole ring of Trp^{215} >10 Å to engage the catalytic His^{57} on the opposite side of the active site cleft (Fig. 4). The drastic rearrangement of the 215–217 β-strand propagates the perturbation up to the peptide bond between Glu^{192} and Gly^{193} that is flipped relative to the conformation of the *E* form (7) and destroys the architecture of the oxyanion hole (Fig. 4). These significant structural changes occur away from the site of mutation in the autolysis loop, where the shortened sequence $^{144}LKGQ^{151}$ shows Lys^{145} connected directly to Gly^{150} (Fig. 4). Hence, the thrombin mutants D102N and Δ146–149e crystallize in the same *E** form, notwithstanding differences in sequence and crystallization conditions. The inactive form *E** is therefore a genuine conformation of thrombin accessible to the enzyme in addition to its active form *E* (9, 35). The *E** form is stabilized by mutations that compromise activity of the enzyme and is selectively converted to the active *E* form under suitable conditions.

DISCUSSION

The new paradigm emerged from analysis of recent crystal structures of trypsin-like proteases (6, 7, 15–23) supports the existence of the *E**-*E* equilibrium as a critical feature of the trypsin fold (9). This allosteric equilibrium explains several important aspects of protease biology. For proteases that are poorly active until interaction with a cofactor, as observed for some clotting and complement factors (29), the onset of catalytic activity can be attributed to the *E** → E conversion. The *E** form acts in this case as a resting state for the enzyme and a spring-loaded mechanism that can be turned on when required

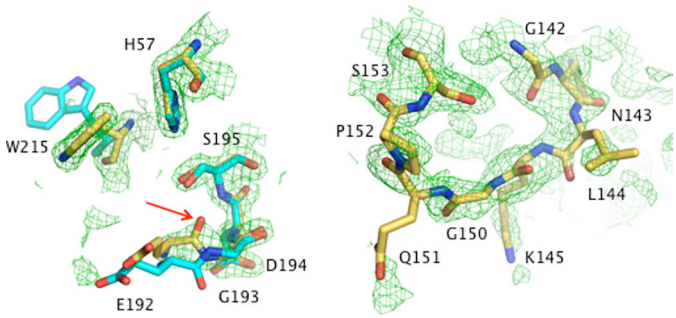

FIGURE 4. *Left,* details of the collapse of Trp^{215} into the active site and disruption of the oxyanion hole in the thrombin mutant Δ146–149e (CPK, *yellow*) are shown. The conformation of the same residues in the *E* form is shown by comparison (CPK, *cyan*). The peptide bond between Glu^{192} and Gly^{193} is flipped in the Δ146–149e mutant (*red open arrowhead*), as seen in the *E** form (6, 7, 9), causing disruption of the oxyanion hole contributed by the N atoms of Gly^{193} and Ser^{195}. The $2F_o - F_c$ electron density map (*green mesh*) is contoured at 2.0σ. *Right,* deletion of residues ^{146}ETWTANVGK^{149e} in the autolysis loop of the Δ146–149e mutant results in a new peptide bond connection between Lys^{145} and Gly^{150} (CPK, *yellow*). The autolysis loop is rarely seen in its entirety in thrombin structures, and considerable disorder remains in the mutant Δ146–149e where the sequence ^{144}LKGQ^{151} must be contoured at 0.5σ in the $2F_o - F_c$ electron density map (*green mesh*).

by the biological context. The *E*-E* equilibrium also provides context to interpret the effect of mutations associated with loss of biological activity in highly active proteases. In some cases, as documented by thrombin (8, 58), the molecular origin of the effect is unclear because the mutation does not affect residues in direct contact with substrate. Stabilization of *E** through molecular conduits not necessarily involved in substrate recognition may offer a plausible explanation.

The allosteric *E*-E* equilibrium has far reaching implications for protein engineering. Stabilization of *E** by selected mutations, coupled with a transition to *E* triggered by suitable cofactors, may result in expression of protease activity on demand in a biological context. Thrombin exists predominantly in the *E* form, which functions as an ensemble partitioned between Na^+-free and Na^+-bound conformations (5, 8) because of the extremely fast rates of binding and dissociation of Na^+ with the enzyme (59). However, a thrombin mutant stabilized in the *E** form that converts to *E* upon interaction with thrombomodulin and protein C would be an anticoagulant of potential clinical relevance. Such mutant would show little or no activity toward fibrinogen and PAR1 but would retain activity toward protein C. A number of thrombin mutants have been reported with an altered specificity that favors protein C activation over fibrinogen cleavage (31–34, 49, 60, 61). Among these mutants, E217K and W215A/E217A are effective as anticoagulants and antithrombotics in non-human primates (33, 34, 62, 63) and have been crystallized at 2.5–2.8 Å resolution (52, 64). The structures show a partial collapse of the 215–217 β-strand and disruption of the oxyanion hole that resembles the conformation of *E** (7). It is possible that these mutants are stabilized in an *E**-like form, but it is equally possible that the perturbed structures are the result of the mutations introduced at residues on the critical 215–217 β-strand. Substantial crystallographic packing interactions especially evident in the E217K mutant also bias the conformation, unlike the structures of the mutants D102N (7) and Δ146–149e reported here. Additional structural work is necessary to validate the collapsed conformations of E217K and W215A/E217A.

The mutant Δ146–149e was previously identified for its significant anticoagulant profile (49) and carries a deletion of nine residues in the highly disordered autolysis loop, whose role in the function of the enzyme remains elusive. Importantly, residues of the autolysis loop are separate from the 215–217 β-strand or the oxyanion hole that undergoes substantial rearrangement in the *E*-E* transition (6, 7). Yet the mutant Δ146–149e crystallizes in a collapsed conformation that is practically identical (r.m.s.d. 0.154 Å) to the *E** form identified recently (6, 7). This result is notable for two reasons. First, it confirms the existence of the inactive form *E** in essentially the same incarnation as first identified in the structure of the thrombin mutant D102N under different crystallization conditions. Second, it provides proof of principle that the anticoagulant profile often caused by a mutation of the thrombin scaffold finds its likely molecular origin into stabilization of the inactive *E** form. The mutant Δ146–149e was previously reported to feature reduced Na^+ affinity (49), which supports the conclusion that its active *E* form is essentially Na^+-free. This confirms the tenet that abrogation of the procoagulant effect of Na^+ (32, 65) is necessary to switch thrombin into an anticoagulant.

There is no contradiction between the modest effect of thrombomodulin on chromogenic substrate hydrolysis (Fig. 1) and structural evidence of the *E** to *E* transition upon exosite I binding (6). Crystallographic evidence that the D102N mutant assumes the *E** form when free and the *E* form when bound to exosite I does not imply an all-or-none distribution of *E** and *E* in solution. In fact, a significant fraction of D102N does exist in the *E* form in solution (7), but this conformation is not favored under the crystallization conditions so far explored (7). Thermodynamic principles (66, 67) establish that an allosteric effector can only shift the *E*-E* equilibrium in favor of *E* by an amount equal to the ratio of affinities of the two forms. Because exosite I, unlike the active site, is similarly accessible in the *E** and *E* form (6–8, 35), binding of thrombomodulin to the two forms cannot result in extreme perturbations of the *E*-E* equilibrium. Hence, when the equilibrium is shifted drastically in favor of *E**, as seen for the Δ146–149e mutant but not the D102N mutant, binding of thrombomodulin is insufficient to populate significantly the active form *E*. On the other hand, the combined action of protein C and thrombomodulin may have a more profound effect on the *E*-E* equilibrium by accessing additional regions of the thrombin surface beyond exosite I (57), thereby ensuring almost complete restoration of activity.

Elucidation of the molecular mechanism underscoring the anticoagulant profile of thrombin mutants like Δ146–149e provides new impetus to the effort of rationally engineering thrombin mutants with exclusive activity toward protein C for clinical applications. The molecular underpinnings of the *E*-E* equilibrium have been revealed by structural biology (6), along with precise targets for mutagenesis aimed at stabilizing the *E** form. An exclusive protein C activator would have several advantages compared with the direct administration of activated protein C currently marketed for the treatment of sepsis (68). Activated protein C acts as an anticoagulant when it inactivates clotting factor Va with the assistance of the cofactor

protein S and as a cytoprotective agent when it cleaves PAR1 on the surface of endothelial cells with the assistance of endothelial protein C receptor (69). Importantly, activated protein C generated *in situ* with the anticoagulant thrombin mutant W215A/E217A offers cytoprotective advantages over activated protein C administered to the circulation (70). Furthermore, the thrombin mutant W215A/E217A acts as a potent antithrombotic by blocking the interaction of von Willebrand factor with the platelet receptor GpIb (71), a property of which activated protein C is naturally devoid and that challenges the efficacy of low molecular weight heparins (63). These intriguing properties of the mutant W215A/E217A, its well established potency as an anticoagulant in non-human primates (62, 63) and the current elucidation of the role of E^* in switching thrombin into an anticoagulant, will facilitate the rational engineering of a thrombin mutant with exclusive activity toward protein C.

REFERENCES

1. Page, M. J., and Di Cera, E. (2008) *Cell. Mol. Life Sci.* **65,** 1220–1236
2. Bode, W., and Huber, R. (1976) *FEBS Lett.* **68,** 231–236
3. Hedstrom, L. (2002) *Chem. Rev.* **102,** 4501–4524
4. Bode, W., Schwager, P., and Huber, R. (1978) *J. Mol. Biol.* **118,** 99–112
5. Bah, A., Garvey, L. C., Ge, J., and Di Cera, E. (2006) *J. Biol. Chem.* **281,** 40049–40056
6. Gandhi, P. S., Chen, Z., Mathews, F. S., and Di Cera, E. (2008) *Proc. Natl. Acad. Sci. U.S.A.* **105,** 1832–1837
7. Pineda, A. O., Chen, Z. W., Bah, A., Garvey, L. C., Mathews, F. S., and Di Cera, E. (2006) *J. Biol. Chem.* **281,** 32922–32928
8. Di Cera, E. (2008) *Mol. Aspects Med.* **29,** 203–254
9. Di Cera, E. (2009) *IUBMB Life* **61,** 510–515
10. Fehlhammer, H., Bode, W., and Huber, R. (1977) *J. Mol. Biol.* **111,** 415–438
11. Wang, D., Bode, W., and Huber, R. (1985) *J. Mol. Biol.* **185,** 595–624
12. Reiling, K. K., Krucinski, J., Miercke, L. J., Raymond, W. W., Caughey, G. H., and Stroud, R. M. (2003) *Biochemistry* **42,** 2616–2624
13. Fersht, A. R. (1972) *J. Mol. Biol.* **64,** 497–509
14. Fersht, A. R., and Requena, Y. (1971) *J. Mol. Biol.* **60,** 279–290
15. Rohr, K. B., Selwood, T., Marquardt, U., Huber, R., Schechter, N. M., Bode, W., and Than, M. E. (2006) *J. Mol. Biol.* **357,** 195–209
16. Krojer, T., Garrido-Franco, M., Huber, R., Ehrmann, M., and Clausen, T. (2002) *Nature* **416,** 455–459
17. Jing, H., Babu, Y. S., Moore, D., Kilpatrick, J. M., Liu, X. Y., Volanakis, J. E., and Narayana, S. V. (1998) *J. Mol. Biol.* **282,** 1061–1081
18. Hink-Schauer, C., Estébanez-Perpiñá, E., Wilharm, E., Fuentes-Prior, P., Klinkert, W., Bode, W., and Jenne, D. E. (2002) *J. Biol. Chem.* **277,** 50923–50933
19. Shia, S., Stamos, J., Kirchhofer, D., Fan, B., Wu, J., Corpuz, R. T., Santell, L., Lazarus, R. A., and Eigenbrot, C. (2005) *J. Mol. Biol.* **346,** 1335–1349
20. Carvalho, A. L., Sanz, L., Barettino, D., Romero, A., Calvete, J. J., and Romão, M. J. (2002) *J. Mol. Biol.* **322,** 325–337
21. Rickert, K. W., Kelley, P., Byrne, N. J., Diehl, R. E., Hall, D. L., Montalvo, A. M., Reid, J. C., Shipman, J. M., Thomas, B. W., Munshi, S. K., Darke, P. L., and Su, H. P. (2008) *J. Biol. Chem.* **283,** 34864–34872
22. Ponnuraj, K., Xu, Y., Macon, K., Moore, D., Volanakis, J. E., and Narayana, S. V. (2004) *Mol. Cell* **14,** 17–28
23. Barrette-Ng, I. H., Ng, K. K., Mark, B. L., Van Aken, D., Cherney, M. M., Garen, C., Kolodenko, Y., Gorbalenya, A. E., Snijder, E. J., and James, M. N. (2002) *J. Biol. Chem.* **277,** 39960–39966
24. Eisenmesser, E. Z., Bosco, D. A., Akke, M., and Kern, D. (2002) *Science* **295,** 1520–1523
25. Lu, H. P., Xun, L., and Xie, X. S. (1998) *Science* **282,** 1877–1882
26. Sytina, O. A., Heyes, D. J., Hunter, C. N., Alexandre, M. T., van Stokkum, I. H., van Grondelle, R., and Groot, M. L. (2008) *Nature* **456,** 1001–1004
27. Erlandson, K. J., Miller, S. B., Nam, Y., Osborne, A. R., Zimmer, J., and Rapoport, T. A. (2008) *Nature* **455,** 984–987
28. Zimmer, J., Nam, Y., and Rapoport, T. A. (2008) *Nature* **455,** 936–943
29. Gros, P., Milder, F. J., and Janssen, B. J. (2008) *Nat. Rev. Immunol.* **8,** 48–58
30. Carrell, C. J., Bush, L. A., Mathews, F. S., and Di Cera, E. (2006) *Biophys. Chem.* **121,** 177–184
31. Cantwell, A. M., and Di Cera, E. (2000) *J. Biol. Chem.* **275,** 39827–39830
32. Dang, Q. D., Guinto, E. R., and di Cera, E. (1997) *Nat. Biotechnol.* **15,** 146–149
33. Gibbs, C. S., Coutré, S. E., Tsiang, M., Li, W. X., Jain, A. K., Dunn, K. E., Law, V. S., Mao, C. T., Matsumura, S. Y., Mejza, S. J., Paborsky, L. R., and Leung, L. L. (1995) *Nature* **378,** 413–416
34. Tsiang, M., Paborsky, L. R., Li, W. X., Jain, A. K., Mao, C. T., Dunn, K. E., Lee, D. W., Matsumura, S. Y., Matteucci, M. D., Coutré, S. E., Leung, L. L., and Gibbs, C. S. (1996) *Biochemistry* **35,** 16449–16457
35. Pineda, A. O., Carrell, C. J., Bush, L. A., Prasad, S., Caccia, S., Chen, Z. W., Mathews, F. S., and Di Cera, E. (2004) *J. Biol. Chem.* **279,** 31842–31853
36. Prasad, S., Wright, K. J., Banerjee Roy, D., Bush, L. A., Cantwell, A. M., and Di Cera, E. (2003) *Proc. Natl. Acad. Sci. U.S.A.* **100,** 13785–13790
37. Ayala, Y. M., Cantwell, A. M., Rose, T., Bush, L. A., Arosio, D., and Di Cera, E. (2001) *Proteins* **45,** 107–116
38. Vindigni, A., and Di Cera, E. (1996) *Biochemistry* **35,** 4417–4426
39. Tanaka, K. A., Gruber, A., Szlam, F., Bush, L. A., Hanson, S. R., and Di Cera, E. (2008) *Blood Coagul. Fibrinolysis* **19,** 465–468
40. Otwinowski, Z., and Minor, W. (1997) *Methods Enzymol.* **276,** 307–326
41. Bailey, S. (1994) *Acta Crystallogr. D Biol. Crystallogr.* **50,** 760–763
42. Murshudov, G. N., Vagin, A. A., and Dodson, E. J. (1997) *Acta Crystallogr. D Biol. Crystallogr.* **53,** 240–255
43. Emsley, P., and Cowtan, K. (2004) *Acta Crystallogr. D Biol. Crystallogr.* **60,** 2126–2132
44. Morris, A. L., MacArthur, M. W., Hutchinson, E. G., and Thornton, J. M. (1992) *Proteins* **12,** 345–364
45. Spraggon, G., Everse, S. J., and Doolittle, R. F. (1997) *Nature* **389,** 455–462
46. Coughlin, S. R. (2000) *Nature* **407,** 258–264
47. Coughlin, S. R. (2005) *J. Thromb. Haemost.* **3,** 1800–1814
48. Esmon, C. T. (2003) *Chest* **124,** 26S-32S
49. Dang, Q. D., Sabetta, M., and Di Cera, E. (1997) *J. Biol. Chem.* **272,** 19649–19651
50. DiBella, E. E., and Scheraga, H. A. (1996) *Biochemistry* **35,** 4427–4433
51. Le Bonniec, B. F., Guinto, E. R., and Esmon, C. T. (1992) *J. Biol. Chem.* **267,** 19341–19348
52. Pineda, A. O., Chen, Z. W., Caccia, S., Cantwell, A. M., Savvides, S. N., Waksman, G., Mathews, F. S., and Di Cera, E. (2004) *J. Biol. Chem.* **279,** 39824–39828
53. Vindigni, A., White, C. E., Komives, E. A., and Di Cera, E. (1997) *Biochemistry* **36,** 6674–6681
54. Vindigni, A., Dang, Q. D., and Di Cera, E. (1997) *Nat. Biotechnol.* **15,** 891–895
55. Bah, A., Chen, Z., Bush-Pelc, L. A., Mathews, F. S., and Di Cera, E. (2007) *Proc. Natl. Acad. Sci. U.S.A.* **104,** 11603–11608
56. Pineda, A. O., Cantwell, A. M., Bush, L. A., Rose, T., and Di Cera, E. (2002) *J. Biol. Chem.* **277,** 32015–32019
57. Xu, H., Bush, L. A., Pineda, A. O., Caccia, S., and Di Cera, E. (2005) *J. Biol. Chem.* **280,** 7956–7961
58. Papaconstantinou, M. E., Bah, A., and Di Cera, E. (2008) *Cell. Mol. Life Sci.* **65,** 1943–1947
59. Gianni, S., Ivarsson, Y., Bah, A., Bush-Pelc, L. A., and Di Cera, E. (2007) *Biophys. Chem.* **131,** 111–114
60. Griffin, J. H. (1995) *Nature* **378,** 337–338
61. Wu, Q. Y., Sheehan, J. P., Tsiang, M., Lentz, S. R., Birktoft, J. J., and Sadler, J. E. (1991) *Proc. Natl. Acad. Sci. U.S.A.* **88,** 6775–6779
62. Gruber, A., Cantwell, A. M., Di Cera, E., and Hanson, S. R. (2002) *J. Biol. Chem.* **277,** 27581–27584
63. Gruber, A., Marzec, U. M., Bush, L., Di Cera, E., Fernández, J. A., Berny, M. A., Tucker, E. I., McCarty, O. J., Griffin, J. H., and Hanson, S. R. (2007) *Blood* **109,** 3733–3740
64. Carter, W. J., Myles, T., Gibbs, C. S., Leung, L. L., and Huntington, J. A. (2004) *J. Biol. Chem.* **279,** 26387–26394
65. Dang, O. D., Vindigni, A., and Di Cera, E. (1995) *Proc. Natl. Acad. Sci.*

U.S.A. **92,** 5977–5981
66. Wyman, J., and Gill, S. J. (1990) *Binding and Linkage*, University Science Books, Mill Valley, CA
67. Di Cera, E. (1995) *Thermodynamic Theory of Site-Specific Binding Processes in Biological Macromolecules*, Cambridge University Press, Cambridge, UK
68. Levi, M. (2008) *Curr. Opin. Hematol.* **15,** 481–486
69. Riewald, M., Petrovan, R. J., Donner, A., Mueller, B. M., and Ruf, W. (2002) *Science* **296,** 1880–1882
70. Feistritzer, C., Schuepbach, R. A., Mosnier, L. O., Bush, L. A., Di Cera, E., Griffin, J. H., and Riewald, M. (2006) *J. Biol. Chem.* **281,** 20077–20084
71. Berny, M. A., White, T. C., Tucker, E. I., Bush-Pelc, L. A., Di Cera, E., Gruber, A., and McCarty, O. J. (2008) *Arterioscler. Thromb. Vasc. Biol.* **28,** 329–334

CHAPTER IV

Investigating the Role of the 145-150 Loop in Thrombin Allostery

In the previous chapters, we demonstrated that human thrombin exists in equilibrium between inactive E* and active E conformations (*1-3*), and that deletion of the nine residues ^{146}ETWTANVGKG^{149e} from the autolysis loop of human thrombin results in stabilization of its E* conformation (*4*). As a result, relative to the wild type enzyme the activity of Δh146-149e was significantly but identically compromised for all synthetic and physiological substrates tested including protein C in the absence but not in the presence of TM. Hence, the TM-PC complex can trigger the E* to E transition and restore almost full catalytic enhancement of PC activation (*4*).

Furthermore, structural and kinetic studies have demonstrated that murine thrombin unlike its human counterpart, lacks Na^+ activation (*5*). However, the enzyme is functionally stabilized in an E:Na^+-like conformation and retains high catalytic activity towards all its physiological substrates (*5, 6*). Obviously the thirty-two amino acids that differ between human and murine thrombin are responsible for these different functional and structural characteristics between the two enzymes. Six of the thirty-two amino acids residues are located the autolysis loop. The contribution of these six substitutions in the differences in Na^+ dependent allostery between human and murine thrombin is presently unknown.

In this chapter, we build upon these data and investigate further what role the length and amino acid composition of the autolysis loop play in thrombin allostery, particularly its effects in the E* to E transition and stabilization of E and E:Na^+ conformations of thrombin. Here, we report the generation and characterization of two autolysis loop

mutants (Table 4.1). The first is Δh145-150 in which ^{145}KG^{150} were further deleted from Δh146-149e to generate an eleven residue deletion mutation. In the second mutant, hm145-150, the human autolysis loop was replaced with the autolysis loop from its murine counterpart by substituting the six ^{145}K, ^{149a}A and ^{149c}VGKG^{150} to the corresponding murine residues (Table 4.1).

Enzyme	Sequence	Description
hwt	^{140} GWGNLKETWTANVGKGQPSV^{154}	Human wild type
mwt	GWGNLRETWTTN I NE I QPSV	Murine wild type
Δh146-149e	GWGNLK - - - - - - - - - - GQPSV	Human with 9 residue deletion
Δh145-150	GWGNL- - - - - - - - - - - QPSV	Human with 11 residue deletion
hm145-150	GWGNLRETWTTN I NE I QPSV	Human with murine autolysis loop

Table 4.1 Amino Acid sequence of autolysis loop constructs generated in this chapter

MATERIALS & METHODS

Human thrombin mutants Δh145-150 and hm145-150 (Table 4.1) were constructed, expressed and characterized as described in chapters 2 and 3.

RESULTS & DISCUSSION

Δh145-150

Mutagenesis studies on the autolysis loop of human thrombin have previously shown that shorter loops disproportionately compromise the procoagulant/prothrombotic substrates

compared to the anticoagulant protein C (*4, 7, 8*). Molecular determinants of this effect originates from the stabilization of the E* conformation (*1*). Hence, the Δh145-150 mutant was designed and constructed in anticipation that it will be relatively more stabilized in the E* conformation compared to Δh146-149e. As a result of deleting two more residues, we expected to generate a mutant with a significantly more compromised catalytic activity towards all substrates, but one whose activation of protein C in the presence of TM will be comparable to the hwt enzyme as observed in Δh146-149e. When successful, these properties will increase its anticoagulant and antithrombotic profile relative to Δh146-149e, thereby making it a better therapeutic agent.

The functional properties of Δh145-150 were tested under physiological conditions against a diverse set of chromogenic and macromolecular substrates (Figure 4.1). The value of k_{cat}/K_M for substrate hydrolysis is significantly affected relative to the wt for all substrates but the extent of the effect varies with each substrate. More importantly, the activation of protein C is not restored relative to the wt in the presence of TM resulting in no gain in the anticoagulant profile. This observation is directly contrary to what will be expected from an exclusive E* stabilization in which we would observe a similar effect on k_{cat}/K_M irrespective of substrate and restoration of protein C activation in the presence of TM, as demonstrated for Δh146-149e in chapter 3. Several plausible explanations can account for this unexpected observation including; the longer deletion (i) affects the E* to E transition and/or (ii) interferes with the intrinsic catalytic properties of the enzyme.

To investigate the molecular origins of its observed kinetic profile, crystals of Δh145-150 were grown in the presence and absence of Na^+. Structure of the mutant in the absence of Na^+ was obtained in the E* conformation of thrombin. All the structural signatures of E* were observed (Figure 4.2 and Figure 4.3); abrogation of the Na^+ binding site, collapse of the 215-217 β-strand into the active site and a disruption of oxyanion hole. The structure of Δh145-150 in the absence of Na^+ is practically similar to the E* form of Δh146-149e.

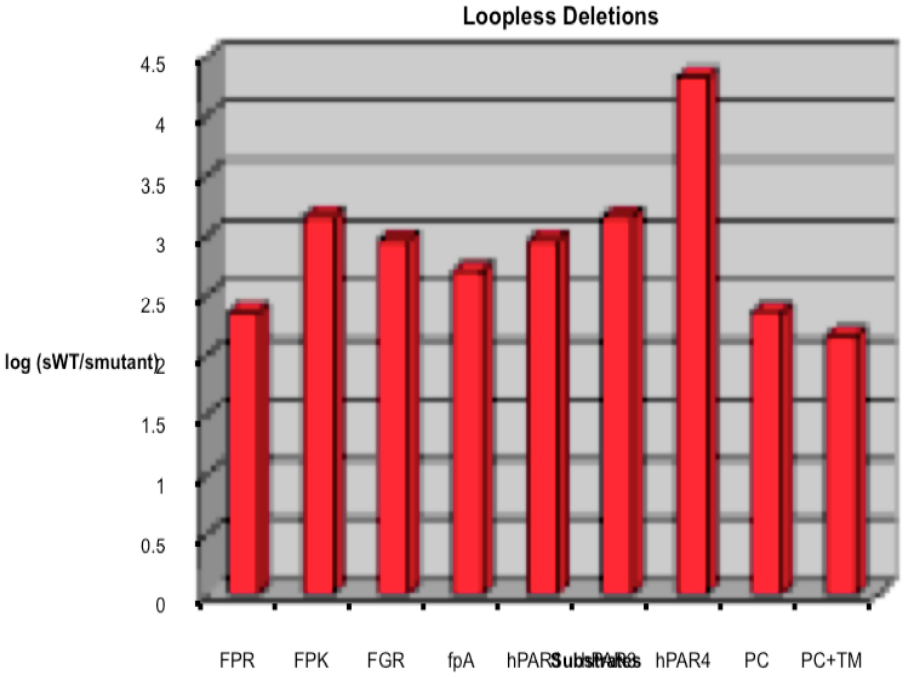

Figure 4.1. Functional properties of the thrombin mutant Δh145-150. Shown are the values of $s=k_{cat}/K_M$ for the hydrolysis of chromogenic substrates FGR, FPK and FPR, fibrinogen (FpA), PAR1, PAR3, PAR4, protein C (PC) and protein C (PC+TM) in the presence of 100 nM thrombomodulin and 5 mM $CaCl_2$ for the thrombin mutant Δh145-150 (s_{mut}) relative to wild-type (s_{wt}). Each substrate experiences a different loss of activity that cannot be reconciled with an exclusive perturbation of the E*-E equilibrium in favor of the inactive form E*, as recently reported for the Δ146-149e mutant (chapter 3). Experimental conditions are: 5 mM Tris, 0.1% PEG8000, 145 mM NaCl, pH 7.4 at 37 °C. The values of s_{wt} are: 0.52±0.05 $\mu M^{-1}s^{-1}$ (FGR), 4.2±0.2 $\mu M^{-1}s^{-1}$ (FPK), 37±1 $\mu M^{-1}s^{-1}$ (FPR), 17±1 $\mu M^{-1}s^{-1}$ (FpA), 39±1 $\mu M^{-1}s^{-1}$ (PAR1), 0.35±0.02 $\mu M^{-1}s^{-1}$ (PAR3), 0.34±0.01 $\mu M^{-1}s^{-1}$ (PAR4), 59±3 $M^{-1}s^{-1}$ (PC), 0.22±0.01 $\mu M^{-1}s^{-1}$ (PC+TM).

On the other hand, in the presence of Na^+, Δh145-150 is stabilized in the canonical E: Na^+ conformation, but with one notable exception. Although the collapse of the 215-217 β-strand into the active site is corrected with Trp-215 moving back into the position observed in the E: Na^+ form of wt, the disruption of the of the oxyanion hole is not restored to its proper architecture. Collectively, these functional and structural data indicate that in addition to the E* to E equilibrium pertubation, the intrinsic catalytic properties of the enzyme are affected by the longer deletion mutation.

The kinetic and structural properties of Δh145-150 are not unique to this mutant, however. Similar properties were recently observed in the N143P mutant of human thrombin. Each substrate analyzed was perturbed to a different extent, an E* conformation was crystallographically observed in the absence of Na^+ and the Na^+-bound structure also features a disruption of the oxyanion hole. A proper architecture of the oxyanion hole is required to stabilize the tetrahedral intermediate during substrate hydrolysis and is directly under the control of the bound Na^+ *(3, 4)*.

Comparison between the N143P and Δh145-150 Na^+-bound conformations indicate that in both structures, despite the different mutations, a highly conserved H-bond between the carbonyl O atom of residue 192 and the backbone N atom of residue 143 on the adjacent β-strand is broken (Figure 4.3). When this important H-bond interaction is lost, the 192-193 peptide bond flips and the oxyanion hole pocket is disrupted. As in the case of the N143P mutant, Na^+ has lost the ability to regulate the architecture of the oxyanion hole in Δh145-150, thereby affecting the intrinsic kinetic properties of both enzymes.

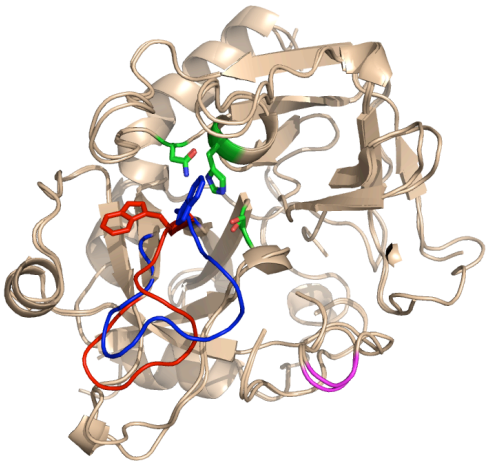

A

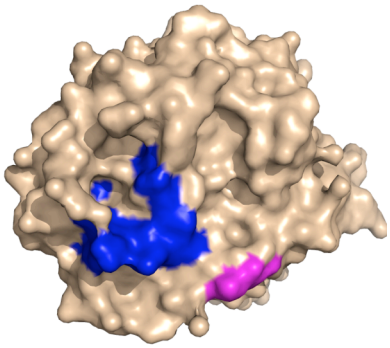

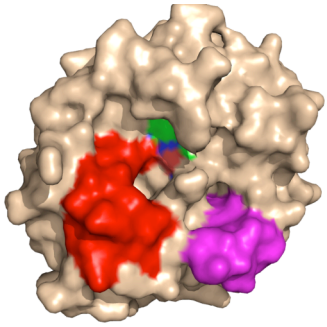

B C

Figure 4.2 Crystal Structure of Δh145-150 in the E* and E: Na^+ forms. A. Structural alignment of Δh145-150 E* and Δh145-150 E:Na^+ in cartoon representation. Occlusion of the active site cleft in the E* by the 215-217 B-strand (blue) compared to E: Na^+ conformation (red). B and C are surface representation of Δh145-150 E* and E: Na^+ structures respectively. Note how the catalytic residues and active site cleft are completely occluded in B and accessible in C.

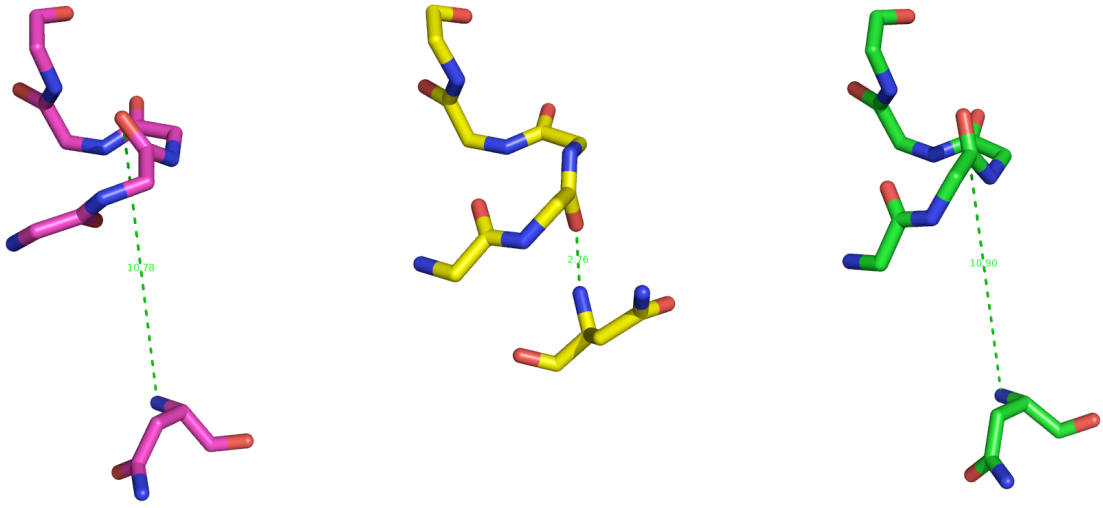

A B C

Figure 4.3 Achitecture of the oxyanion hole in (A) Δh145-150 E* (B) hWT and (C) Δh145-150 E:Na^+. Conserved H-bond between carbonyl O atom of Glu-192 and backbone N atom of 143 is broken in Δh145-150 E* and Δh145-150 E: Na^+ but not in hWT. As a result, the 192-193 peptide bond flips and the oxyanion hole is disrupted.

Mutants that are stabilized in the E* confirmation and whose catalytic properties are significantly compromised have great potential application for *in vivo* studies. Such mutants can complement functional studies of anticoagulant and antithrombotic mutants such as W215A/E217A (WE). For instance, Berny *et. al.* have shown that although WE cannot activate platelets, it can interact with platelets through GPIb and disrupts the GPIb-dependent binding to von Willebrand factor-collagen under shear (*9*). Wt or the catalytically inactive S195A mutant cannot produce these effects, indicating that some unique feature (s) of WE is responsible for its antagonistic properties against GPIb. To date, the molecular basis of this antithrombotic property of WE is unknown. However,

the E* features, the specific mutation effects or some yet unknown characteristic of WE is definitely causing this anomalous and extraordinary interaction of WE with GPIb. Therefore, Δh145-150 can be an excellent control to test the hypothesis that WE's E* nature is responsible for antagonizing GPIb.

hm145-150

Previous attempts to mimic the activating effects of Na^+ in human thrombin or other type II- Na^+ activating enzymes were moderately successful as they generally results in poor activity enzymes both in the presence and absence of Na^+ (*6, 10, 11*). However, structural and kinetic studies reveal that murine thrombin has successfully mimicked the E:Na^+ conformation of human thrombin (*5*). The origin of this remarkable property is not fully understood as the swapping of the entire Na^+ binding loops of murine thrombin into the human enzyme did not result in a high activity Na^+ independent enzyme (*6*).

However, biochemical studies have shown that one of the effects of Na^+ binding to human thrombin is to stabilize the highly flexible autolysis loop (*12*), which in the murine enzyme is intrinsically stable due to intra-loop interactions (*13, 14*). These interactions originate from six critical amino acid substitutions that differ between the autolysis loop of murine and human thrombin (Table 4.1). The contribution of amino acid composition of the autolysis loop in the Na^+ dependent allostery of human thrombin has not been previously investigated although this loop is not highly conserved in thrombin

molecules from different species (*15*). In this section, we directly addressed the role of the autolysis loop in the different Na^+ response between murine and human thrombin.

When the human autolysis loop is replaced with its murine counterpart, the catalytic properties of the mutant are intermediate between those of the two enzymes. In the absence of Na^+, the activity of the hm145-150 is higher than that of human but less than murine thrombin, while the converse is true in the presence of Na^+. Figure 4.4 shows that k_{cat}/K_M of hm145-150 for FPR hydrolysis was enhanced 7-fold relative to hwt thrombin in the absence of Na^+, and that the effect of Na^+ on the kinetic properties of the mutant was drastically reduced as demonstrated by only a 3-fold compared to a 27-fold enhancement in k_{cat}/K_M in hm145-150 and hWT respectively. Similar results were obtained for other chromogenic and macromolecular substrates tested. These data indicate that most of the Na^+ independent high activity effect of murine thrombin and low activity of slow form of human thrombin originate from the amino acid composition of their respective autolysis loops.

Furthermore, kinetics and thermodynamic of Na^+ binding studies were performed to assess the effect of the autolysis loop swap on the Na^+ dependent allostery. Na^+ binding to hWT thrombin is biphasic in kinetics and is characterized by large enthalpy and entropy change of -22 kcal/mol and -64 cal/mol/K respectively (*1, 10, 16*). A major contribution to these thermodynamic parameters originate from the six ligating interactions involving Na^+, and the uptake and re-ordering of water molecules that transmit Na^+ binding through the water channel to activity in the active site(*17*). In

addition, Na^+ binding is accompanied by a large intrinsic heat capacity change of -500 cal/mol/K, but the molecular origins of this effect have not been uncovered so far (*16*)

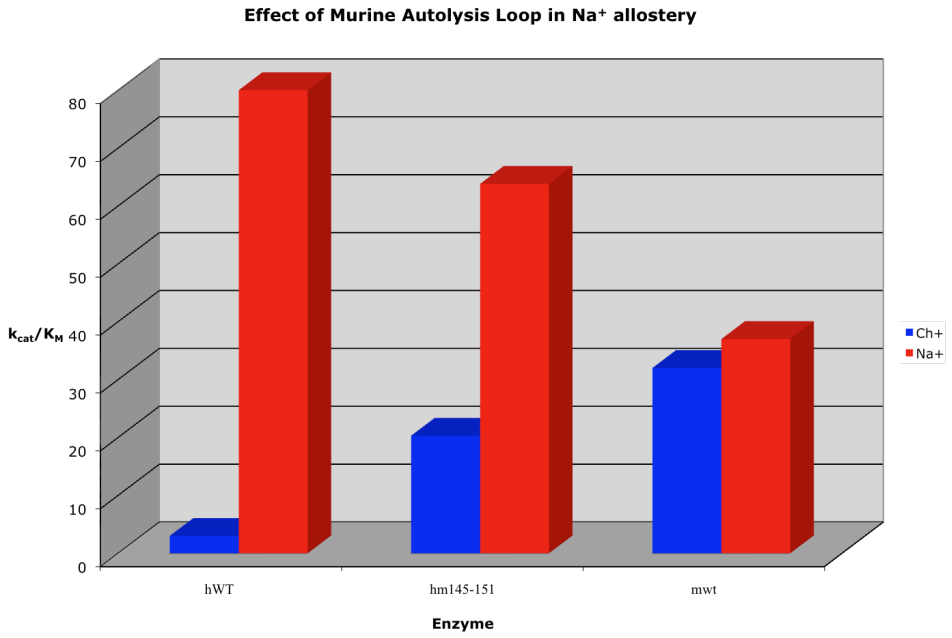

Figure 4.4. Effect of Na^+ on FPR substrate hydrolysis. Shown are the values of $s=k_{cat}/K_M$ for the hydrolysis of chromogenic substrate FPR in the presence or absence of Na^+ by human wild type (hWT), hm145-150 and murine wild thrombin (mWT). Experimental conditions are: 5 mM Tris, 0.1% PEG8000, 200 mM NaCl or ChCl, pH 8 at 25°C.

Stopped flow fluorescence measurements of Na^+ binding to hm145-150 shows a similar biphasic binding mechanism as observed in the hwt, indicating the presence of E*, E and E: Na^+ forms (Figure 4.6). However, as highlighted from the amplitude of the slow phase in Figure 4.6 and data fitting analysis, in hm145-150, the E* to E equilibrium is shifted more towards E and that Na^+ binds with a higher affinity relative to hWT. In addition, equilibrium-binding measurements using static fluorescence were performed in the temperature range from 5 to 40 ^oC to investigate the thermodynamic signatures of Na^+

binding. Under all the conditions tested, hm145-150 has a higher binding affinity compared to the hWT. Moreover, van't Hoff plot of Na^+ binding to hm145-150 shows a linear relationship between log K versus T^{-1} where K is the apparent Na^+ binding affinity and T is the absolute temperature in Kelvin (Figure 4.8). Lack of curvature in the van't Hoff plot indicates that unlike the hwt enzyme, no heat capacity change is associated with Na^+ binding for this hm145-150 (*1*).

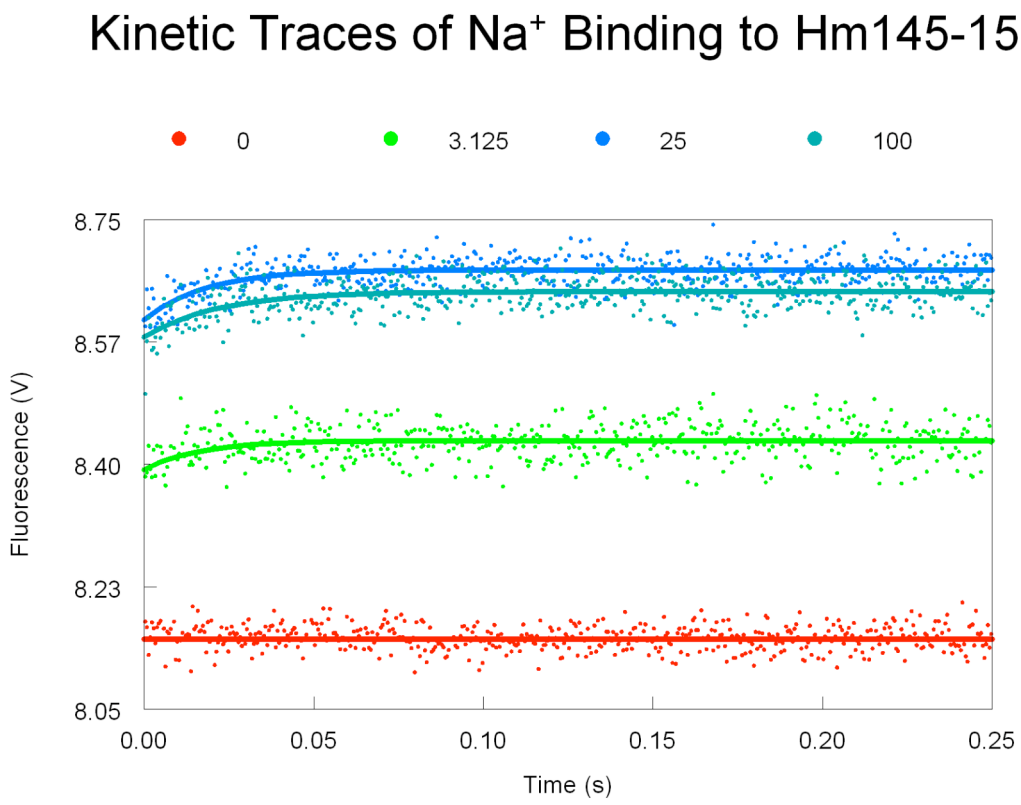

Figure 4.5 Kinetic traces of Na^+ binding to hm145-150 in the 0–250-ms time scale. Notice how the binding of Na^+ obeys a two-step mechanism, with a fast phase completed within the dead time (<0.5 ms) of the spectrometer, followed by a single-exponential slow phase. Shown are the traces obtained at 0 (*red circles*), 3.125 (*green circles*), 25

(*blue circles*), and 100 (*cyan circles*) mM Na^+. Experimental conditions were 50 nM thrombin, 50mMTris, 0.1% PEG, pH 8.0, at 15 °C. Continuous lines were drawn using the expression $a\{1-\exp(-k_{obs}t)\}+b$ with best-fit parameter values: *red circles*, a = 0.000 ± 0.000 V, k_{obs} = 0.0 ± 0.0 s^{-1}, b = 8.15 ± 0.011 V ; green *circles*, a = 0.0414 ± 0.0001 V, k_{obs} = 60.7 ± 15.1 s^{-1}, b =8.393 ±0.001 V ; *blue circles*, a =0.0714 ±0.0002 V, k_{obs} = 56.3± 6.4 s^{-1}, b =8.647 ± 0.012 V ; *cyan circles*, a =0.0645 ± 0.001V, k_{obs} =45.79 ± 5.6 s^{-1}, b =8.5825 ± 0.0024 V ;

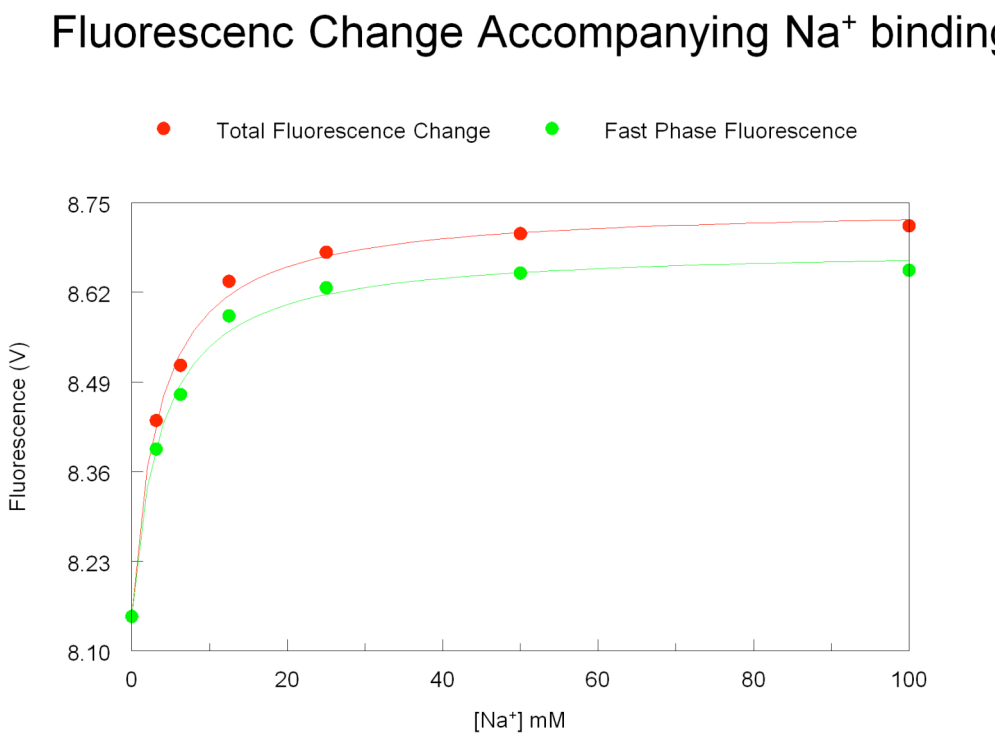

Figure 4.6 Na^+ binding to hm145-150. Binding isotherm obtained from total fluorescence change and amplitude of fast phase. Note how the contribution of the slow phase, which represents the E* to E transition is negligible. $K_{Aapp} \sim K_A = 288\ M^{-1}$

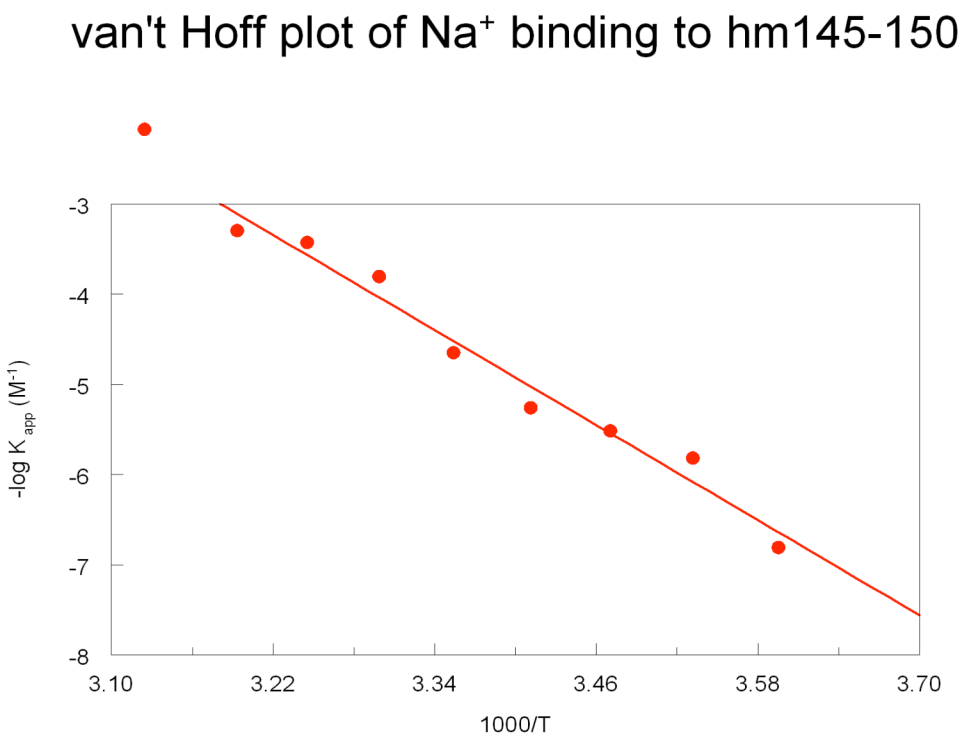

Figure 4.7 van't Hoff plot Na+ binding to hm145-150. Continuous line was drawn with best-fit parameter values of ΔH= -17.43 kcal/mol, ΔS= -49.48 kcal/mol.K and ΔC_p= 0.0

To gain further insight into the molecular origins of the Na^+ effects in hm145-150, crystal structures of the mutant were solved in the presence and absence of Na^+. In hwt thrombin, there are subtle but important structural differences between the E and E: Na^+ forms. These include (i) an ion-pair between Arg187 and Asp222 that stabilizes the Na^+ binding site, (ii) the rotation of the Asp 189 in the primary specificity pocket, (iii) H-bonding of catalytic Ser195 and His57 and (iv) the architecture of the water channel that spans from the Na^+ site to the active site. In hm145-150 structures, these differences between E and E: Na^+ forms are not observed and both structures are similar to the E: Na^+ form of hWT. Most notably, the entire autolysis loop was defined, and unlike hWT,

E and E: Na^+ structures are basically identical. These structural characterizations gives a plausible rationale for the observed catalytic properties, high Na^+ affinity and lack of heat capacity change associated with Na^+ binding.

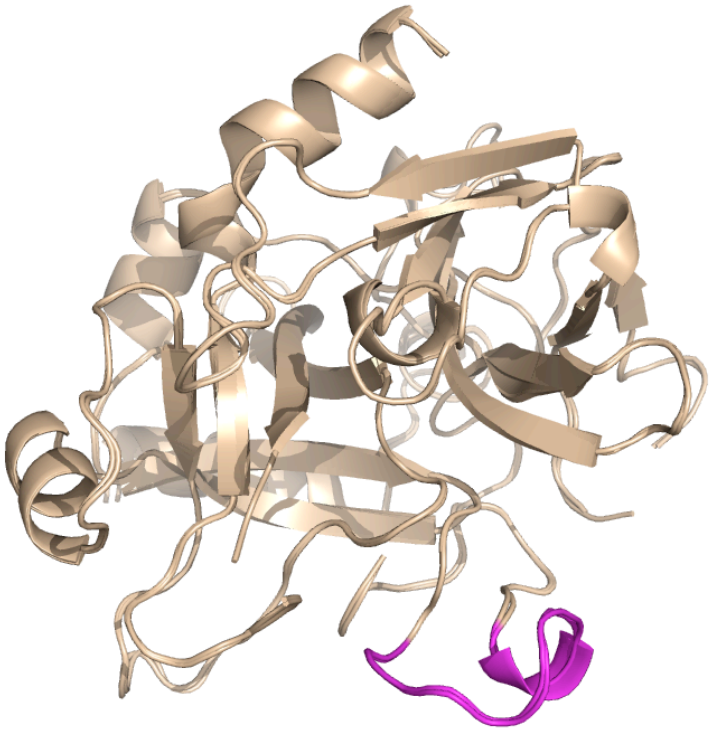

Figure 4.8 Alignment of the Crystal Structures of hm145-150 in the presence and absence of Na^+. Na^+-free and Na^+-bound forms of hm145-150 are practically identical and are similar to Na^+-bound form of hWT [rmsd = 0.257 Å].

What is the molecular mechanism responsible for the remarkable involvement of this loop in thrombin allostery? Structural and thermodynamic analysis may hold a key to this answer. When the first crystal structures of human thrombin were solved, it was hypothesized that the main function of the autolysis loop was to restrict access to the active site cleft, endowing thrombin and other clotting factors that have longer loops with relatively narrow substrate specificity. However, data emerging from this thesis indicate

this loop is critical in allostery as well. In many human thrombin structures, the autolysis loop is either not defined due to poor electron density or it assumes different conformations depending on crystallization conditions, demonstrating an inherently flexible region. However, Na^+ and other effector binding have been shown to rigidify and stabilize this loop, thereby reducing exposure to proteolysis cleavage (*12*). Therefore, the flexibility of the human autolysis reduces the affinity of Na^+ due to an entropic cost associated with its stabilization by Na^+.

However, amino acid composition analysis of the autolysis loop in murine thrombin indicates that this loop has a lower flexibility tendency due in part to the replacement of two Gly residues with Ile. Indeed, intra-molecular interactions within this loop stabilize it and as a result it is almost always well defined in crystal structures. A stable autolysis loop in murine thrombin has been observed in structures whether free or bound to different ligands (*13, 14*). Similar evidence came from the structural characterization of hm145-150 that shows that amino acid composition of the autolysis loop can stabilize the loop through intra loop interaction irrespective of Na^+.

Revealing the mechanism of the molecular mimicry of Na^+ activation in murine thrombin and its engineering in human thrombin has great potential for understanding other mechanism of type II M^+ activation. The knowledge gained in these studies can facilitate the rational redesign and engineering of more proficient proteases.

References:

1. Bah, A., Garvey, L. C., Ge, J., and Di Cera, E. (2006) Rapid kinetics of Na+ binding to thrombin, *J Biol Chem 281*, 40049-40056.
2. Gianni, S., Ivarsson, Y., Bah, A., Bush-Pelc, L. A., and Di Cera, E. (2007) Mechanism of Na+ binding to thrombin resolved by ultra-rapid kinetics, *Biophys Chem 131*, 111-114.
3. Pineda, A. O., Chen, Z. W., Bah, A., Garvey, L. C., Mathews, F. S., and Di Cera, E. (2006) Crystal structure of thrombin in a self-inhibited conformation, *J Biol Chem 281*, 32922-32928.
4. Bah, A., Carrell, C. J., Chen, Z., Gandhi, P. S., and Di Cera, E. (2009) Stabilization of the E* form turns thrombin into an anticoagulant, *J Biol Chem 284*, 20034-20040.
5. Bush, L. A., Nelson, R. W., and Di Cera, E. (2006) Murine thrombin lacks Na+ activation but retains high catalytic activity, *J Biol Chem 281*, 7183-7188.
6. Marino, F., Chen, Z. W., Ergenekan, C., Bush-Pelc, L. A., Mathews, F. S., and Di Cera, E. (2007) Structural basis of Na+ activation mimicry in murine thrombin, *J Biol Chem 282*, 16355-16361.
7. Dang, Q. D., Sabetta, M., and Di Cera, E. (1997) Selective loss of fibrinogen clotting in a loop-less thrombin, *J Biol Chem 272*, 19649-19651.
8. Le Bonniec, B. F., Guinto, E. R., and Esmon, C. T. (1992) Interaction of thrombin des-ETW with antithrombin III, the Kunitz inhibitors, thrombomodulin and protein C. Structural link between the autolysis loop and the Tyr-Pro-Pro-Trp insertion of thrombin, *J Biol Chem 267*, 19341-19348.
9. Berny, M. A., White, T. C., Tucker, E. I., Bush-Pelc, L. A., Di Cera, E., Gruber, A., and McCarty, O. J. (2008) Thrombin mutant W215A/E217A acts as a platelet GpIb antagonist, *Arterioscler Thromb Vasc Biol 18*, 329-334.
10. Prasad, S., Wright, K. J., Roy, D. B., Bush, L. A., Cantwell, A. M., and Di Cera, E. (2003) Redesigning the monovalent cation specificity of an enzyme, *Proceedings of the National Academy of Sciences of the United States of America 100*, 13785-13790.
11. Page, M. J., Bleackley, M. R., Wong, S., MacGillivray, R. T. A., and Di Cera, E. (2006) Conversion of trypsin into a Na+ activated enzyme, *Biochemistry 45*, 2987-2993.
12. De Filippis, V., De Dea, E., Lucatello, F., and Frasson, R. (2005) Effect of Na+ binding on the conformation, stability and molecular recognition properties of thrombin, *The Biochemical journal 390*, 485-492.
13. Bah, A., Chen, Z., Bush-Pelc, L. A., Mathews, F. S., and Di Cera, E. (2007) Crystal structures of murine thrombin in complex with the extracellular fragments of murine protease-activated receptors PAR3 and PAR4, *Proc Natl Acad Sci USA 104*, 11603-11608.
14. Gandhi, P. S., Page, M. J., Chen, Z., Bush-Pelc, L. A., and Di Cera, E. (2009) Mechanism of the anticoagulant activity of the thrombin mutant W215A/E217A, *J Biol Chem 284*, 24098-24105.
15. Banfield, D. K., and MacGillivray, R. T. (1992) Partial characterization of vertebrate prothrombin cDNAs: amplification and sequence analysis of the B

chain of thrombin from nine different species, *Proceedings of the National Academy of Sciences of the United States of America 89*, 2779-2783.
16. Guinto, E. R., and Di Cera, E. (1996) Large heat capacity change in a protein-monovalent cation interaction, *Biochemistry 35*, 8800-8804.
17. Pineda, A. O., Carrell, C. J., Bush, L. A., Prasad, S., Caccia, S., Chen, Z. W., Mathews, F. S., and Di Cera, E. (2004) Molecular dissection of Na+ binding to thrombin., *J Biol Chem 279*, 31842-31853.

CHAPTER V

Discovery of E* in other vitamin K dependent clotting factors

Kinetic and structural studies of the mechanism of Na^+ binding to thrombin demonstrate that the Na^+ -free form (slow form) of thrombin exists in dynamic equilibrium between two conformations E* and E (*1-4*). E is the active conformation of the enzyme responsible for the catalytic activity of the enzyme in the absence of Na^+ (*5*). However, E* is an inactive conformation which is unable to interact with either Na^+ or substrates and is structurally distinct from the active forms (E and E:Na^+).

The structural features of E* are not unique to thrombin. The collapse of the 215-217 β-strand into the active site while still maintaining an intact Ile-16 – Asp-194 has been observed in the structures of several members of the trypsin-like serine protease (*6*). A plausible hypothesis resulting from the widespread observation of inactive conformations of trypsins is that the E*--E equilibrium is a universal property of a plastic trypsin fold that optimizes activity and specificity after the occurrence of zymogen activation. To begin to test this hypothesis, we investigate the existence of E* in all vitamin K -dependent clotting factors. Here we report that like thrombin and meizo-thrombin desF1, E* exists in equilibrium with E in Factor Xa, Factor IXa and activated protein C.

MATERIALS AND METHODS

Expression, purification and activation of human α-thrombin (thrombin) were performed as described elsewhere (*7, 8*). Gla-domainless activated protein C (GDPC) was expressed using a HPC4-modified pRc/RSVvector (a gift from Dr. A. Rezaie) using baby hamster kidney cell line. Purification and activation were done as described in (*9*). Human Factor

Xa (FXa) and human Factor IXa (FIXa) were obtained from Hematologic Technologies Inc (Essex Junction, VT) while Gla-domainless Factor VIIa (GDFVIIa) was obtained from Enzyme Research Laboratories Inc (South Bend, IN).

Intrinsic protein fluorescence was used to study the kinetic mechanism of Na^+ binding to FXa, FIXa, aGDPC and GDFVIIa in an Applied Photophysics SX20 stopped flow spectrophotometer, using an excitation wavelength of 283 nm and a 305 nm cutoff filter as reported in (*1,4*) with one important modification. Due to the interaction and inhibitory effects of quaternary ammonium compounds with the vitamin K dependent clotting factors (*10*), choline chloride could not be used as an inert ion for maintaining a constant ionic strength as previously done for thrombin. Therefore, samples of each clotting factor at a final concentration of 100 nM in 50 mM Tris-HCl and 0.1 % PEG, pH 8 at 15 ^oC was mixed in 1:1 ratio with the same buffer containing increasing concentration of NaCl. To check and ensure that nonspecific ionic effects are not affecting our results, Na^+ binding to human thrombin was repeated without maintaining a constant ionic strength and results obtained were similar to the previously published data.

The fluorescence change accompanying Na^+ binding is characterized by a two-step binding mechanism, an initial fast phase that is too rapid to be resolved within the dead time of the instrument and a single exponential slow phase whose observed rate constant (k_{obs}) decreases hyperbolically with increasing concentration of Na^+ (see "Results"). The initial fast phase shows an increase in fluorescence for FIIa, FXa, FIXa and GDFVIIa but not for GDaPC where it shows a fluorescence quenching. The total change in

fluorescence, F, calculated from the sum of the amplitudes of the slow and fast phases is therefore expected to decrease for GDaPC accordingly. The value of F as a function of Na^+ was fit according to Equation 1 (*11*)

$$F = \frac{\left(F_0 + F_1 K_{app}[Na^+]\right)}{\left(1 + K_{app}[Na^+]\right)} \qquad \text{Equation 1}$$

where F_0 and F_1 are the values of F in the absence and under saturating $[Na^+]$ and K_{app} is the apparent equilibrium association constant for Na^+ binding. However, due to the small fluorescence change observed for Na^+ binding to GDFVIIa (Figue 5.1e), its K_{app} could not be obtained with confidence from data analysis using equation 1.As previously described for human thrombin (*1*), the simplest kinetic scheme accounting for the two-step mechanism of Na^+ binding to each clotting factor is

$$E^* \underset{k_{-1}}{\overset{k_1}{\rightleftharpoons}} E \quad \overset{K_A}{\Leftrightarrow} \quad E:Na^+ \qquad \text{Scheme 1}$$

where the free enzyme exists in dynamic equilibrium between two forms, ***E**** and ***E***, that interconvert with kinetic rate constants k_1 and k_{-1}. However, only ***E*** can interact with Na^+ with an equilibrium intrinsic association constant K_A to generate ***E:Na***$^+$, which results in the fast phase. The slow phase is the result of the inter-conversion between ***E**** and ***E*** with a observed rate constant, k_{obs} given by

$$k_{obs} = k_1 + k_{-1}\frac{1}{1 + K_A[Na^+]} \qquad \text{Equation 2}$$

According to scheme 1 the value of k_{obs} is expected to decrease with increasing $[Na^+]$ from (k_1+k_{-1}) to k_1 when $[Na^+]$ increases from 0 to ∞. Analysis of k_{obs} according to equation 2 yields the rates of conversion of $k_1$and k_{-1}, as well as K_A. There is a relationship between the apparent equilibrium association constant K_{app} from equation 1 and K_A because of the presence of ***E**** and ***E***,

$$K_{app} = \frac{K_A}{1 + \frac{k_{-1}}{k_1}} = \frac{K_A}{1 + r} \qquad \text{Equation 3}$$

where the parameter r=[E*]/[E] measures the population of E* relative to E (Table 1).

RESULTS

The stopped flow fluorescence measurements for Na^+ binding to FXa, GDaPC and FIXa clearly reveals a two step binding mechanism as previously shown for thrombin and meizo-thrombin desF1 (Figure 5.1), thereby indicating similar molecular conformational changes. A rapid fast phase that occurs within the dead time of the instrument is followed by a single exponential slow phase whose k_{obs} decreases hyperbolically with increasing $[Na^+]$ (Figure 5.2). The k_{obs} dependence on $[Na^+]$ is consistent with the mechanism shown in scheme 1 and Equation 3. This supports the conclusion that, like thrombin, FXa, GDaPC and FIXa exist in equilibrium between two inter-converting conformations, E* and E where only E can interact with Na^+ giving rise to the fast phase. The observed slow phase is due to the inter-conversion between E* and E that occurs on the time scale of milliseconds while the fast phase occurs on microsecond time scale.

The total fluorescence change accompanying Na^+ binding is obtained from the sum of the amplitudes of the slow and fast phases and it increases hyperbolically with increasing [Na^+] (Figure 5.3) and equation 1. Analysis of Na^+ binding curves enables the determination of K_{app} while the analysis of k_{obs} as a function of [Na^+] gives a direct measurement of K_A, k_1 and k_{-1} using equation 2 (Figure 2 and Table 1).

It is of interest to note that of all the clotting factors, only GDaPC shows a decrease in fluorescence due to Na^+ binding (fast phase) preceding an increase in fluorescence in the E* to E conversion. This observation was totally missed when using steady state fluorescence to monitor monovalent cation binding and could account in part for the lower %F change compared to thrombin and FXa. Na^+ binding to FXa shows more significant fluorescent change compared to the thrombin although it has fewer number of tryptophan residues. Increase in fluorescence change when some tryptophan residues where mutated in thrombin have also been observed (*1*). Because of the presence of several tryptophan residues which are distributed throughout the protease molecule, the changes in fluorescence induced by Na^+ implies these conformational transitions are global effects as was convincingly demonstrated in thrombin through systematic replacements of each tryptophan residue (*1*).

DISCUSSION

The results presented in this study complements the investigation of the molecular mechanisms of Na^+ binding to all vitamin K dependent clotting enzymes, and

demonstrates the existence of E*, E and E: Na^+ in FIXa, FXa and GDaPC. Using steady state measurements of intrinsic fluoresce and kinetic effects linked to Na^+ binding, previous studies have shown the presence of E and E:Na^+. This study revealed for the first time, that E is indeed in dynamic equilibrium with E*. The discovery of E* in the vitamin K dependent clotting enzymes have mechanistic significance in understanding the allosteric pathways, linkage effects of cations and macromolecular cofactors as well as rationalize the effects of mutagenesis studies linked to Na^+. For instance, it has been demonstrated that the Na^+ and Ca^{2+} sites on the protease domains of FVIIa, FIXa, FXa and aPC are thermodynamically linked, but the molecular basis of this observation is unknown. The presence of E* may explain this mechanism, for binding of Ca^{2+} on E will shift the equilibrium away from E* (*12*) resulting in an increase in K_{app}. Secondly, the presence of E* may explain the drastic catalytic properties of some mutants in the absence of Na^+, Ca^{2+} and cofactors.

Like thrombin, activated protein C is involved in multiple distinct functions in the anticoagulant and cytoprotective protein C pathways. Understanding the intrinsic molecular mechanisms may aid in dissociating its functions through rational protein engineering. Activated protein C utilizes both Na^+ and Ca^{2+} for optimal catalytic activity (*13*). In vivo, efficient inactivation of Factor Va, requires both Na^+ and Ca^{2+} and mutations that disrupts the Na^+ allostery are significantly compromised in Ca^{2+} binding and activity towards Factor Va (*13*). Although, the Na^+ site and the Ca^{2+} are thermodynamically, only the former is linked to the active site (*14*).

Factor IXa and Factor Xa function in the tenase and prothrombinase complexes respectively (*15*) and in this context, it has been shown Na^+ is not required neither for the assembly nor for the catalytic enhancement of these membrane complexes (*16, 17*). However, Na^+ in conjunction with Ca^{2+} are needed for the optimal amidolytic properties of each of these enzymes when free in solution (*18, 19*). Therefore, the either the relevant *in vivo* complexes utilitize novel pathways to enhance the catalytic properties of these enzymes or they simply replace the effects of Na^+. Several mutagenesis studies seem to support the latter in that in both FIXa and FXa Y225P mutants whose Na^+ machinery are severely weakened, the catalytic properties are significantly compromised in the presence or absence of $Ca^{2+}$when free in solution. However, when these mutants are assembled in the tenase and prothrombinase complexes, the K_m but not the k_{cat} effect for both small chromogenic and macromolecular substrates are fully restored to that of the wild type (*17, 18*). In addition, both Na^+ and Ca^{2+} ions are required for the effective inhibition of wild type FIXa and FXa and here too, their Y225P mutants are significant compromised for inhibition by antithrombin. These data seem to support that, *in vivo*, because of the roles of $Ca^{2+}$and macromolecular cofactors in mediating the interaction of enzymes and substrates on the surfaces of membranes and their linkage to the Na^+ site, the effect of Na^+ is drastically reduced in wild type FXa and FIXa when incorporated in the tenase and prothombinase complexes respectively. This is reminiscent of role of Na^+ in the presence of thrombomodulin. Not only do these cofactors provide the beneficial effects of Na^+ allostery, they can increase their effects through protein-protein and protein-membrane interactions.

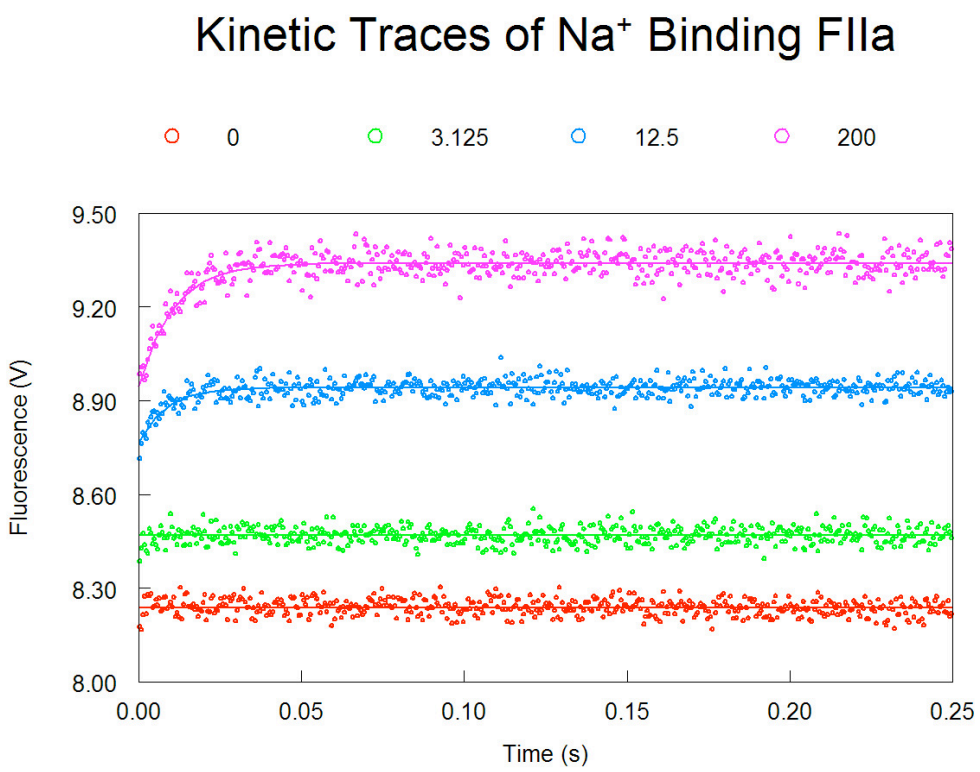

FIGURE 5. 1. Kinetic traces of Na^+ binding to vitamin K dependent clotting factors in the 0–250-ms time scale. Notice how the binding of Na^+ obeys a two-step mechanism, with a fast phase completed within the dead time (<0.5 ms) of the spectrometer, followed by a single-exponential slow phase. The k_{obs} for the slow phase decreases with increasing [Na^+] (see also Fig. 2), as is evident from the plot.

Human α-thrombin. Shown are the traces obtained at 0 (*red circles*), 3.125 (*green circles*), 25 (*blue circles*), and 200 (*magenta circles*) mM Na^+. Experimental conditions were 100 nM thrombin, 50mMTris, 0.1% PEG, pH 8.0, at 15 °C. Continuous lines were drawn using the expression a {1-exp ($-k_{obs}t$)}+ b with best-fit parameter values: *red circles*, a = 0.000 ± 0.000 V, k_{obs} = 0.0 ± 0.0 s^{-1}, b = 8.239 ± 0.016 V; green *circles*, a = 0.000 ± 0.000 V, k_{obs} =0.0 ± 0.0 s^{-1}, b

=8.470 ±0.001 V; *blue circles*, a =0.1754 ±0.0099 V, k_{obs} = 120.0± 9.5 s^{-1}, b =9.1174 ± 0.0012 V; *magenta circles*, a =0.3921 ± 0.0013V, k_{obs} =95.6 ± 4.3 s^{-1}, b =9.7321 ± 0.0025 V ;

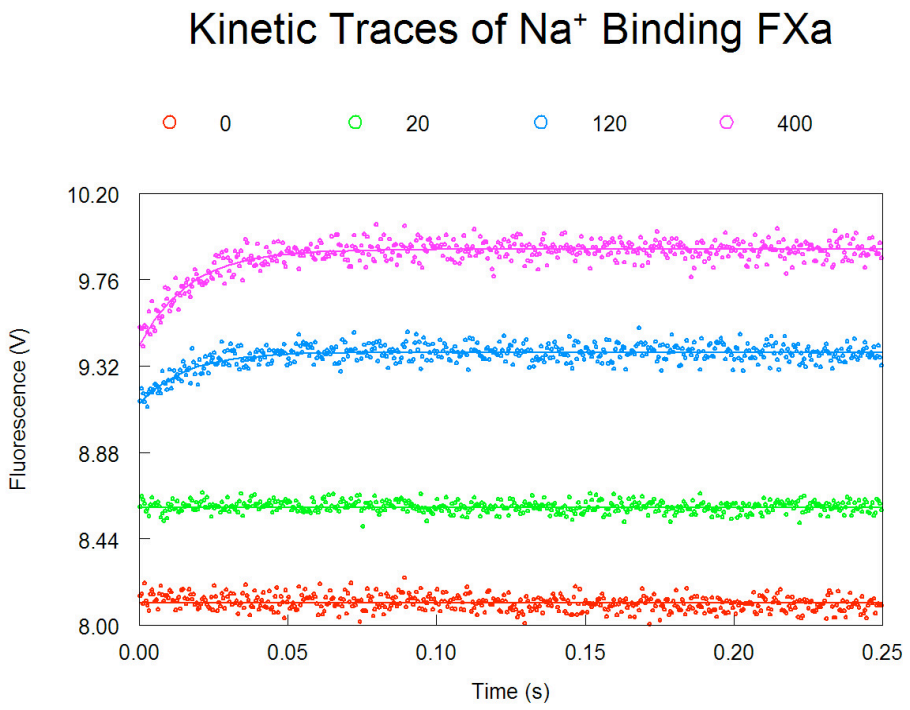

Factor Xa. Shown are the traces obtained at 0 (*red circles*), 20 (*green circles*), 120 (*blue circles*), and 400 (*magenta circles*) mM Na^+. Experimental conditions were 100 nM FXa, 50mMTris, 0.1% PEG, pH 8.0, at 15 °C. Continuous lines were drawn using the expression *a* {1-exp (-$k_{obs}t$)}+ *b* with best-fit parameter values: *red circles*, a = 0.000 ± 0.000 V, k_{obs} = 0.0 ± 0.0 s^{-1}, b = 8.1120 ±0.0001 V; green *circles*, a = 0.000 ± 0.000 V, k_{obs} =0.0 ± 0.0 s^{-1}, b =8.6010 ±0.0019 V; *blue circles*; a =0.2613 ± 0.0017 V, k_{obs} = 64.1 ± 3.9 s^{-1}, b = 9.1297±0.0012 V *magenta circles*, a =0.4876 ±0.0011 V, k_{obs} = 60.3 ± 1.2s^{-1}, b = 9.4274 ± 0.0015 V ;

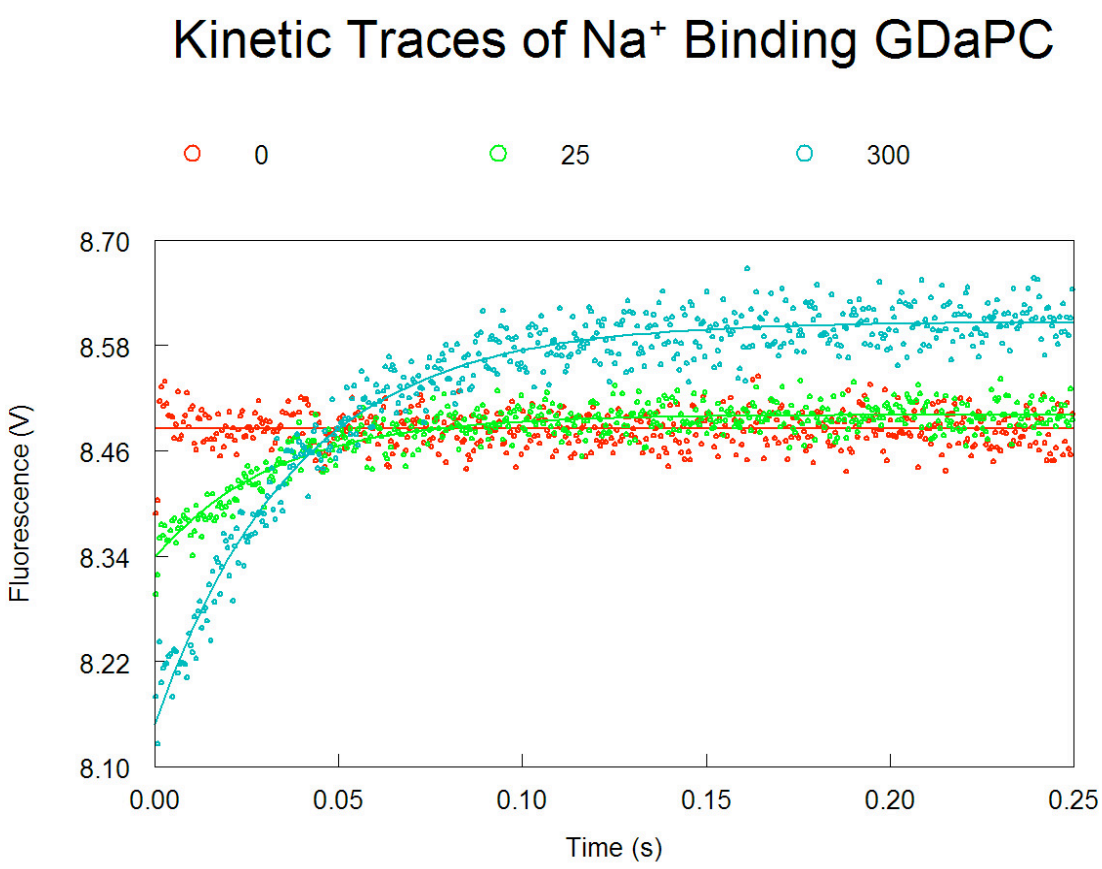

GDaPC. Shown are the traces obtained at 0 (*red circles*), 25 (*green circles*) and 300 (*blue circles*) mM Na^+. Experimental conditions were 100 nM GDaPC, 50mMTris, 0.1% PEG, pH 8.0, at 15 °C. Continuous lines were drawn using the expression a {1-exp ($-k_{obs}t$)}+ b with best-fit parameter values *red circles*, a = 0.000 ± 0.000 V, k_{obs} = 0.0 ± 0.0 s^{-1}, b = 8.4850 ± 0.0013 V; green *circles*, a =0.1617 ±0.0011 V, k_{obs} = 30.7 ± 0.9 s^{-1}, b = 8.3393± V; *blue circles*, a =0.4578± 0.0012V, k_{obs} =26.5 ± 0.4 s^{-1}, b = 8.1492± 0.0011 V

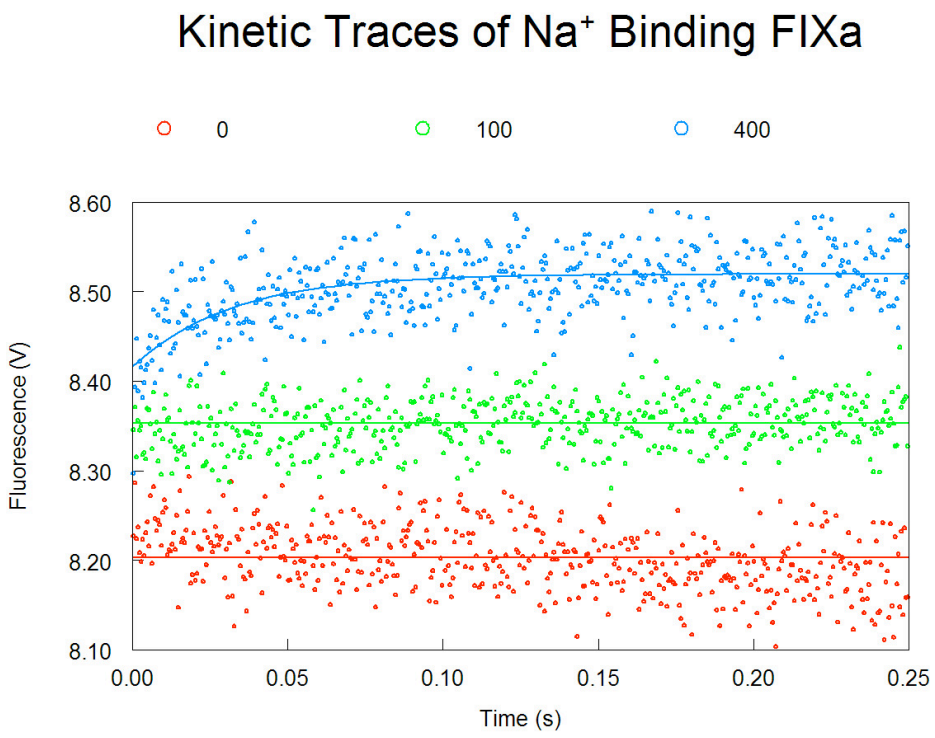

FIXa. Shown are the traces obtained at 0 (*red circles*), 100 (*green circles*) and 400 (*blue circles*) mM Na^+. Experimental conditions were 100 nM FIXa, 50mMTris, 0.1% PEG, pH 8.0, at 15 °C. Continuous lines were drawn using the expression $a\ \{1\text{-exp}\ (-k_{obs}t)\}+ b$ with best-fit parameter values *red circles*, a = 0.000 ± 0.000 V, k_{obs} = 0.0 ± 0.0 s^{-1}, b = 8.2030 ± 0.0012 V; green *circles*, a =0.000 ±0.0000 V, k_{obs} = 0.0 ± 0.0 s^{-1}, b = 8.3530± V; *blue circles*, a =0.1031± 0.0009V, k_{obs} =31.6 ± 0.9 s^{-1}, b = 8.4165± 0.0018 V

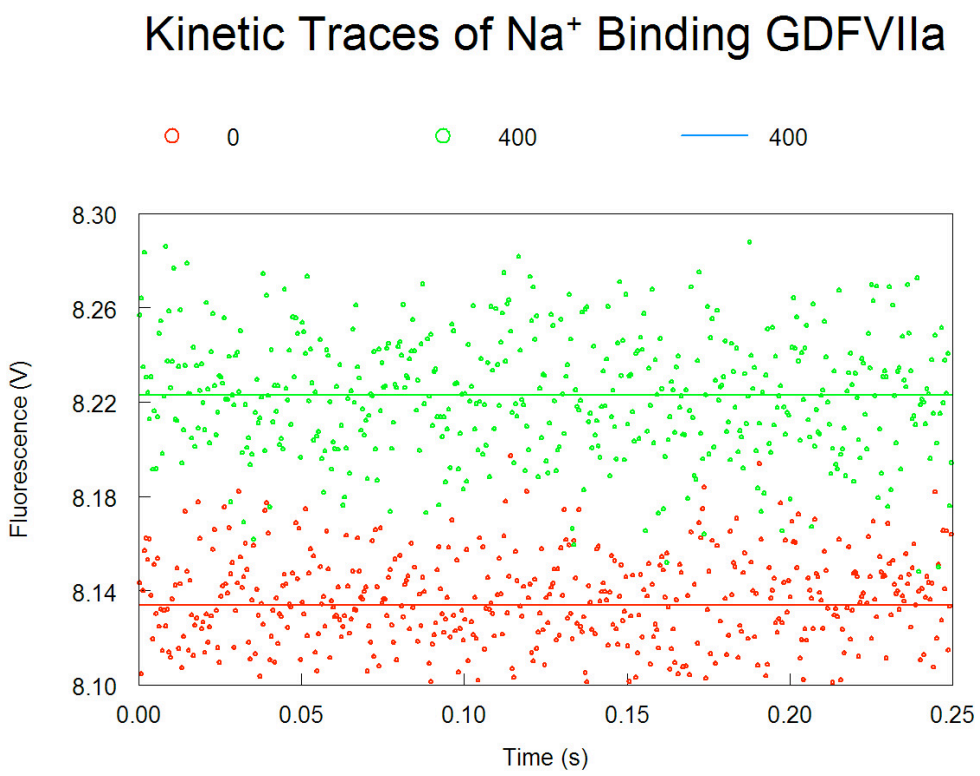

GDFVIIa. Shown are the traces obtained at 0 (*red circles*) and 400 (*green circles*) mM Na^+. Experimental conditions were 100 nM GDFVIIa, 50mMTris, 0.1% PEG, pH 8.0, at 15 °C. Continuous lines were drawn using the expression a {1-exp ($-k_{obs}t$)}+ b with best-fit parameter values *red circles*, a = 0.000 ± 0.000 V, k_{obs} = 0.0 ± 0.0 s^{-1}, b = 8.1340 ± 0.001 V; green *circles*, a =0.000 ±0.0000 V, k_{obs} = 0.0 ± 0.0 s^{-1}, b = 8.2230± 0.0001V

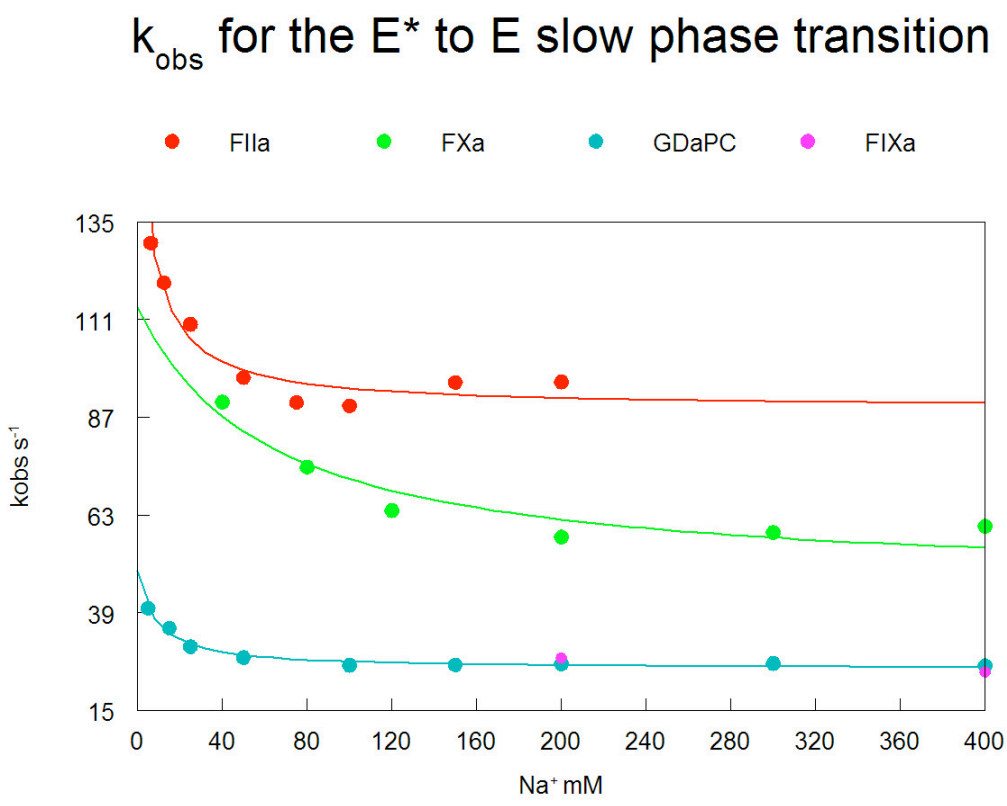

FIGURE 2. Values of *k*obs for the slow phase of fluorescence increase due to Na^+ binding to clotting factors (see Fig. 1) as a function of [Na^+]. Shown are the results pertaining to FIIa (*red circles*), FXa (*green circles*), GDaPC (*blue circles*) and FIXa (*magenta circles*). Continuous lines were drawn according to Equation 2 under "Materials and Methods" with best-fit parameter values listed in Table 1. Continuous lines were drawn according to Equation 3 under "Materials and Methods" with best-fit parameter values listed in Table 1.

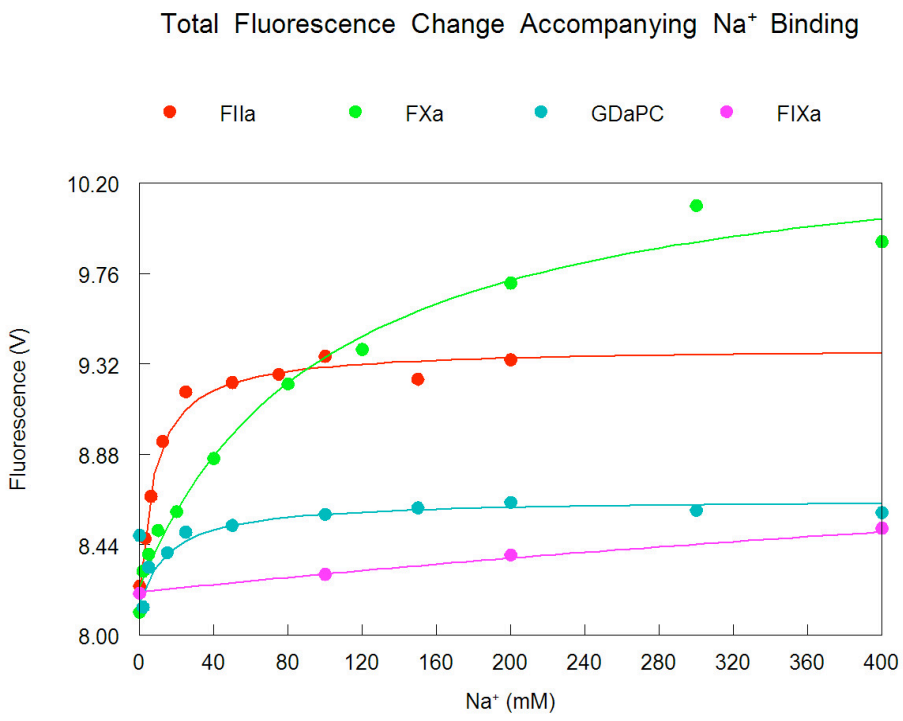

FIGURE 5.3. Na^+ binding curves of clotting factors obtained from the total change in intrinsic fluorescence measured as the sum of the amplitudes of the fast and slow phases determined by stopped-flow kinetics (see Fig. 1). Shown are the results pertaining to FIIa (*red circles*), Fxa (*green circles*), GDaPC (*blue circles*) and FIXa (*magenta circles*). Continuous lines were drawn according to Equation 2 under "Materials and Methods" with best-fit parameter values listed in Table 1.

Clotting Factor	F_0	F_1	$\Delta F/F_0$	K_{app}	K_A	k_1	k_{-1}	r
	V	V	%	M^{-1}	M^{-1}	s^{-1}	s^{-1}	
FIIa	8.20 ± 0.05	9.39 ± 0.03	14.5	119±12	162 ± 20	89±2	85±9	0.95
FXa	8.23 ± 0.05	10.47 ± 0.16	27.2	10 ± 2	16 ± 4	45± 4	68 ± 12	1.49
GDaPC	8.15 ± 0.03	8.66 ± 0.02	6.1	59 ± 3	116 ± 15	25 ± 1	24 ± 3	0.95
FIXa	8.21 ± 0.01	8.51± 0.03	3.6	~ 0.8 ± 0.1	-	-	-	-
GDFVIIa	8.13 ± 0.02	8.22 ± 0.01	1.1	-	-	-	-	-

TABLE 5.1 Fluorescence and binding parameters for Na^+ binding to the Vitamin K dependent clotting factors. The parameters F_0, F_1 and $\Delta F=F_1-F_0$ and K_{app} were derived from analysis of the data in Figure 3 using Equation 1 under "Materials and Methods". The value of K_A, k_1,k_{-1} and $r=k_{-1}/k_1$ were derived from analysis of the data from figure 2 using Equation 2 .

References:

1. Bah, A., Garvey, L. C., Ge, J., and Di Cera, E. (2006) Rapid kinetics of Na+ binding to thrombin, *J Biol Chem 281*, 40049-40056.
2. Pineda, A. O., Chen, Z. W., Bah, A., Garvey, L. C., Mathews, F. S., and Di Cera, E. (2006) Crystal structure of thrombin in a self-inhibited conformation, *J Biol Chem 281*, 32922-32928.
3. Lai, M. T., Di Cera, E., and Shafer, J. A. (1997) Kinetic pathway for the slow to fast transition of thrombin. Evidence of linked ligand binding at structurally distinct domains, *J Biol Chem 272*, 30275-30282.

4. Papaconstantinou, M. E., Gandhi, P. S., Chen, Z., Bah, A., and Di Cera, E. (2008) Na(+) binding to meizothrombin desF1, *Cell Mol Life Sci 65*, 3688-3697.
5. Wells, C. M., and Di Cera, E. (1992) Thrombin is a Na(+)-activated enzyme, *Biochemistry 31*, 11721-11730.
6. Di Cera, E. (2009) Serine proteases, *IUBMB life 61*, 510-515.
7. Dang, Q. D., Guinto, E. R., and Di Cera, E. (1997) Rational engineering of activity and specificity in a serine protease, *Nat Biotechnol 15*, 146-149.
8. Guinto, E. R., Vindigni, A., Ayala, Y. M., Dang, Q. D., and Di Cera, E. (1995) Identification of residues linked to the slow-->fast transition of thrombin, *Proceedings of the National Academy of Sciences of the United States of America 92*, 11185-11189.
9. Rezaie, A. R., and Esmon, C. T. (1992) The function of calcium in protein C activation by thrombin and the thrombin-thrombomodulin complex can be distinguished by mutational analysis of protein C derivatives, *J Biol Chem 267*, 26104-26109.
10. Monnaie, D., Arosio, D., Griffon, N., Rose, T., Rezaie, A. R., and Di Cera, E. (2000) Identification of a binding site for quaternary amines in factor Xa, *Biochemistry 39*, 5349-5354.
11. Prasad, S., Wright, K. J., Roy, D. B., Bush, L. A., Cantwell, A. M., and Di Cera, E. (2003) Redesigning the monovalent cation specificity of an enzyme, *Proceedings of the National Academy of Sciences of the United States of America 100*, 13785-13790.
12. Gandhi, P. S., Chen, Z., Mathews, F. S., and Di Cera, E. (2008) Structural identification of the pathway of long-range communication in an allosteric enzyme, *Proc Natl Acad Sci USA 105*, 1832-1837.
13. He, X., and Rezaie, A. R. (1999) Identification and characterization of the sodium-binding site of activated protein C, *J Biol Chem 274*, 4970-4976.
14. Schmidt, A. E., Padmanabhan, K., Underwood, M. C., Bode, W., Mather, T., and Bajaj, S. P. (2002) Thermodynamic linkage between the S1 site, the Na+ site, and the Ca2+ site in the protease domain of human activated protein C (APC). Sodium ion in the APC crystal structure is coordinated to four carbonyl groups from two separate loops, *J Biol Chem 277*, 28987-28995.
15. Mann, K. G. (2003) Thrombin formation, *Chest 124*, 4S-10S.
16. Gopalakrishna, K., and Rezaie, A. R. (2006) The influence of sodium ion binding on factor IXa activity, *Thromb Haemost 95*, 936-941.
17. Camire, R. M. (2002) Prothrombinase assembly and S1 site occupation restore the catalytic activity of FXa impaired by mutation at the sodium-binding site, *J Biol Chem 277*, 37863-37870.
18. Schmidt, A. E., Stewart, J. E., Mathur, A., Krishnaswamy, S., and Bajaj, S. P. (2005) Na+ site in blood coagulation factor IXa: effect on catalysis and factor VIIIa binding, *Journal of molecular biology 350*, 78-91.
19. Underwood, M. C., Zhong, D., Mathur, A., Heyduk, T., and Bajaj, S. P. (2000) Thermodynamic linkage between the S1 site, the Na+ site, and the Ca2+ site in the protease domain of human coagulation factor xa. Studies on catalytic efficiency and inhibitor binding, *J Biol Chem 275*, 36876-36884.

20. Rezaie, A. R., and He, X. (2000) Sodium binding site of factor Xa: role of sodium in the prothrombinase complex, *Biochemistry 39*, 1817-1825.

CHAPTER VI

Summary, Discussion & Future Directions

Data from this thesis as well as from recent kinetic and structural observations on thrombin and other S1 proteases support a considerable and unexpected plasticity of the trypsin fold (*1*). Through protein conformational dynamics, the protease can inter-convert between inactive E* and active E forms. E* features a collapse of the 215-217 β-strand into the active site, a disruption of the oxyanion hole due to a flip of the peptide bond between Glu192 and Gly193, and abrogation of the Na^+ site (*2, 3*). Consequently, E* is basically unable to interact with either substrate or bind Na^+.

The structural differences between E and E:Na^+ are subtle, but the E* structure differs significantly from both, as such the E* to E transition involves unprecedented conformational changes (*4*). More importantly however, an intact ion-pair between Ile16 and Asp194 is still maintained in all the structures of E*, suggesting that this conformation is not equivalent to the zymogen form, which is characterized by a broken Ile16-Asp194 ion-pair and lack of a collapse of the 215-217 β-strand (*5, 6*). Furthermore, stopped-flow experiments show that the E* to E transition takes place on a time scale <10 msec compared to the zymogen – protease conversion that occurs on a longer (100-1000 msec) time scale (*7, 8*).

E* is not unique to the vitamin K-dependent clotting factors, however. Structural features of E* like collapse of the 215-217 β-strand into the active site or the disruption of the oxyanion hole have also been observed in other structures of serine proteases such as tryptases and complement factors (*1*). These observations support E* as an inactive form that is in allosteric equilibrium with the active form E of the protease. Serine

proteases are therefore allosteric enzymes whose activity can be fine tuned by modulating the E*-E equilibrium. Allostery is more often discussed in multimeric proteins like hemoglobin where large scale conformational transitions are usually evident (*9*). The structural plasticity demonstrated in monomeric proteins like serine proteases supports the idea that allostery is an intrinsic property of all dynamic proteins closely intertwined with catalysis (*10*). As shown in this thesis work, conformational plasticity is an integral part of protease function, regulation and substrate specificity.

What is the physiological advantage of the E*-E equilibrium? Depending on the activity requirement of each protease, the E* to E equilibrium can be set to optimize the function of that protease. For low activity proteases, the equilibrium favors E* while the reverse is true for high activity protease.

FUTURE DIRECTIONS

I. THROMBIN AND ANTICOAGULANT THERAPY

Safe and effective anticoagulants are needed for treatment and prevention of thrombotic disorders such as venous thrombosis and acute myocardial infarction (*11*). Current anticoagulant therapy is dominated by heparinoids, which are involved in antithrombin inhibition of thrombin and factor Xa; and warfarin, a generic inhibitor of the synthesis of all vitamin K -dependent clotting factors. Amongst the limitation of heparin and warfarin are a narrow therapeutic window and an unpredictable dose-response profile (*12*). Direct thrombin inhibitors like hiruden and bivalirudin are highly selective for thrombin, yet do no have a superior therapeutic efficacy and safety compared with low molecular weight

or even unfractionated heparins. Therefore new strategies are needed to generate more efficacious anticoagulants (*12*).

Because of its paradoxical roles in the procoagulant and anticoagulant pathways, thrombin mutants with selective specificity toward the anticoagulant protein C pathway have been rationally engineered and show potent and safe anticoagulant and antithrombotic effects in vivo. α-Thrombin mutants, E217K and W215A/E217A that show anticoagulant and antithrombotic effects in non-human primates both exhibit some structural features of ***E**** like partial collapse of the 215-217 β-strand and disruption of the oxyanion hole (*13-15*). Thus stabilization of ***E**** through mutagenesis or binding of a small molecule can provide an elegant regulatory control that can fine tune specificity along a particular pathway (*3*). The presence of E* in thrombin have significance mechanistic importance in generating a completely anticoagulant thrombin with no or minimal effect on fibrinogen and PAR1. Because of the collapsed active site, a mutant completely stabilized in E* will not interact with substrates or bind inhibitors. However, when such mutant interacts with TM-protein C complex, it can regain its ability to activate protein C. Stabilization of E* provides a novel strategy for generating anticoagulant thrombins and it can be pursued through mutagenesis or binding by small molecules identified through high throughput screening techniques.

II. E* in other proteolytic enzymes

In this thesis project, we have investigated the presence of inactive E* conformations in vitamin K- dependent clotting factors using Na^+ as a probe to perturb the E* to E

equilibrium. However, for proteolytic enzymes that do not interact or interact weakly with Na^+, this strategy cannot be used. Therefore, specific active site or exosite probes should be generated to investigate whether E*-like conformations are present in solution. In addition, to detect structural features of E*, crystallographic studies should be pursued in the absence of salts or inhibitors to prevent any allosteric transitions caused by these effectors. Alternatively, proteolytic enzymes that are amenable to NMR studies, structural and kinetic characterization of E* can be performed simultaneously using specific experiments based on CPMG relaxation dispersion that have been develop to investigate the low-populated transiently-formed conformations in proteins. These techniques can be very useful for instance to investigate changes in dynamics of the E* to E transition in the presence of effectors.

III. Role of the autolysis loop in S1 proteases

Sequence comparison of S1 serine proteases shows a lack of conservation in amino acid composition and length in the 145-150-loop region. However, this loop is strategically located between the 186- and 220 loops (the Na^+ binding site in some cases), the active site and exosite I/Ca^{2+} binding site. In many enzymes with longer loops, this region is highly flexible and susceptible to proteolysis, and in crystal structures it is either not defined or assumes different conformations depending on the crystallization conditions. Therefore, it became very difficult to allocate a definite function and it was proposed that the main function of this loop is to restrict access to the active site cleft. However, studies from our lab and others as well as data from this project shows that composition of the autolysis loop plays a major role in protease allostery and specificity. For instance,

deletion of the nine residues from human thrombin have stabilized that E* conformation whilst substitution of this loop with it murine counterpart resulted not only in a high activity human enzyme in the absence of Na^+, it generated a thrombin mutant with a higher Na^+ binding affinity compared to the WT (Chapters 3 & 4). Taken together, these results indicate that this loop is at the heart of protease allostery due to its strategic location, and can be used to modulate specificity by optimizing its sequence composition and length. Therefore, protease engineering efforts focusing on this loop in other trypsin-like serine proteases have the potential to modulate activity and generate more proficient enzymes especially for biological or industrial purposes.

References:

1. Di Cera, E. (2009) Serine proteases, *IUBMB life 61*, 510-515.
2. Pineda, A. O., Chen, Z. W., Bah, A., Garvey, L. C., Mathews, F. S., and Di Cera, E. (2006) Crystal structure of thrombin in a self-inhibited conformation, *J Biol Chem 281*, 32922-32928.
3. Bah, A., Carrell, C. J., Chen, Z., Gandhi, P. S., and Di Cera, E. (2009) Stabilization of the E* form turns thrombin into an anticoagulant, *J Biol Chem 284*, 20034-20040.
4. Gandhi, P. S., Chen, Z., Mathews, F. S., and Di Cera, E. (2008) Structural identification of the pathway of long-range communication in an allosteric enzyme, *Proc Natl Acad Sci USA 105*, 1832-1837.
5. Neurath, H., and Dixon, G. H. (1957) Structure and activation of trypsinogen and chymotrypsinogen, *Fed Proc 16*, 791-801.
6. Wang, D., Bode, W., and Huber, R. (1985) Bovine chymotrypsinogen A X-ray crystal structure analysis and refinement of a new crystal form at 1.8 A resolution, *Journal of molecular biology 185*, 595-624.
7. Bah, A., Garvey, L. C., Ge, J., and Di Cera, E. (2006) Rapid kinetics of Na+ binding to thrombin, *J Biol Chem 281*, 40049-40056.
8. Fersht, A. R., and Requena, Y. (1971) Equilibrium and rate constants for the interconversion of two conformations of -chymotrypsin. The existence of a catalytically inactive conformation at neutral p H, *Journal of molecular biology 60*, 279-290.
9. Tsai, C. J., del Sol, A., and Nussinov, R. (2008) Allostery: absence of a change in shape does not imply that allostery is not at play, *Journal of molecular biology 378*, 1-11.

10. Goodey, N. M., and Benkovic, S. J. (2008) Allosteric regulation and catalysis emerge via a common route, *Nat Chem Biol 4*, 474-482.
11. Bates, S. M., and Weitz, J. I. (2006) The status of new anticoagulants, *Br J Haematol 134*, 3-19.
12. Di Cera, E. (2003) Thrombin interactions, *Chest 124*, 11S-17S.
13. Pineda, A. O., Chen, Z. W., Caccia, S., Cantwell, A. M., Savvides, S. N., Waksman, G., Mathews, F. S., and Di Cera, E. (2004) The anticoagulant thrombin mutant W215A/E217A has a collapsed primary specificity pocket, *J Biol Chem 279*, 39824-39828.
14. Gandhi, P. S., Page, M. J., Chen, Z., Bush-Pelc, L. A., and Di Cera, E. (2009) Mechanism of the anticoagulant activity of the thrombin mutant W215A/E217A, *J Biol Chem 284*, 24098-24105.
15. Carter, W. J., Myles, T., Gibbs, C. S., Leung, L. L., and Huntington, J. A. (2004) Crystal structure of anticoagulant thrombin variant E217K provides insights into thrombin allostery, *J Biol Chem 279*, 26387-26394.